NORTHWESTERN UNIVERSITY

Bursting Deep Dorsal Horn Neurons: Potential Contributor to Muscle Spasms

A DISSERTATION

SUBMITTED TO THE GRADUATE SCHOOL

IN PARTIAL FULFILLMENT OF THE REQUIREMENTS

for the degree

DOCTOR OF PHILOSOPHY

Field of Northwestern University Interdepartmental Neuroscience Program (NUIN)

By

Theeradej Thaweerattanasinp

EVANSTON, ILLINOIS

March 2017

ABSTRACT

Bursting Deep Dorsal Horn Neurons: Potential Contributor to Muscle Spasms

Theeradej Thaweerattanasinp

Loss of inhibitory control from descending serotonergic (5-HT) fibers deregulates the excitability of spinal motoneurons and interneurons following spinal cord injury (SCI). Exaggerated synaptic activity triggers long-lasting excitatory postsynaptic potentials (long EPSPs) in hyperexcitable motoneurons to ultimately drive muscle spasms at the chronic stage of SCI. Deep dorsal horn (DDH) neurons with burst firing behavior could play a role in generating the long EPSPs. Modifying the 5-HT or glutamatergic transmission could influence the firing activity of the bursting DDH neurons and thus muscle spasms following SCI. Using extracellular electrophysiology, we investigate the firing behaviors of DDH neurons in the isolated sacral spinal cords of adult mice following acute and chronic spinal transection while administering NMDA or 5-$HT_{1B/1D}$ receptor agonist zolmitriptan. We also quantify polysynaptic reflexes in the ventral roots during NMDA administration. Upon dorsal root stimulation, DDH neurons can exhibit one of the three major firing response types with distinct evoked and spontaneous firing behaviors: bursting, single spiking, or spontaneously tonic firing. The bursting DDH neurons likely contribute to generating the long EPSPs due to their burst firing behavior and a slight increase in their excitability over time following SCI. Moreover, during zolmitriptan and NMDA administration, only the bursting DDH neurons exhibit significant changes in their firing properties. Zolmitriptan suppresses the bursting DDH neurons by, for example, reducing their evoked spike count, with stronger effects over time following SCI. In contrast, NMDA facilitates them by, for example, enhancing their spontaneous firing rate, with weaker effects over time following SCI. In addition, NMDA can induce bursting activity in the

ventral roots with no significant change in the magnitudes of its effect over time following SCI. These results support the functional contribution of the bursting DDH neurons to generation of the long EPSPs and muscle spasms, whose mechanisms may function independently from NMDA-induced bursting ventral root activity following chronic SCI.

ACKNOWLEDGEMENTS

I would like to express my appreciation and gratitude to all the people helping me in this project. To my committee, Drs. Vicki Tysseling, CJ Heckman, David Bennett, David McLean, and Matthew Tresch, who have imparted me the world-class process of becoming an independent scholar. To my mice, which devoted their lives and souls to the advance of the spinal cord research. To Mingchen Jiang, who has taught me the sacral cord preparation and electrophysiological techniques and has built and installed the entire recording chamber. To Derin Birch, Alyssa Puritz, and Erica Benelli, who has helped me in spinal transection surgery and bladder expression. To Jack Miller, who has maintained the rig and has helped me to order surgical tools and chemicals. To my family and friends, who have been by my side from the very beginning. I am sincerely thankful for everyone's contribution to helping me completing this project.

LIST OF ABBREVIATIONS

5-HT	5-hydroxytryptamine or serotonin
ACSF	Artificial cerebrospinal fluid
AMPA	*Alpha*-amino-3-hydroxy-5-methyl-4-isoxazolepropionic acid
ANOVA	Analysis of variance
CPG	Central pattern generator
DDH	Deep dorsal horn
DMSO	Dimethyl sulfoxide
EPSP	Excitatory postsynaptic potential
GABA	*Gamma*-Aminobutyric acid
G protein	Guanine nucleotide-binding protein
LLR	Long-lasting reflex
LPR	Long polysynaptic reflex
NMDA	*N*-methyl-D-aspartate
PIC	Persistent inward current
POC	Persistent outward current
SCI	Spinal cord injury
SEM	Standard error of the mean
SPR	Short polysynaptic reflex

TABLE OF CONTENTS

LIST OF FIGURES

I. INTRODUCTION

Spinal cord injury (SCI) results from a physical damage to the spinal cord. The location and severity level of the injury determine the degree of disruption to the spinal functions, ranging from no effect to muscle weakness to complete loss of function. Muscle spasm is one of the common complications sustained in patients with chronic SCI. It is characterized by a sudden, involuntary contraction of a muscle or group of muscles, which can interfere with postural and locomotor functions (Young 1994).

SCI interrupts the descending monoaminergic projections from the brainstem to spinal cord. The interruption results in the imbalance of excitatory and inhibitory input to spinal motoneurons by favoring excitatory input over inhibitory one. One of those SCI-interrupted projections is the raphespinal tract whose fibers release the neuromodulator serotonin (5-HT) in the intact spinal cord. The descending 5-HT fibers to the spinal cord originate from a group of raphe nuclei within the rostral ventromedial medulla, including the nucleus raphe magnus, raphe pallidus, and raphe obscuris, with their axon terminals distributed at all segmental levels of the spinal cord (Schmidt and Jordan 2000; Millan 2002). The 5-HT raphespinal fibers project from the raphe pallidus and obscuris via the ventral and ventrolateral funiculi to innervate ventral horn neurons (Schmidt and Jordan 2000; Watson and Harvey 2009). Raphespinal 5-HT facilitates spinal motor output (Schmidt and Jordan 2000; Heckman et al. 2005). It activates excitatory G_q protein-coupled receptors, such as 5-HT_2 receptors, on ventral horn motoneurons (Heckman et al. 2005; Hochman et al. 2001), which innervate muscles. Activation of 5-$HT_{2A/2B/2C}$ receptors on motoneurons lowers the spike threshold and facilitates voltage-gated persistent inward currents (PICs) which are mediated by both sodium (Na^+) channels and L-typed calcium (Cav1.3) channels (Li and Bennett 2003; Harvey et al. 2006a; Li et al. 2007; Murray et al. 2011a). These PICs normally induce plateau potentials which, in turn, amplify synaptic inputs to motoneurons

and prolong their firing patterns (Heckman et al. 2005; Harvey et al. 2006a), thus enhancing input-output rate modulation of motoneurons.

However, the number of raphespinal 5-HT fibers significantly decreases in the spinal segments below the lesion (Hadjiconstantinou et al. 1984; Murray et al. 2010). Even though the spinal cord itself can produce and release 5-HT from a small number of 5-HT neurons in the dorsal horn and central canal as well as 5-HT-containing afferent fibers (Yoshimura and Furue 2006), the nearly total deprivation of 5-HT in the spinal cord after complete transection indicates that the majority of spinal 5-HT arises from the supraspinal sources (Yoshimura and Furue 2006; Hadjiconstantinou et al. 1984; Murray et al. 2010). Therefore, denervation of the 5-HT fibers dramatically reduces the excitability of motoneurons (Li et al. 2004a; Heckman et al. 2005), and thus the acute stage of SCI results in spinal shock, presenting with hyporeflexia and paralysis (Ditunno et al. 2004). Surprisingly, rat sacral motoneurons recover or even over-recover their excitability spontaneously over weeks after the injury (Harvey et al. 2006b; Murray et al. 2010). More importantly, at the chronic stage of SCI, large PICs reemerge as $5\text{-HT}_{2B/2C}$ receptors on motoneurons become constitutively active in the reduced level of endogenous 5-HT (Harvey et al. 2006b; Murray et al. 2010; Murray et al. 2011a). As a result, this constitutive receptor activity restores the excitability of motoneurons but without proper descending regulation from the brainstem (Murray et al. 2010). These hyperexcitable motoneurons thus contribute to hyperreflexia and muscle spasms as common complications after SCI (Bennett el al. 2004; Li et al. 2004a; Ditunno et al. 2004). Although the hyperexcitable motoneurons are the major contributor to generation of muscle spasms, growing evidence from prior studies suggests that spinal interneurons in the dorsal horn may also contribute to muscle spasms following SCI.

The spinal dorsal horn can be organized into different laminae along the dorsoventral axis based on their cellular composition (Watson and Kayalioglu 2009; Brown 1982; Abraira and

Ginty 2013). Laminae I and II are the outermost layer of the dorsal horn, while the deep laminae III through VI comprise the rest of the dorsal horn and have neurons of larger cell bodies than those of the outermost laminae (Watson and Kayalioglu 2009; Brown 1982; Abraira and Ginty 2013). Primary afferent fibers convey sensory inputs of different modalities from the skin, viscera, muscles, and joints throughout the body and have lamina-specific central projections in the spinal dorsal horn via excitatory glutamatergic transmission (Heise and Kayalioglu 2009; Brown 1982; Abraira and Ginty 2013; Todd 2010). Small-diameter unmyelinated C (or group IV) fibers, which mediate temperature, itch, and pain sensation, terminate mainly in laminae I and II (Heise and Kayalioglu 2009; Brown 1982; Abraira and Ginty 2013; Todd 2010; Li et al. 2011). Medium-diameter myelinated Aδ (or group III) fibers for temperature, pain, and high-threshold tactile sensation terminate in laminae I through III and also lamina V (Heise and Kayalioglu 2009; Abraira and Ginty 2013; Todd 2010; Li et al. 2011). Large-diameter myelinated Aβ (or group II) fibers for low-threshold tactile sensation terminate in laminae III through V (Heise and Kayalioglu 2009; Abraira and Ginty 2013; Todd 2010; Li et al. 2011). Lastly, large-diamter myelinated Aα (or group I) fibers for body-position sensation terminate in lamina V through lamina VII, where premotor interneurons, such as Ia inhibitory interneurons, are located in the ventral horn, and lamina IX of spinal motoneurons (Heise and Kayalioglu 2009; Brown 1982; Levine et al. 2014).

In addition to primary afferent fibers, the dorsal horn also receives descending inputs from the brain, such as the corticospinal and raphespinal tracts (Watson and Harvey 2009; Brown 1982). In mammals, the corticospinal tract descends mainly from the primary motor, premotor, and somatosensory cortical areas and terminates mainly in the medial parts of laminae III through VI in the dorsal horn or even lamina VII in the ventral horn (Watson and Harvey 2009; Brown 1982). Corticospinal fibers from sensory cortical areas terminate more dorsally in the dorsal

horn than those from motor cortical areas (Brown 1982). In the dorsal horn, activation of the corticospinal tract results in presynaptic inhibition of primary afferents (Andersen et al. 1964; Brown 1982) and inhibition or excitation of dorsal horn neurons (Fetz 1968; Brown 1982). Moreover, direct corticospinal projections to motoneurons in lamina IX are predominantly found in primates (Watson and Harvey 2009). These direct corticomotoneuronal connections are presumably correlated with the development of highly skilled motor control, particularly in humans (Watson and Harvey 2009). As a result, denervation of the corticospinal fibers results in loss of fine voluntary movements in SCI patients (Ditunno et al. 2004).

The raphespinal fibers, which contain 5-HT, descend from the raphe magnus of the brainstem via the dorsolateral funiculi to innervate dorsal horn neurons in laminae I through V and the medial part of lamina VI (Schmidt and Jordan 2000; Watson and Harvey 2009; Brown 1982). Raphespinal 5-HT normally suppresses spinal sensory transmission, for example, of tactile and pain information to motoneurons and ascending projections to the brain via activation of inhibitory G_i protein-coupled 5-HT_1 receptors on presynaptic afferent axons or excitatory dorsal horn neurons (Schmidt and Jordan 2000; Hochman et al. 2001; Millan 2002; Yoshimura and Furue 2006). Activation of 5-$HT_{1A/1B/1D}$ receptors, which are expressed densely in the spinal dorsal horn (Millan 2002; Yoshimura and Furue 2006), opens potassium (K^+) channels and closes calcium (Ca^{2+}) channels through a decrease in the intracellular level of cyclic adenosine monophosphate (Millan, 2002; Yoshimura and Furue, 2006), thus suggesting the inhibitory effect of 5-HT_1 receptors in the dorsal horn. As a result, SCI-induced loss of descending 5-HT inhibitory control results in exaggerated sensory transmission, for example, long-lasting excitatory postsynaptic potentials (long EPSPs) to motoneurons for driving muscle spasms following chronic SCI (Li et al. 2004a; Baker and Chandler 1987; Bennett et al. 2004). However, application of 5-HT can suppress muscle spasms via activation of 5-$HT_{1B/1D}$ receptors (Li et al.

2004b; Murray et al. 2011b; D'Amico et al. 2013). Zolmitriptan, the more selective agonist for 5-$HT_{1B/1D}$ receptors, can suppress long EPSPs and muscle spasms without affecting the intrinsic membrane properties of the hyperexcitable motoneurons (Murray et al. 2011b), thus suggesting the contribution of other spinal neurons to generation of long EPSPs and muscle spasms. Despite the depletion of 5-HT, the spinal cord continues to produce glutamate for locomotor activity mediated by NMDA receptors following SCI (Chau et al. 2002; Giroux et al. 2003). Activation of NMDA receptors can generate longer-lasting EPSPs than activation of AMPA receptors (Blanke and VanDongen 2009). Therefore, NMDA receptors may potentially contribute to generation of the long EPSPs in the hyperexcitable motoneurons that trigger muscle spasms (Murray et al. 2011b).

The majority of neurons in the dorsal horn are interneurons with local axonal and dendritic projections within the spinal cord (Abraira and Ginty 2013; Todd 2010). A small fraction of dorsal horn neurons are projection neurons with ascending projections to the brain, which are primarily found in lamina I and distributed throughout laminae III through VI (Abraira and Ginty 2013; Todd 2010). Neurons in the superficial dorsal horn (laminae I-II), which are important for thermoreception (temperature sensation) and nociception (noxious stimulus or pain sensation), have been the most extensively studied dorsal horn neurons (Abraira and Ginty 2013; Todd 2010). In contrast, neurons in the deep dorsal horn (laminae III-VI), perhaps important for mechanoreception (tactile or mechanical sensation) and proprioception (body-position sensation), are poorly understood (Abraira and Ginty 2013; Todd 2010). Nonetheless, the extensive, but incomplete, studies of the superficial dorsal horn neurons will provide some basic backgrounds for future characterization of the deep dorsal horn neurons.

Neurons in lamina I are the major source of ascending projections conveying discriminative aspects of nociception and thermoreception to the brain (Carstens and Trevino 1978; Willis et

al. 1979; Heise and Kayalioglu 2009). Lamina I neurons receive afferent inputs mainly from C and Aδ fibers (Christensen and Perl 1970; Heise and Kayalioglu 2009), and they can be classified into three major functional cell types based on their modality-specific responses: nociceptive-specific neurons, polymodal nociceptive neurons, and thermoreceptive-specific neurons (Christensen and Perl 1970; Heise and Kayalioglu 2009). Wide dynamic range neurons, which are responsive to nociceptive stimuli and innocuous mechanoreceptive stimuli, are also found in this lamina (Feerington et al. 1987; Heise and Kayalioglu 2009). These functional cell types of lamina I neurons correlate with their morphological cell types (Han et al. 1998; Heise and Kayalioglu 2009). Nociceptive-specific neurons can be associated with fusiform cells, polymodal nociceptive neurons with multipolar cells, and thermoreceptive-specific neurons with pyramidal cells (Han et al. 1998; Heise and Kayalioglu 2009). Moreover, lamina I neurons can be classified into four firing-pattern types based on their responses to sensory stimulation, perhaps reflecting differences in sensory input processing (Prescott and De Koninck 2002; Heise and Kayalioglu 2009). Tonic cells discharge continuously with a low-frequency firing throughout the stimulation and may act as integrators. Phasic cells discharge a high-frequency burst firing of variable duration and may act as coincidence detectors. Delayed-onset cells discharge irregularly with a significant delay to the first spike and may act as integrators. Single-spike cells discharge only one spike even during the strong stimulation and may act as coincidence detectors (Prescott and De Koninck 2002; Heise and Kayalioglu 2009). These physiological cell types of lamina I neurons also correlate with their morphological cell types (Prescott and De Koninck 2002; Heise and Kayalioglu 2009). Tonic cells can be associated with fusiform cells, phasic cells with pyramidal cells, and delayed-onset and single-spike cells with multipolar cells (Prescott and De Koninck 2002; Heise and Kayalioglu 2009). Therefore, the morphological diversity of lamina I neurons likely reflects a functional system for transmission of modality-specific information (Heise and Kayalioglu 2009).

Neurons in lamina II are primarily interneurons which modulate transmission of nociceptive information and have axon collaterals to deep dorsal horn laminae III through V (Heise and Kayalioglu 2009; Light and Kavookjian 1988). Lamina II neurons can respond to either nociceptive stimuli or innocuous mechanoreceptive stimuli (Light et al. 1979; Bennett et al. 1980; Light and Wilcockson, 1999). Although a large number of them remain unclassified, lamina II neurons can be classified into four major morphological cell types: islet, central, vertical, and radial cells (Grudt and Perl 2002; Hantman et al. 2004; Todd 2010). Islet cells are inhibitory GABAergic neurons receiving afferent inputs mainly from C fibers, while radial and most vertical cells are excitatory glutamatergic neurons receiving afferent inputs from both C and Aδ fibers, and central cells are of either type receiving afferent inputs mainly from C fibers (Grudt and Perl 2002; Hantman et al. 2004; Todd 2010). Therefore, the morphological diversity of lamina II neurons reflects a functional system that can be involved in integration of primary afferent input, modulation of projection neuron output from the surrounding laminae, and transmission of nociceptive information to deeper dorsal horn laminae (Light et al. 1979; Millan 1999; Heise and Kayalioglu 2009).

Deep dorsal horn (DDH) neurons in laminae III through VI are either interneurons or projection neurons conveying innocuous mechanoreceptive information to the brain (Heise and Kayalioglu 2009). Many DDH neurons extend their dendrites dorsoventrally across their own laminae into surrounding laminae (Heise and Kayalioglu 2009). Several lamina III-IV neurons have their dendrites spreading into more superficial lamina II, and some even into lamina I (Schoenen 1982; Maxwell et al. 1983; Heise and Kayalioglu 2009). Lamina III-IV neurons receive afferent inputs from Aβ and Aδ fibers (Brown 1982; Light and Perl 1979; Heise and Kayalioglu 2009), and those with dendrites extending into lamina II may also receive and respond to afferent inputs from C fibers as well as getting modulated by lamina II interneurons (Perl 1980; Maxwell

1985; Todd 1989; Heise and Kayalioglu 2009). DDH neurons in lamina III and IV respond to low-threshold (e.g. light touch) or high-threshold (e.g. strong pressure) mechanoreceptive stimuli (Bennett et al. 1984; Cervero et al. 1988; Maxwell et al. 1983; Heise and Kayalioglu 2009). Moreover, wide dynamic range neurons that respond to nociceptive stimuli are also present in these laminae (De Koninck et al. 1992; Heise and Kayalioglu 2009).

DDH neurons in laminae V and VI have their dendrites spreading into more superficial laminae III and II and also reaching deeper lamina VII (Heise and Kayalioglu 2009). Lamina V-VI neurons receive monosynaptic inputs from Aβ and Aδ fibers and polysynaptic inputs from C fibers as well as collateral axons of Aα muscle spindle (i.e. group Ia) fibers (Heise and Kayalioglu 2009; Brown and Fyffe 1978). Some DDH neurons in these laminae are involved in functional circuits for reflex and sensory modulation of locomotor output (Bui et al. 2013; Levine et al. 2014; Duysens and Pearson 1976; Quevedo et al. 2005). Lamina V neurons can be classified into at least three functional cell types with distinct morphological features: multireceptive wide dynamic range neurons, nociceptive-specific neurons, and mechanoreceptive neurons (Ritz and Greenspan 1985; Heise and Kayalioglu 2009). Multireceptive neurons have differential responses to innocuous and noxious mechanical stimuli and have large cell bodies with extensive dendrites spreading in all directions as well as axons ascending in the contralateral ventral white matter. Nociceptive-specific neurons respond only to noxious stimuli and have smaller cell bodies with similar extensive dendritic trees. Mechanoreceptive neurons respond to innocuous mechanical stimuli without nociceptive input and have a less extensive dendritic spread than the other two cell types (Ritz and Greenspan 1985; Heise and Kayalioglu 2009).

Therefore, DDH neurons, particularly in lamina V, can contribute to synaptic integration and transmission of somatosensory information from multiple sources to motoneurons. They receive

diverse sensory afferent inputs via glutamatergic synapses, ranging from proprioceptive to mechanoreceptive to nociceptive inputs (Brown 1982; Woolf 1987; Heise and Kayalioglu 2009), for sensory input processing and then relay the processed information via their axon collaterals to neurons in the ventral horn (Brown 1982; Heise and Kayalioglu 2009). Moreover, these lamina V neurons can express PIC-induced plateau potentials for amplifying and prolonging their firing responses to synaptic inputs (Derjean et al. 2003; Morisset and Nagy 1998, 1999), similar to motoneurons (Li and Bennett 2003; Harvey et al. 2006a; Li et al. 2007; Murray et al. 2011a). Some DDH neurons in medial lamina V even receive direct synaptic input from the corticospinal tract and provide monosynaptic input to motoneurons (Levine et al. 2014). These neurons also extend their axons across multiple spinal segments to connect functionally associated motoneuron pools for coordinating patterns of motoneuron activation or motor synergies (Levine et al. 2014). Perhaps, targeting these medial lamina V neurons to drive motor synergies could facilitate voluntary and reflexive movements in SCI patients (Levine et al. 2014).

Taken together, the findings from prior studies lead to the hypothesis that loss of 5-HT inhibition of DDH neurons following SCI can reduce their threshold for generating plateau potentials in response to low-threshold sensory inputs. The disinhibited DDH neurons then develop the burst firing behavior and thus become capable of triggering long EPSPs in motoneurons for driving muscle spasms. Nowadays, the majority of SCI research aims at repair of the primary lesion and regeneration of descending axons. However, regulation of the plastic changes in spinal neurons and networks below the lesion is no less important. Detail studies of plastic changes in the intrinsic membrane properties of spinal motoneurons following SCI are already prevalent. In contrast, the plasticity of dorsal horn neurons following SCI remains poorly understood as a muscle spasm mechanism. The understandings of the differential plasticity of all individual neuronal substrates in the spinal networks following SCI are important for designing

pharmacological interventions to restore spinal functions and alleviate pathological symptoms such as muscle spasms and chronic pain. Therefore, the goal of this thesis is to understand the firing behavior of DDH neurons over time following SCI by characterizing their firing properties during various pharmacological conditions at both acute and chronic stages of SCI.

This thesis is organized into chapters, with each in the format of journal manuscript. Chapter 2 has been published (Thaweerattanasinp et al. 2016). Chapters 3 and 4 are parts of manuscripts for submission to a peer-reviewed journal. Chapter 2 describes results of an experiment which investigates the firing characteristics of DDH neurons following acute spinal transection during administration of zolmitriptan and NMDA. The chapter tests the hypothesis that DDH neurons with burst firing behavior emerge following SCI and have significant firing responses to the effects of both drugs. It also establishes a baseline for investigating whether these bursting DDH neurons change their firing behavior from acute to chronic SCI. In chapter 3, the bursting DDH neurons are further investigated for their firing characteristics following chronic spinal transection during administration of zolmitriptan and NMDA. The chapter tests the hypothesis that the bursting DDH neurons maintain their burst firing behavior and continue to respond to the effects of both drugs over time following SCI. Chapter 4 describes results of ventral root activity following acute and chronic spinal transection during administration of NMDA. The chapter establishes a baseline for investigating the functional relationship between locomotor network and muscle spasm-generating network in the spinal cord following SCI. Future studies may use these results to identify the bursting DDH neurons via genetic labeling for better understandings of their functional contribution to muscle spasm mechanisms and their functional connectivity with other neurons in the spinal networks. Identification of the bursting DDH neurons would facilitate the process of designing pharmacological treatments for SCI and its related complications.

II. THE FIRING CHARACTERISTICS OF DEEP DORSAL HORN NEURONS FOLLOWING ACUTE SPINAL TRANSECTION DURING ADMINISTRATION OF AGONISTS FOR 5-$HT_{1B/1D}$ AND NMDA RECEPTORS

(Thaweerattanasinp T, Heckman CJ, Tysseling VM. *J Neurophysiol* 116: 1644-1653, 2016)

Abstract. Spinal cord injury (SCI) results in a loss of serotonin (5-HT) to the spinal cord and a loss of inhibition to deep dorsal horn (DDH) neurons, which produces an exaggerated excitatory drive to motoneurons. The mechanism of this excitatory drive could involve the DDH neurons triggering long excitatory postsynaptic potentials (EPSPs) in motoneurons, which may ultimately drive muscle spasms. Modifying the activity of DDH neurons with drugs such as NMDA or the 5-$HT_{1B/1D}$ receptor agonist zolmitriptan could have a large effect on motoneuron activity and, therefore, on muscle spasms. In this study, we characterize the firing properties of DDH neurons following acute spinal transection in adult mice during administration of zolmitriptan and NMDA, using the *in vitro* sacral cord preparation and extracellular electrophysiology. DDH neurons can be categorized into three major types with distinct evoked and spontaneous firing characteristics: burst (bursting), simple (single-spiking), and tonic (spontaneously tonic-firing) neurons. The burst neurons likely contribute to muscle spasm mechanisms due to their bursting behavior. Only the burst neurons show significant changes in their firing characteristics during zolmitriptan and NMDA administration. Zolmitriptan suppresses the burst neurons by reducing their evoked spikes, burst duration, and spontaneous firing rate. Conversely, NMDA facilitates them by enhancing their burst duration and spontaneous firing rate. These results suggest that zolmitriptan may exert its anti-spastic effect on the burst neurons via activation of 5-$HT_{1B/1D}$ receptors in the dorsal horn, whereas activation of NMDA receptors may facilitate the burst neurons in contributing to muscle spasm mechanisms following SCI.

INTRODUCTION

One of the descending brain projections to the spinal cord interrupted by spinal cord injury (SCI) is the projection from the brainstem raphe nuclei. In the intact spinal cord, raphespinal fibers release the neuromodulator serotonin (5-HT), which inhibits spinal sensory input (Schmidt and Jordan 2000). Raphespinal 5-HT activates inhibitory G_i protein-coupled receptors, such as 5-HT_1 receptors, especially on excitatory dorsal horn neurons involved in polysynaptic spinal reflexes (e.g. flexion withdrawal reflex; Schouenborg and Sjolund 1983) and sensory perception (Hochman et al. 2001; Millan 2002; Yoshimura and Furue 2006). Particularly, activation of 5-$HT_{1A/1B/1D/1F}$ receptors causes postsynaptic inhibition and reduced excitability of dorsal horn neurons (Yoshimura and Furue 2006; Millan 2002), thus attenuating sensory transmission to motoneurons and ascending projections to the brain.

SCI significantly reduces the number of raphespinal 5-HT fibers in the spinal segments below the transection (Hadjiconstantinou et al. 1984; Murray et al. 2010). Loss of tonic 5-HT inhibition of the spinal sensory input following SCI results in exaggerated sensory transmission, including the appearance of unusually long-lasting excitatory postsynaptic potentials (long EPSPs; up to 1 s) in cat lumbar (Baker and Chandler 1987) and rat sacral (Li et al. 2004a) motoneurons evoked by stimulation of low-threshold group I and II primary afferents from muscle and skin (Li et al. 2004a; Baker and Chandler 1987) via polysynaptic connections (Murray et al. 2011b). At the acute stage of SCI, the long EPSPs do not activate voltage-gated persistent inward currents (PICs) in virtually unexcitable motoneurons (Li et al. 2004a). In contrast, at the chronic stage of SCI, these exaggerated long EPSPs, in turn, activate the uncontrolled large PICs in hyperexcitable motoneurons, ultimately driving muscle spasms in rats (Bennett et al. 2004; Li et al. 2004a). Interestingly, before injury, the same stimulation for the long EPSPs instead suppresses ongoing muscle activity (Bennett et al. 2004), suggesting the predominance of

inhibitory control of sensory transmission in the intact spinal cord. Unlike 5-HT, glutamate is an intrinsically produced transmitter in the spinal cord and thus still contributes to locomotion mediated by NMDA receptors in the spinal cord after SCI (Chau et al. 2002; Giroux et al. 2003). However, the contribution of NMDA to muscle spasms after SCI remains unknown. The long duration of the EPSPs that trigger muscle spasms suggests the potential involvement of NMDA receptors in its generation (Murray et al. 2011b).

Prior studies demonstrated that exogenous application of 5-HT can suppress muscle spasms in chronic SCI rats (Li et al. 2004b) via its action on inhibitory 5-$HT_{1B/1D/1F}$ receptors (Murray et al. 2011b; D'Amico et al. 2013). Unlike excitatory 5-$HT_{2B/2C}$ receptors on motoneurons (Harvey et al. 2006b; Murray et al. 2010; Murray et al. 2011a), 5-$HT_{1B/1F}$ receptors do not develop constitutive activity (Murray et al. 2011b). Instead, they remain silent in the reduced level of endogenous 5-HT after chronic SCI (Murray et al. 2011b) without developing 5-HT supersensitivity (D'Amico et al. 2013). Moreover, the anti-spastic effect of 5-$HT_{1B/1D/1F}$ receptor agonist zolmitriptan can suppress long EPSPs and muscle spasms without affecting the sacral motoneuron properties, including PICs, in chronic SCI rats (Murray et al. 2011b). Despite the known inhibitory effects of 5-HT on spinal sensory transmission, the location of 5-$HT_{1B/1D/1F}$ receptors or where the anti-spastic effect of zolmitriptan takes place remains largely unknown. Possibly, these 5-HT_1 receptors are on axon terminals of low-threshold group I and II afferents (Murray et al. 2011b; Millan 2002). Another possibility is that these 5-HT_1 receptors are located on the excitatory spinal deep dorsal horn (DDH) neurons, which also receive group II afferent inputs, by either pre- or post-synaptically modulating the activity of these neurons (Dougherty et al. 2005; Murray et al. 2011b).

Taken together, evidence from prior studies suggests the possible involvement of disinhibited DDH neurons in providing exaggerated excitatory drive, i.e. long EPSPs, to motoneurons,

ultimately producing muscle spasms following SCI. We hypothesize that the disinhibited DDH neurons contributing to muscle spasm mechanisms will exhibit bursting responses following SCI. Moreover, it remains unknown how the activation of 5-$HT_{1B/1D}$ and NMDA receptors would affect the responses of the DDH neurons following SCI. Therefore, as the first step in our long-term goal of understanding DDH neuron behavior following SCI, we characterize the firing properties of the DDH neurons following acute spinal transection. We also examine their responses during administration of zolmitriptan, the selective 5-$HT_{1B/1D}$ receptor agonist, and NMDA. We predict that zolmitriptan will suppress the firing activity of the bursting DDH neurons for its anti-spastic effect, while NMDA will instead facilitate the bursting DDH neurons.

Combining the *in vitro* sacral preparation in adult mice (Jiang and Heckman 2006; Jiang et al. 2009) with extracellular electrophysiology, we demonstrate that there are distinct types of DDH neurons with their own evoked and spontaneous firing characteristics following acute spinal transection, which we studied as a model of the acute stage of complete SCI. Moreover, their firing characteristics respond differently to zolmitriptan and NMDA administration. Of particular interest, bursting DDH neurons or the “burst neurons” exhibit diminished firing activity during zolmitriptan administration. On the other hand, NMDA moderately facilitates the firing activity of the burst neurons. Therefore, this study in acute spinal transection establishes a first step for investigating bursting DDH neurons further in chronic SCI as these neurons likely contribute to muscle spasm mechanisms.

MATERIALS AND METHODS

Animal models

Adult mice (C57BL/6, BALB/c; aged > 8 weeks; *N* = 81) received acute spinal transection during the *in vitro* sacral cord (S1-S3) preparation. The whole sacral cord was removed from the animals with complete transection at the sacral edge of the lumbar enlargement (i.e. between L6 and S1 segments) and maintained *in vitro* for extracellular recordings of deep dorsal horn neurons, as detailed below. All experimental procedures were reviewed and approved by the Institutional Animal Care and Use Committee of Northwestern University and were in accordance with the National Institute of Health Guide for the Care and Use of Laboratory Animals.

In vitro sacral cord preparation

The animal surgery was based on the detail described in Jiang and Heckman (2006) and Jiang et al (2009). The animals were deeply anesthetized with intraperitoneal (IP) injections of urethane (0.18g/100g). After a few minutes, a foot-pinching test with forceps was used to determine whether the animals needed additional urethane IP injections. During the surgery, animals were supplied with 95% O_2/ 5% CO_2 via a face mask. The spinal cord was exposed by dorsal laminectomy and removal of lateral portions of the vertebrae. That is, the spinal column was cut open between low thoracic and caudal segments while immediately perfusing the spinal cord with artificial CSF (ACSF). The ACSF consisted of the following chemicals (in mM): 126 NaCl, 3 KCl, 1 NaH_2PO_4, 1.5 $MgSO_4$, 2.5 $CaCl_2$, 26 $NaHCO_3$, and 10 glucose. The ACSF was bubbled with 95% O_2/ 5% CO_2, and circulated at 5-7 ml/min. The dura below lumbar segments was slit transversely using angled Iris scissors, and the cord was transected at the L1-L2 spinal

segments immediately after decapitation. The transected spinal cord with the attached dorsal and ventral roots was rapidly transferred to a 100 mm Petri dish filled with the ACSF bubbled with 95% O_2/ 5% CO_2. The dorsal and ventral roots at the caudal cord were cut at their spinal outlets. After separating the sacral ventral roots (S1-S3) and the corresponding sacral dorsal roots, the cord was cut at the sacral edge of the lumbar enlargement. To wash out the residual anesthetic before recording, the cord was maintained in the dissection Petri dish for 1.0-1.5 hrs at room temperature. After that, the cord was transferred to a recording chamber filled with ACSF. The chamber consisted of two arrays, one on each side, of bipolar recording electrodes for the ventral roots (S1-S3). Each bipolar electrode consisted of two monopolar electrodes separated by 5 mm. Another bipolar electrode was used to stimulate each dorsal root. All Teflon-coated stainless-steel wire electrodes for stimulating and recording were mounted on a plastic plate. The dorsal and ventral roots were placed on the electrodes and sealed with a mineral oil/petroleum jelly (2:1) mixture, and the chamber was perfused with ACSF. The ACSF was bubbled with 95% O_2/5% CO_2, and the fluid rate was adjusted to 2.5-3 ml/min.

Stimulation and recordings

Extracellular recordings of DDH neurons of the sacral (S1-S3) spinal cord were made with sharp glass microelectrodes. The electrodes were pulled from glass capillary tubes (1.5-mm OD; A-M Systems) using a micropipette puller (P-97, Sutter) and filled with 3 M potassium acetate (KCH_3COO) as an internal solution, with impedances of 30-50 MΩ. Electrode tips were advanced perpendicularly through the dorsal surface of the sacral cord using a stepper-motor micromanipulator (2660, Kopf) to be in the vicinity of DDH neurons located at the depth of approximately 100-500 μm from the dorsal surface, where the deep dorsal laminae III-V are located in the sacral spinal segments (S1-S3; Watson et al. 2009). Many neurons in these

laminae receive descending monoaminergic input from the brainstem, and they also have projections to deeper laminae, including motoneurons, in the ventral horn (Brown 1982; Heise and Kayalioglu 2009). On either the left or right side of the sacral cord, electrode penetration was made at the halfway point between the midline dorsal vein and the most lateral edge. A sudden shift in potential during the search reflected the first indication of a cell. The DDH neurons were identified by orthodromic dorsal root stimulation with 20-μA electrical pulses (0.2 ms). Only DDH neurons with reliable orthodromic synaptic activity were included in the study. Data collection was made with Axoclamp 2A intracellular ampliflier (Axon Instruments) running in discontinuous current-clamp mode (Bridge).

The recorded DDH neurons received synaptic activation via dorsal root stimulation using an isolation unit (PSIU6E, Grass Instruments) that was connected to a stimulator (S88, Grass Instruments). The dorsal roots were stimulated with 0.2-ms electrical pulses at four stimulus intensities, i.e. 1X (3-10 μA), 2X, 5X, and 10X, to reliably evoke mono- and poly-synaptic ventral root reflexes. Reflex threshold is comparable with afferent threshold (Bennett et al. 2004). At a given intensity, the dorsal roots were stimulated 5 times at intervals of 30 seconds to avoid reflex depression. The recording electrodes on the ventral roots were connected to an amplifier (DAM 50, WPI) in differential mode with 1000X gain, high-pass filtering at 300 Hz, and low-pass filtering at 20 kHz. The recording outputs of both DDH neurons and ventral root reflexes were transferred to an analog-to-digital interface (1401plus, CED), and the analog signals were digitized at 20-50 kHz and acquired into a Dell computer controlled by Spike2 software (CED).

Drug solutions and actions

Drugs that were added to the ACSF (its composition described in the above section) included NMDA and zolmitriptan, the selective 5-$HT_{1B/1D}$ receptor agonist (all purchased from Sigma-

Aldrich). Before added to ACSF, NMDA was first dissolved as a 10 mM stock in purified water, while zolmitriptan was dissolved in a 1 mM stock in DMSO.

The effects of NMDA (15, 50, and 100 μM) and zolmitriptan (1 μM) were studied via bath administration on the firing properties of DDH neurons in response to dorsal root stimulation. In each experiment, the sacral dorsal roots were stimulated with the same 5 stimuli (or 5 trials) at a given stimulus intensity for four stimulus intensities (i.e. 1X, 2X, 5X, and 10X; 20 stimuli in total).

The dorsal roots were stimulated for 20 stimuli at intervals of 30 s (~10 min) during drug administration, and followed by other 20 stimuli at the same intervals (~10 min) during drug washout. These same 20 stimuli (~10 min) also preceded the drug administration as controls. The drugs were washed in and out for approximately 2-3 minutes prior to the first dorsal root stimulation during the drug administration and washout, respectively.

Data analysis

The following firing properties of DDH neurons were measured offline in Spike2 (CED): evoked spike count, field potential, first-spike latency, and spontaneous firing rate. Evoked spike count was measured in each trial by counting the number of spikes within the first 1-second time window from a stimulus onset, after determining the first evoked spike. Measuring first-spike latency in each trial helped identify the first evoked spike by taking the time difference between the stimulus onset and the onset of the first evoked spike (maximally capped at 30 ms). Only the non-zero values of first-spike latency were used for statistical analyses. Field potential was measured from a peak-to-peak voltage of a hyperpolarization which usually happened shortly after a stimulus artifact. Moreover, we calculated spontaneous firing rate in each trial from the number of spikes within the last 1 second prior to a stimulus onset. Specifically for the burst

neurons (see Results), burst duration was measured in the same software by taking the time difference between the first and last evoked spikes. For a recorded DDH neuron, the mean of each firing property was calculated from the measurements in the 5 trials (or fewer in cases with some missed trials) of each stimulus intensity. Moreover, the final mean of evoked spike count was corrected for post-stimulus spontaneous spikes by subtracting the mean of spontaneous firing rate (within 1 second pre-stimulus) from the pre-corrected mean of evoked spike count (within 1 second post-stimulus).

Due to a large difference in the number of data across the analyzed groups (i.e. unbalanced data), a two-way unbalanced ANOVA via multiple regression analysis ($\alpha = 0.05$) was used for all comparisons of the firing properties from DDH neuron types or drug conditions at four stimulus intensities. If statistically significant, a post-hoc pairwise comparison (*t*-test) of group means ($\alpha = 0.05$) with the Bonferroni correction was then used to identify specific significant differences between DDH neuron types or drug conditions at four stimulus intensities. Because of a large number of trial measurements from a large population of the recorded DDH neurons, the group mean of each firing property will approximately approach a normal distribution, according to the central limit theorem. Only the significant main effects of DDH neuron types and drug conditions are shown on figures. Statistical analyses were performed using Microsoft Excel 2007 (Redmond, WA) with the Real Statistics Resource Pack add-in (release 4.5; copyright 2013-2015; Charles Zaiontz; www.real-statistics.com). Data are means ± SEM.

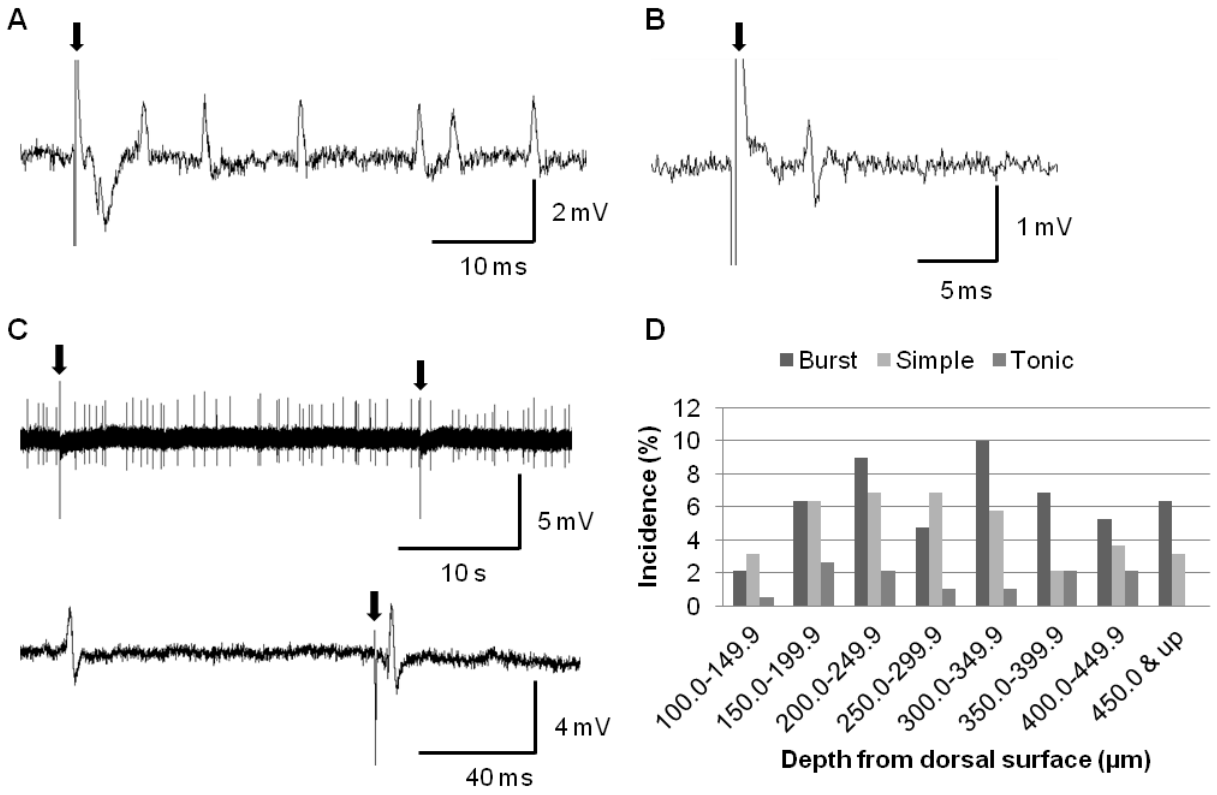

Figure 1. Three firing response types of DDH neurons and their distribution in the dorsal horn. Representative recording traces showing three distinct firing response types of DDH neurons upon 0.2-ms dorsal root stimulation (stimulus artifacts, arrows) in a single trial. *A*: burst neuron. *B*: simple neuron. *C*: tonic neuron (top) with its evoked spike (bottom). *Bottom*: an expanded view of the second arrow (top) for a better view of the evoked spike. An evoked spike was also found in an expanded view of the first arrow (not shown). *D*: Distribution of DDH neuron types as incidence (%) across various depths measured from the dorsal surface (*N* = 190).

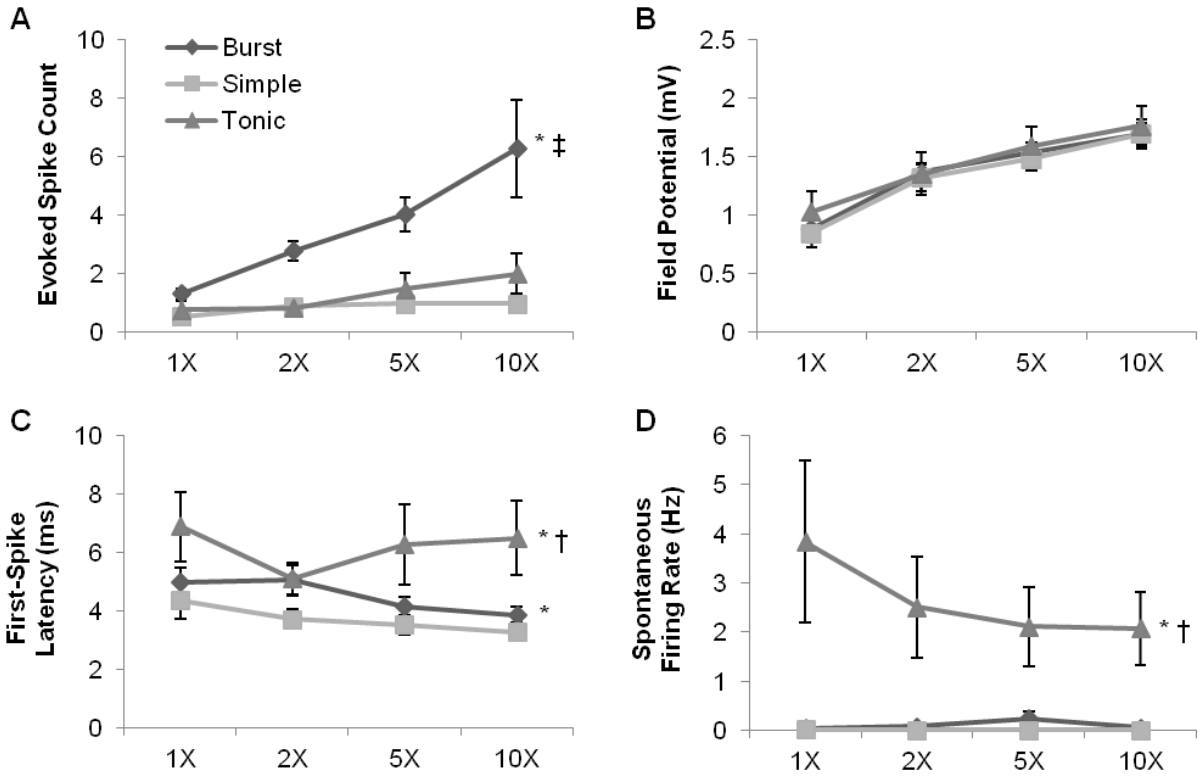

Figure 2. Firing properties of three distinct neuron types following acute spinal transection. Group data comparing firing properties (mean ± SEM) of the burst (♦), simple (■), and tonic (▲) neurons in response to increasing stimulus intensity in control. *A*: evoked spike count for the burst (*N* = 96; except *N* = 95 at 10X), simple (*N* = 72), and tonic (*N* = 22) neurons. *B*: field potential for the burst (*N* = 96; except *N* = 95 at 10X), simple (*N* = 72), and tonic (*N* = 22) neurons. *C*: first-spike latency (only nonzero values) for the burst (*N* = 64, 1X; *N* = 92, 2X; *N* = 96, 5X; *N* = 94, 10X), simple (*N* = 39, 1X; *N* = 64, 2X; *N* = 69, 5X; *N* = 69, 10X), and tonic (*N* = 16, 1X; *N* = 18, 2X; *N* = 20, 5X; *N* = 21, 10X) neurons. *D*: spontaneous firing rate for the burst (*N* = 96; except *N* = 95 at 10X), simple (*N* = 72), and tonic (*N* = 22) neurons. Significant difference from the simple (*$P < 0.017$), burst (†$P < 0.017$), and tonic (‡$P < 0.017$) neurons using a post-hoc pairwise comparison (*t*-test) of group means with the Bonferroni correction.

RESULTS

Extracellular recordings of 190 DDH neurons were obtained from 81 adult mice with acute spinal transection. Among the recorded DDH neuron population, 112 neurons were studied during the bath administration of either NMDA (*N* = 62) or zolmitriptan (*N* = 50) obtained from 69 adult mice. We also analyzed four parameters for the measurement of DDH neuron firing properties: evoked spike count; field potential; first-spike latency; and spontaneous firing rate (see details in Methods).

Firing response types of DDH neurons following acute spinal transection

Single-pulse (0.2 ms) dorsal root stimulation revealed three firing response types of DDH neurons: burst, simple, and tonic neurons (Fig. 1). We categorized these neurons based on the number of evoked spikes and on the presence of spontaneous firing. Burst neurons (*N* = 96; Fig. 1A) consistently fired two or more spikes in response to single stimuli of dorsal root stimulation with sporadic spontaneous firing. Simple neurons (*N* = 72; Fig. 1B) fired only a single spike in response to dorsal root stimulation with sporadic spontaneous firing. However, tonic neurons (*N* = 22) had sustained spontaneous firing (Fig. 1C, *top*) and could fire a single or multiple spikes in response to dorsal root stimulation (Fig 1C, *bottom*). The depth distribution of recorded DDH neurons in the dorsal horn is shown in Figure 1D. We performed further analyses in controls to characterize the firing properties among the three firing response types of DDH neurons (Fig. 2).

Evoked spike count (Fig. 2A) differed significantly among the three DDH neuron types (two-way unbalanced ANOVA, $p = 5.72 \times 10^{-8}$), as expected from their classifications defined in the previous paragraph. The burst neurons (3.59 ± 0.46 spikes) fired more evoked spikes than the

simple (0.82 ± 0.02 spikes; Bonferroni-corrected pairwise *t*-test, $p = 2.83 \times 10^{-8}$) and tonic (1.24 ± 0.25 spikes; $p = .002$) neurons in response to dorsal root stimulation. DDH neurons as a group fired more evoked spikes with more intense stimulation ($p = .035$).

There was no significant interaction between DDH neuron type and stimulus intensity ($p = .055$), indicating that the three neuron types respond similarly to activation of low- versus high-threshold afferents. In addition, field potentials (Fig. 2B) from the vicinity of the three DDH neuron types were not significantly different in magnitude from each other ($p = .65$). The field potentials did become larger in magnitude with more intense stimulation ($p = 6.56 \times 10^{-12}$), but there was no significant interaction between DDH neuron type and stimulus intensity ($p = 1.0$). These results reflect the close proximity of the burst, simple, and tonic neurons in the dorsal horn.

First-spike latency (Fig. 2C) differed significantly among the three DDH neuron types ($p = 2.09 \times 10^{-6}$). The simple neurons fired the earliest spike in response (3.71 ± 0.19 ms) to dorsal root stimulation, followed by the burst (4.51 ± 0.20 ms) and tonic (6.19 ± 0.58 ms) neurons, respectively (simple vs burst, $p = .008$; simple vs tonic, $p = 3.01 \times 10^{-7}$; burst vs tonic, $p = 3.10 \times 10^{-4}$). However, more intense stimulation did not elicit faster responses from DDH neurons ($p = .32$). Also, there was no significant interaction between DDH neuron type and stimulus intensity ($p = .56$). These results indicate that the simple neurons respond most rapidly to single stimuli of dorsal root stimulation and thus may have the most direct connection from the sensory afferents.

Lastly, spontaneous firing rate (Fig. 2D) differed significantly among the three DDH neuron types ($p = 7.84 \times 10^{-31}$). The tonic neurons had the highest spontaneous firing rate (2.63 ± 0.55 Hz; $p = 8.19 \times 10^{-29}$ vs burst; $p = 2.90 \times 10^{-29}$ vs simple), with no significant difference ($p = .49$)

between the burst (0.10 ± 0.04 Hz) and simple (0.00 ± 0.00 Hz) neurons. However, more intense stimulation decreased the spontaneous firing rate of DDH neurons as a group (p = .048). Moreover, a significant interaction between DDH neuron type and stimulus intensity (p = .047) revealed that the tonic neurons had a higher spontaneous firing rate than the burst and simple neurons at all intensities (p < .002 for all post-hoc comparisons). But the tonic neurons had a reduced spontaneous firing rate with more intense stimulation, particularly between 1X (3.84 ± 1.65 Hz) and 10X (2.07 ± 0.75 Hz) intensities ($p = 1.54 \times 10^{-3}$). These results reflect the contribution of the tonic neurons to providing background activity in the dorsal horn. Taken together, these results (Fig. 2A-D) demonstrated that the burst, simple, and tonic neurons belong to distinct groups of DDH neurons with different firing characteristics following acute spinal transection. Because of their bursting behavior in response to short-duration synaptic input, the burst neurons likely contribute to muscle spasm mechanisms following SCI.

Figure 3. Effects of NMDA on the firing properties of the burst neurons following acute spinal transection. *A*: representative recording traces showing the effect of NMDA (bottom) on a burst neuron, compared with that in control (top), upon dorsal root stimulation (0.2 ms; arrow). *B-F*: group data showing the effects of NMDA (■) on the firing properties (mean ± SEM) of the burst neurons in response to increasing stimulus intensity, compared with those during control (♦) and washout (▲) conditions. *B*: evoked spike count during control (*N* = 34 for all intensities), NMDA (*N* = 26, 1X&2X; *N* = 28, 5X; *N* = 32, 10X), and washout (same as NMDA) conditions. *C*: field potential during control (N = 34 for all intensities), NMDA (*N* = 26, 1X&2X; *N* = 28, 5X; *N* = 32, 10X), and washout (same as NMDA) conditions. *D*: burst duration during control (*N* = 34 for all intensities), NMDA (*N* = 26, 1X&2X; *N* = 28, 5X; *N* = 32, 10X), and washout (same as NMDA) conditions. *E*: first-spike latency (only nonzero values) during control (*N* = 18, 1X; *N* = 31, 2X; *N* = 34, 5X&10X), NMDA (*N* = 15, 1X; *N* = 23, 2X; *N* = 26, 5X; *N* = 30, 10X), and washout (*N* = 14, 1X; *N* = 22, 2X; *N* = 26, 5X; *N* = 29, 10X) conditions. *F*: spontaneous firing rate during control (*N* = 34 for all intensities), NMDA (*N* = 26, 1X&2X; *N* = 28, 5X; *N* = 32, 10X), and washout (same as NMDA) conditions. Significant difference from control (**P* < 0.017) and washout (†*P* < 0.017) conditions using a post-hoc pairwise comparison (*t*-test) of group means with the Bonferroni correction.

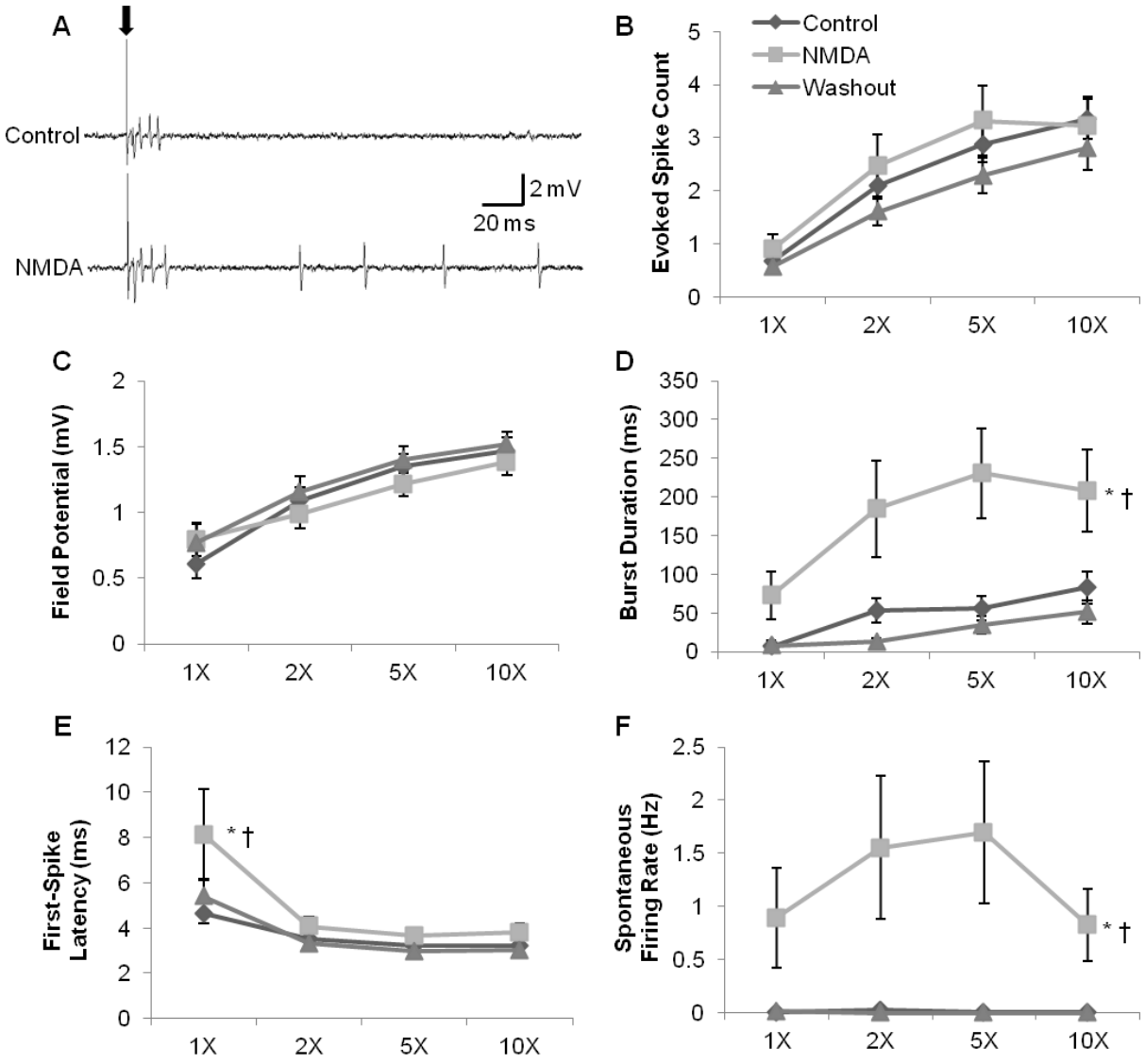
A
Control
2 mV
20 ms
NMDA
B
Control
NMDA
Washout
Evoked Spike Count
0
1
2
3
4
5
1X
2X
5X
10X
C
Field Potential (mV)
0
0.5
1
1.5
2
1X
2X
5X
10X
D
Burst Duration (ms)
0
50
100
150
200
250
300
350
* †
1X
2X
5X
10X
E
First-Spike Latency (ms)
0
2
4
6
8
10
12
* †
1X
2X
5X
10X
F
Spontaneous Firing Rate (Hz)
0
0.5
1
1.5
2
2.5
* †
1X
2X
5X
10X

NMDA facilitates the burst neurons

The burst neurons are the main interest of this study because they could potentially generate exaggerated excitatory drive, i.e. long EPSPs (Murray et al. 2011b), to motoneurons following SCI. As a result, we studied the effects of NMDA, as NMDA receptor activation is known to generate longer lasting EPSPs than AMPA (α-amino-3-hydroxy-5-methyl-4-isoxazolepropionic acid) receptors activation (Blanke and VanDongen 2009), and zolmitriptan, which is known to reduce long lasting EPSPs that produce muscle spasms (Murray et al. 2011b), on this DDH neuron type.

A total of 96 burst neurons were recorded from the deep dorsal horn; 34 of these neurons were studied during the bath administration of NMDA (N = 21 at 15 μM; N = 4 at 50 μM; N = 9 at 100 μM). In addition to the four firing property parameters (see the previous section), we also measured burst duration specifically for the burst neurons. The results described below were derived from the combined effects of all the three concentrations on the five parameters of the burst neuron firing properties following acute spinal transection (Fig. 3). NMDA moderately facilitated the firing properties of the burst neurons (Fig. 3A) as follows.

NMDA had no significant effect on the evoked spike count of the burst neurons (Fig. 3B; p = .064). The drug also had no significant effect on the field potential magnitude from the vicinity of the burst neurons (Fig. 3C; p = .33), and the overall pattern of increased evoked spike count (p = 2.43×10^{-13}) and field potential (p = 1.36×10^{-15}) with more intense stimulation seen in the control state continued during NMDA administration. However, NMDA did have a significant effect on the burst duration of the burst neurons (Fig. 3D; p = 8.34×10^{-11}). The evoked firing of the burst neurons had significantly longer burst duration during NMDA administration (173.68 ± 26.70 ms), compared with those in control (49.59 ± 8.09 ms; p = 1.88×10^{-8}) and washout

(26.73 ± 5.66 ms; $p = 2.63 \times 10^{-10}$). Moreover, the burst neurons exhibited prolonged burst duration over increasing stimulus intensity ($p = .004$).

NMDA also had a significant effect on the first-spike latency of the burst neurons (Fig. 3E; $p = 1.98 \times 10^{-4}$). Surprisingly, NMDA delayed the first-spike latency of the burst neurons (4.92 ± 0.39 ms), compared with control (3.65 ± 0.14 ms; $p = 1.05 \times 10^{-4}$) and washout (3.66 ± 0.19 ms; $p = 3.56 \times 10^{-4}$). Moreover, more intense stimulation could elicit faster responses from the burst neurons ($p = 2.62 \times 10^{-10}$), whereas stimulus intensity did not have a significant effect on the whole samples of DDH neurons (see the previous section).

Lastly, NMDA had a significant effect on the spontaneous firing rate of the burst neurons (Fig. 3F; $p = 4.16 \times 10^{-10}$). NMDA significantly increased the spontaneous firing rate of the burst neurons (1.24 ± 0.27 Hz), compared with control (0.01 ± 0.01 Hz; $p = 3.64 \times 10^{-9}$) and washout (0.00 ± 0.00 Hz; $p = 1.40 \times 10^{-8}$). However, stimulus intensity did not significantly affect the spontaneous firing rate of the burst neurons ($p = .50$), whereas more intense stimulation have a decreasing effect on the whole samples of DDH neurons (see the previous section). These results support the effect of NMDA in raising the spontaneous firing rate of the burst neurons.

Taken together, these results (Fig. 3A-F) demonstrated that NMDA moderately facilitates the firing properties of the burst neurons following acute spinal transection by enhancing burst duration and spontaneous firing rate, despite slightly delaying first-spike latency, when compared with controls.

Figure 4. Effects of zolmitriptan on the firing properties of the burst neurons following acute spinal transection. *A*: representative recording traces showing the effect of zolmitriptan (bottom) on a burst neuron, compared with that in control (top), upon dorsal root stimulation (0.2 ms; arrow). *B-F*: group data showing the effects of zolmitriptan (■) on the firing properties (mean ± SEM) of the burst neurons in response to increasing stimulus intensity, compared with those during control (♦) and washout (▲) conditions. *B*: evoked spike count during control (*N* = 25 for all intensities), zolmitriptan (*N* = 24, 1X, 2X, &5X; *N* = 25, 10X), and washout (same as zolmitriptan) conditions. *C*: field potential during control (*N* = 25 for all intensities), zolmitriptan (*N* = 24, 1X, 2X, &5X; *N* = 25, 10X), and washout (same as zolmitriptan) conditions. *D*: burst duration during control (*N* = 25 for all intensities), zolmitriptan (*N* = 24, 1X, 2X, &5X; *N* = 25, 10X), and washout (same as zolmitriptan) conditions. *E*: first-spike latency (only nonzero values) during control (*N* = 18, 1X; *N* = 24, 2X, 5X, &10X), zolmitriptan (*N* = 16, 1X; *N* = 21, 2X; *N* = 22, 5X; *N* = 21, 10X), and washout (*N* = 13, 1X; *N* = 21, 2X, 5X, &10X) conditions. *F*: spontaneous firing rate during control (*N* = 25 for all intensities), zolmitriptan (*N* = 24, 1X, 2X, &5X; *N* = 25, 10X), and washout (same as zolmitriptan) conditions. Significant difference from zolmitriptan (*$P < 0.017$) and washout (†$P < 0.017$) conditions using a post-hoc pairwise comparison (*t*-test) of group means with the Bonferroni correction.

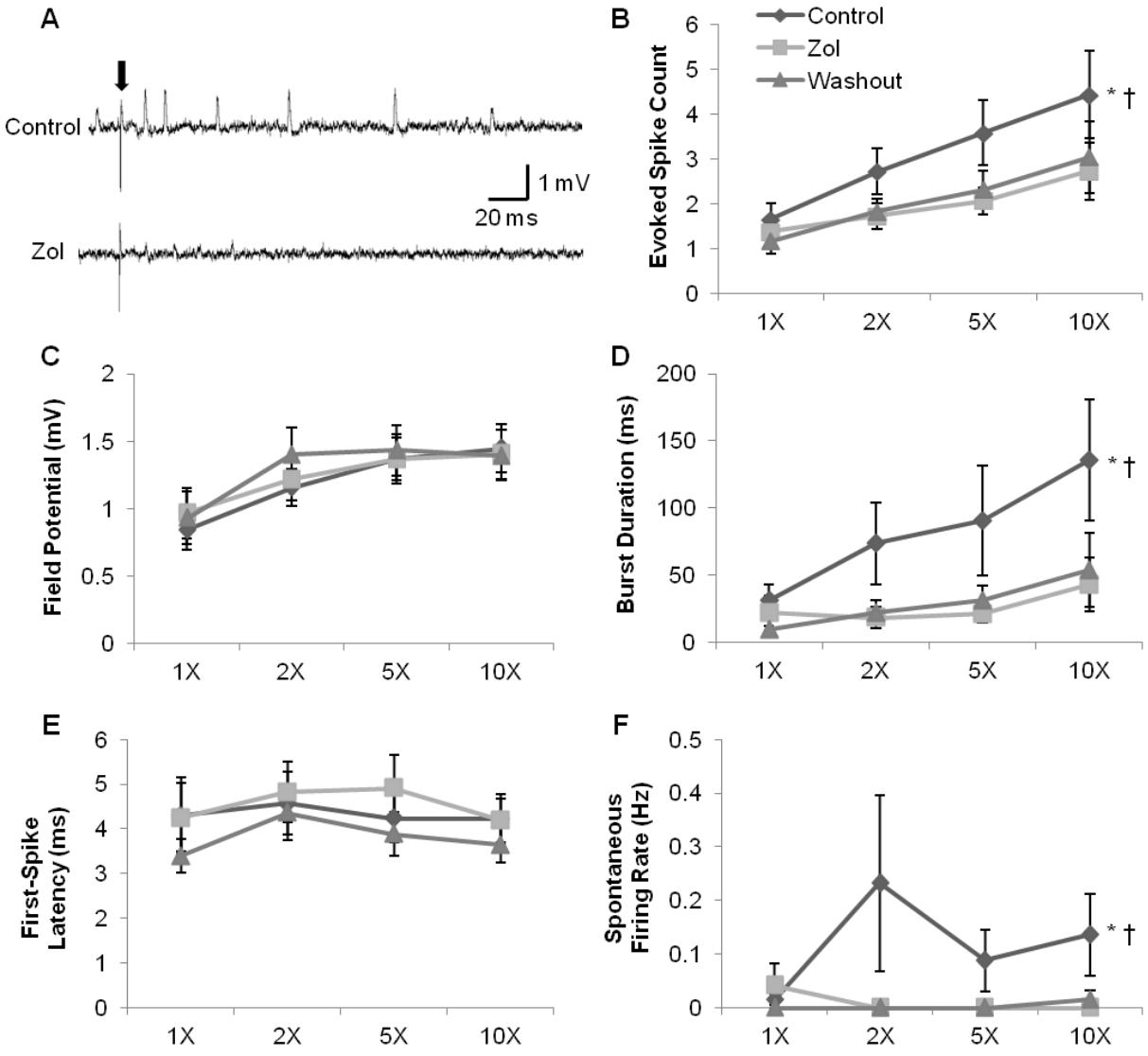
A
Control
1 mV
20 ms
Zol
B
Control
Zol
Washout
Evoked Spike Count
* †
1X
2X
5X
10X
C
Field Potential (mV)
D
Burst Duration (ms)
E
First-Spike Latency (ms)
F
Spontaneous Firing Rate (Hz)

Zolmitriptan suppresses the burst neurons

Among the total number of 96 burst neurons recorded from the deep dorsal horn, 25 neurons were studied during the bath administration of zolmitriptan. Unlike NMDA, only one concentration of zolmitriptan (1 μM) was used to study its effect on the firing properties (Fig. 4). As opposed to the NMDA experiments, a complete washout of zolmitriptan was found to be very challenging (also reported in Murray et al. 2011b), thus resulting in no significant differences in all the firing properties between zolmitriptan and washout conditions. Moreover, in some experiments, we performed the same recording protocol with zolmitriptan administration in the second DDH neurons following the zolmitriptan washout of the first neuron. However, we found that exclusion of the data of these second neurons from the data analysis did not overturn any statistical results in which all the neurons were included. Therefore, despite the difficulty in washing out the drug, we reported the statistical results from the data of all the DDH neurons that had been recorded during zolmitriptan administration in the below sections. Zolmitriptan suppressed the firing properties of the burst neurons (Fig. 4A) as follows.

Zolmitriptan significantly decreased the evoked spike count of the burst neurons (Fig. 4B; two-way unbalanced ANOVA, $p = .007$; 1.97 ± 0.21 spikes vs 3.09 ± 0.36 spikes in control; Bonferroni-corrected pairwise *t*-test, $p = .004$). Zolmitriptan also had a significant effect on the burst duration of the burst neurons (Fig. 4D; $p = 7.19 \times 10^{-4}$), with post-drug duration being 25.96 ± 6.54 ms and pre-drug 82.79 ± 17.46 ms ($p = 7.16 \times 10^{-8}$). In addition, the drug had a significant effect on the spontaneous firing rate of the burst neurons (Fig. 4F; $p = .007$), decreasing to 0.01 ± 0.01 Hz, from a pre-drug value of 0.12 ± 0.05 Hz ($p = .007$). Zolmitriptan had no significant effect on the first-spike latency of the burst neurons (Fig. 4E; $p = .27$) or on the magnitude of the field potential in the vicinity of the burst neurons (Fig. 4C; $p = .79$). These results support the effect of zolmitriptan in decreasing the spontaneous firing rate of the burst

neurons. Taken together, these results (Fig. 4A-F) demonstrated that zolmitriptan suppresses the firing properties of the burst neurons following acute spinal transection by decreasing evoked spike count, burst duration, and spontaneous firing rate, when compared with controls.

Figure 5. Effects of NMDA on the firing properties of the simple neurons following acute spinal transection. *A*: representative recording traces showing the effect of NMDA (bottom) on a simple neuron, compared with that in control (top), upon dorsal root stimulation (0.2 ms; arrow). *B*-*E*: group data showing the effects of NMDA (■) on the firing properties (mean ± SEM) of the simple neurons in response to increasing stimulus intensity, compared with those during control (♦) and washout (▲) conditions. *B*: evoked spike count during control (*N* = 23 for all intensities), NMDA (*N* = 17, 1X&2X; *N* = 21, 5X; *N* = 19, 10X), and washout (same as NMDA) conditions. *C*: field potential during control (*N* = 23 for all intensities), NMDA (*N* = 17, 1X&2X; *N* = 21, 5X; *N* = 19, 10X), and washout (same as NMDA) conditions. *D*: first-spike latency (only nonzero values) during control (*N* = 10, 1X; *N* = 21, 2X; *N* = 23, 5X&10X), NMDA (*N* = 8, 1X; *N* = 13, 2X; *N* = 17, 5X; *N* = 15, 10X), and washout (*N* = 7, 1X; *N* = 13, 2X; *N* = 17, 5X; *N* = 16, 10X) conditions. *E*: spontaneous firing rate during control (*N* = 23 for all intensities), NMDA (*N* = 17, 1X&2X; *N* = 21, 5X; *N* = 19, 10X), and washout (same as NMDA) conditions.

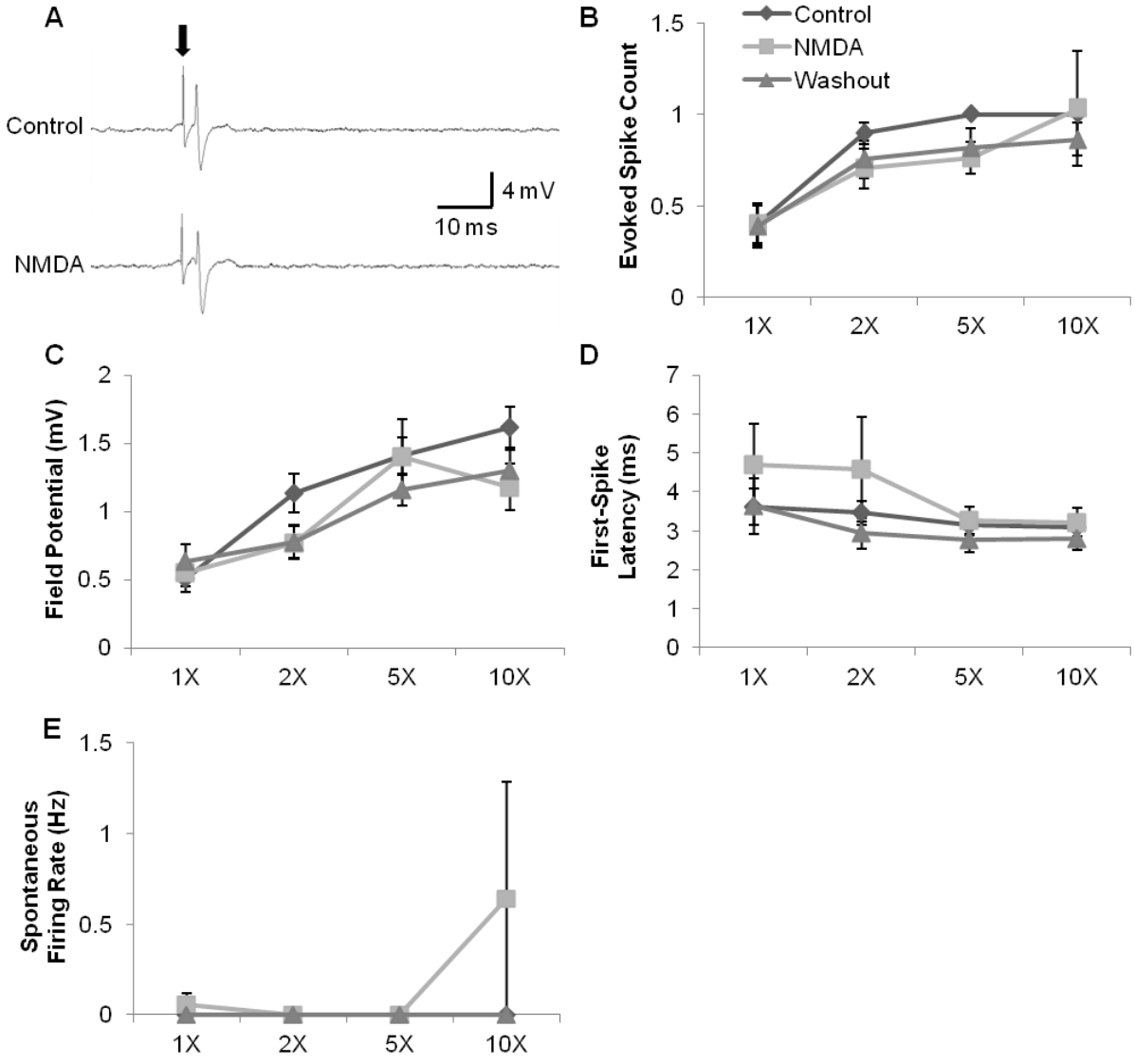
A
Control
4 mV
10 ms
NMDA
B
Control
NMDA
Washout
Evoked Spike Count
1.5
1
0.5
0
1X
2X
5X
10X
C
Field Potential (mV)
2
1.5
1
0.5
0
1X
2X
5X
10X
D
First-Spike Latency (ms)
7
6
5
4
3
2
1
0
1X
2X
5X
10X
E
Spontaneous Firing Rate (Hz)
1.5
1
0.5
0
1X
2X
5X
10X

Figure 6. Effects of zolmitriptan on the firing properties of the simple neurons following acute spinal transection. *A*: representative recording traces showing the effect of zolmitriptan (bottom) on a simple neuron, compared with that in control (top), upon dorsal root stimulation (0.2 ms; arrow). *B-E*: group data showing the effects of zolmitriptan (■) on the firing properties (mean ± SEM) of the simple neurons in response to increasing stimulus intensity, compared with those during control (♦) and washout (▲) conditions. *B*: evoked spike count during control (*N* = 23 for all intensities), zolmitriptan (*N* = 20, 1X, 2X, &5X; *N* = 22, 10X), and washout (*N* = 21, 1X, 2X, &5X; *N* = 22, 10X) conditions. *C*: field potential during control (*N* = 23 for all intensities), zolmitriptan (*N* = 21, 1X, 2X, &5X; *N* = 23, 10X), and washout (*N* = 21, 1X, 2X, &5X; *N* = 22, 10X) conditions. *D*: first-spike latency (only nonzero values) during control (*N* = 15, 1X; *N* = 19, 2X; *N* = 22, 5X&10X), zolmitriptan (*N* = 13, 1X; *N* = 17, 2X; *N* = 19, 5X; *N* = 22, 10X), and washout (*N* = 13, 1X; *N* = 18, 2X&5X; *N* = 20, 10X) conditions. *E*: spontaneous firing rate during control (*N* = 23 for all intensities), zolmitriptan (*N* = 20, 1X, 2X, &5X; *N* = 22, 10X), and washout (*N* = 21, 1X, 2X, &5X; *N* = 22, 10X) conditions.

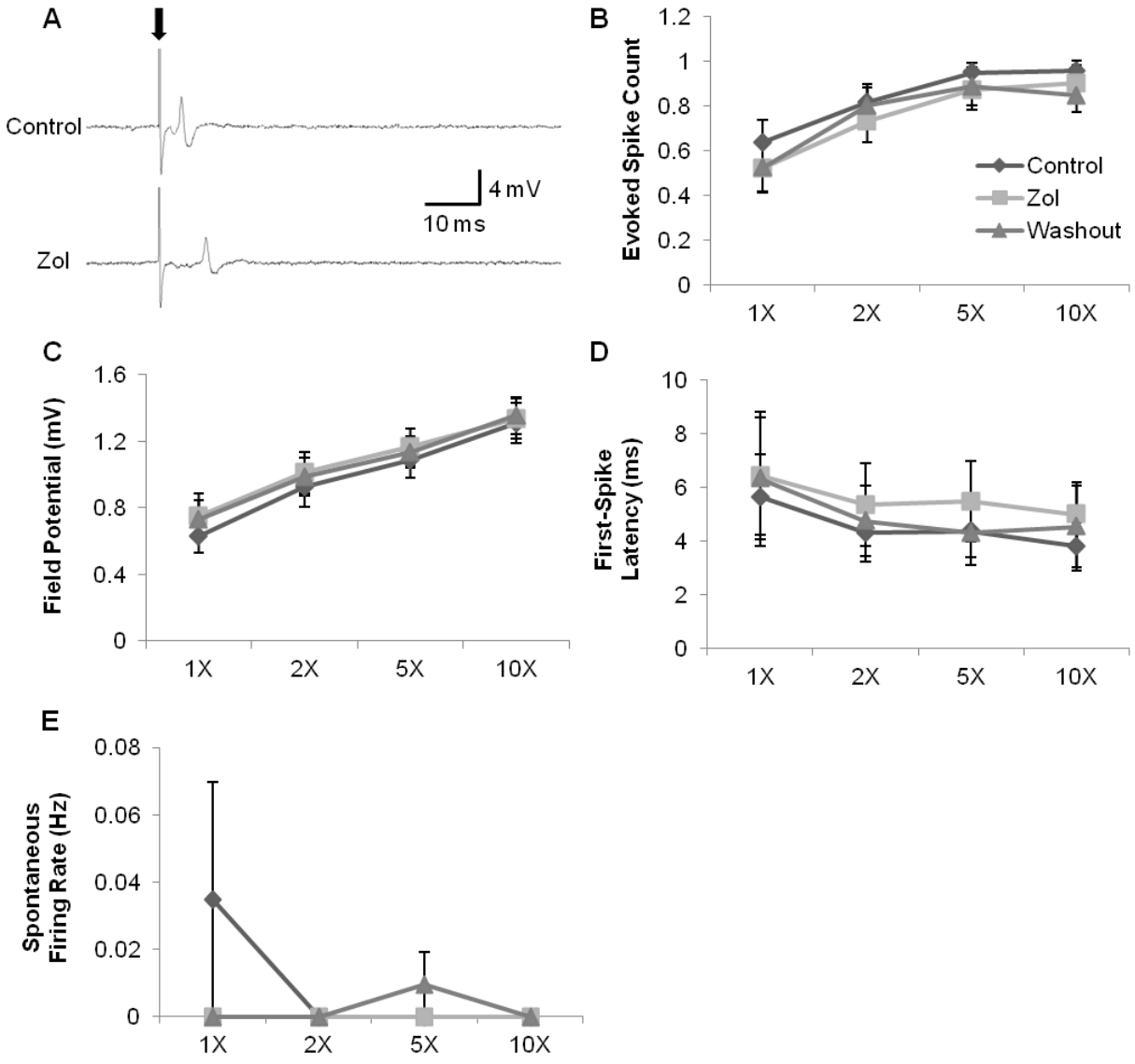
A
Control
Zol
4 mV
10 ms
B
Evoked Spike Count
1.2
1
0.8
0.6
0.4
0.2
0
1X
2X
5X
10X
Control
Zol
Washout
C
Field Potential (mV)
1.6
1.2
0.8
0.4
0
1X
2X
5X
10X
D
First-Spike Latency (ms)
10
8
6
4
2
0
1X
2X
5X
10X
E
Spontaneous Firing Rate (Hz)
0.08
0.06
0.04
0.02
0
1X
2X
5X
10X

Neither NMDA nor zolmitriptan has any significant effects on the simple neurons

There were no significant effects of either NMDA (see Figure 5) or zolmitriptan (see Figure 6) on the simple neurons. Figures 5A and 6A illustrate this lack of effect for evoked spike count on the simple neurons. Unfortunately, we could study only a very small number of tonic neurons during the bath administration of NMDA (N = 5) and zolmitriptan (N = 2). Therefore, we did not include the drug results of the tonic neurons in this study. The difference in effects of these drugs is consistent with a role for bursting but not single-spiking neurons in the generation of long-lasting EPSPs in motoneurons.

DISCUSSION

Our goal was to characterize the firing activity of DDH neurons immediately following a complete transection SCI. We also aimed to assess the effects of 5-$HT_{1B/1D}$ and NMDA receptor activation on the firing characteristics of DDH neurons following this acute spinal transection. In the following discussion, we consider the possibility that the bursting subtype of DDH neurons may become involved in the generation of muscle spasms that develop as acute spinal injury transitions to chronic injury.

This study had two main findings. Firstly, following acute spinal transection, the deep dorsal horn contains at least three major response types of neurons with distinct evoked and spontaneous firing characteristics, single spiking, bursting and tonic firing. Secondly, only the burst neurons have significant changes in their firing activity during administration of zolmitriptan and NMDA, when compared with controls. Zolmitriptan suppresses the burst neurons by decreasing their evoked spike count, burst duration, and spontaneous firing rate. In contrast,

NMDA moderately facilitates them by increasing their burst duration and spontaneous firing rate.

Neurons of distinct firing characteristics reside in the deep dorsal horn

The three major response types of neurons in the deep dorsal horn have distinct evoked and spontaneous firing characteristics upon short-duration synaptic input from dorsal root stimulation (Fig. 2A-D), possibly reflecting functional differences in sensory input processing of DDH neurons. The burst and simple neurons fire spikes virtually at the stimulus onset (Fig. 2C) and thus may play a role as “coincidence detectors” (Abraira and Ginty 2013). The burst neurons may also encode the stimulus intensity (Ruscheweyh and Sandkühler 2002) since they tend to fire more spikes (Fig. 2A, 3B, &4B) and have longer burst duration (Fig. 3D&4D) over increasing stimulus intensities. On the other hand, the tonic neurons may play a role in maintaining excitability of the local neural network in the dorsal horn via their sustained spontaneous firing (Fig. 2D). Prior studies also found similar and other types of neurons in the deep dorsal horn (Hochman et al. 1997; Ruscheweyh and Sandkühler 2002; Rank et al. 2015). Using slice preparations, these *in vitro* patch-clamp studies investigated the intrinsic membrane properties of dorsal horn neurons upon current injection with relatively long duration (>100 ms). However, our *in vitro* sacral cord preparation preserves the sensory afferents in the sacral dorsal roots. Therefore, it allows a direct delivery of natural sensory stimuli to dorsal horn neurons via dorsal root stimulation with much shorter duration (0.2 ms). Although blind patch methods have been implemented in the superficial dorsal horn *in vivo* in the adult spinal cord (Rank et al. 2015), it has not proved possible to implement blind patch methods in the deeper laminae.

However, it can be also argued that the burst, simple and tonic neurons in our findings may not represent three different types of DDH neurons. Instead these neurons may reflect different

firing modes or functional states of individual DDH neurons, specifically the wide dynamic range neurons, at the time of our observation. This argument is based on a previous study reporting that DDH neurons can switch their firing modes (i.e. tonic to plateau or rhythmic bursting patterns) depending on the balance of metabotropic glutamate (mGlu) and $GABA_B$ receptor controls (Derjean et al. 2003). However, without pharmacological manipulation of mGlu and $GABA_B$ receptors similar to that of Derjean et al (2003), we do not expect the drastic changes in the firing modes of DDH neurons during the recordings in our preparation.

Bursting DDH neurons could contribute to muscle spasms following SCI

Several aspects of the data suggest that the burst DDH neurons may contribute to the generation of muscle spasms that develop as the cord transitions from acute to chronic SCI. The burst neurons are capable of firing multiple spikes in response to a single-pulse stimulation (Fig. 1A, 2A, 3B, &4B), and they show longer burst duration upon an increased stimulus intensity (Fig. 3D&4D). Zolmitriptan was found to suppress long EPSPs and muscle spasms in both rats (Murray et al. 2011b) and humans (D'Amico et al. 2013) of chronic SCI. This selective 5-$HT_{1B/1D}$ agonist helps restore inhibition of exaggerated sensory transmission after SCI without affecting the intrinsic membrane properties of motoneurons (Murray et al. 2011b). Our study demonstrates that zolmitriptan suppresses the firing activity of the burst neurons following acute spinal transection (Fig. 4A) by reducing their evoked spike count (Fig. 4B), burst duration (Fig. 4D), and spontaneous firing rate (Fig. 4F). However, the drug has no significant effect on the other DDH neuron types (i.e. simple neurons; Fig. 6). For the mechanism of its action, zolmitriptan may activate 5-$HT_{1B/1D}$ receptors on the cell membranes of the burst neurons, as it has no significant effect on the field potential magnitude recorded from the vicinity of these neurons (Fig. 4C). However, we do not rule out the possibility that zolmitriptan also activates the

receptors on the presynaptic axon terminals of the sensory afferents, especially the unmyelinated C fibers (Li et al. 2016). Despite this uncertainty about the mechanism of this 5-$HT_{1B/1D}$ receptor agonist, our study suggests that the burst neurons could be one of the potential targets of its anti-spastic effect. In contrast, the burst neurons exhibit moderate facilitation of their firing activity via activation of NMDA receptors following acute spinal transection (Fig. 3A). NMDA enhances the burst duration (Fig. 3D) and spontaneous firing rate (Fig. 3F) of the burst neurons, despite slightly delaying their first-spike latency (Fig. 3E). As for zolmitriptan, NMDA does not significantly alter the firing activity of the other DDH neuron types (i.e. the simple neurons; Fig. 5). Also like zolmitriptan, NMDA may activate NMDA receptors on the cell membranes of the burst neurons, as there was an insignificant effect of NMDA on the field potential magnitude from the vicinity of the burst neurons (Fig. 3C). Therefore, our study suggests that activation of NMDA receptors may exacerbate muscle spasms by facilitating the burst neurons in contributing to muscle spasm mechanisms following SCI.

Thus an important goal of this study in acute spinal transection is to establish a baseline for investigating how these interneurons transition in their behavior from acute to chronic SCI. In this acute stage, dorsal root stimulation only evokes very short monosynaptic reflexes in our preparation (data not shown), not the long polysynaptic reflexes (LPRs) which are initiated by the long EPSPs in chronic SCI (Murray et al. 2011b). This is because the loss of descending serotonergic and noradrenergic tracts following the complete transection causes the excitability of motoneurons to plummet (Li et al. 2004a; Heckman et al. 2005; Miller et al. 1996), such that the potentially strong effects of the burst neurons cannot generate long-lasting motor output. The recovery of motoneuron excitability that occurs in the acute to chronic transition would allow the effect of the burst DDH neurons to have a major impact on motoneurons and serve as a contributor to the long-lasting EPSPs that trigger muscle spasms in the chronic stage (Murray et

al. 2011b). The assertion that long-lasting EPSPs trigger PICs and thus muscle spasms is a well established mechanism (Murray et al. 2011b; Baker and Chandler 1987; Bennett et al. 2004; Li et al. 2004a). However, this does not exclude other possibilities, for example, prolonged firing in other populations of spinal interneurons.

Do bursting DDH neurons exist in the intact cord?

In the intact spinal cord, 5-HT exerts its inhibitory effects on the transmission of group II or Aβ cutaneous afferent inputs by activating 5-HT_1 receptors located on the cell membranes of DDH neurons, especially those located in spinal lamina V. This deep-dorsal lamina receives a wide range of primary afferent inputs via glutamatergic synapses. These inputs include monosynaptic inputs from myelinated low-threshold group II (Aβ) and high-threshold group III (Aδ) afferents as well as polysynaptic inputs from unmyelinated high-threshold group IV (C) pain afferents (Brown 1982; Woolf 1987; Heise and Kayalioglu 2009). Moreover, lamina V contains the high density of raphespinal 5-HT terminals descending in the dorsolateral funiculus (Field et al. 1977; Brown 1982). As a result, lamina V neurons can play an important role in synaptic integration of somatosensory information, and most of them primarily provide ascending projections to the brain, for example, via the spinothalamic tract (Brown 1982). However, both projection neurons and interneurons of lamina V also have local connections to deeper laminae in the ventral horn via their axon collaterals for spinal reflex pathways, such as flexion withdrawal reflex (Brown 1982; Heise and Kayalioglu 2009; Schouenborg and Sjolund 1983). In terms of intrinsic membrane properties, the majority (~90%) of lamina V neurons in the rat dorsal horn can express plateau potentials (Derjean et al. 2003). Similar to those observed in motoneurons (Li and Bennett 2003; Harvey et al. 2006a; Li et al. 2007; Murray et al. 2011a) and commissural interneurons (Abbinanti et al. 2012), plateau potentials in lamina V neurons are driven by slowly

activating calcium currents through voltage-gated L-type Ca^{2+} channels (Morisset and Nagy 1998, 1999), which consequently amplify and prolong their responses to synaptic inputs. Moreover, these Ca^{2+}-driven plateau potentials are facilitated by activation of metabotropic glutamate receptors (Morisset and Nagy 1996) but suppressed by activation of metabotropic $GABA_B$ receptors (Voisin and Nagy 2001). As a result, it is possible that following SCI, loss of tonic 5-HT inhibition of lamina V neurons can reduce the threshold for generating plateau potentials in response to excitatory glutamatergic inputs from low-threshold group II or Aβ cutaneous afferents. Subsequently, the disinhibited lamina V neurons exhibit bursting behavior (i.e. becoming the bursting DDH neurons recorded in this study) and thus induce exaggerated long EPSPs in ventral horn motoneurons via polysynaptic connections (Jankowska et al. 2002). In addition to monoaminergic systems, loss of other descending inputs, such as the inotropic component of the reticulospinal system, may also contribute to the disinhibition of the DDH neurons following SCI. In this regard, it is important to note that the cutaneous inputs to motoneurons, which are likely relayed via DDH neurons, generate only short-lasting EPSPs in the intact cord in the decerebrate cats. Acute spinal transection immediately converts these short EPSPs to long-lasting ones (Baker and Chandler 1987). An important question for our further studies of DDH neurons is whether they maintain their propensity for generating bursts as the acute stage transitions to the chronic stage.

Deep dorsal horn is another potential target for SCI intervention

The SCI-induced plasticity of dorsal horn neurons remains relatively unstudied as a mechanism of spasms following SCI. A therapeutic strategy for muscle spasms that focuses on reduction of motoneuron excitability may not be suitable for most SCI patients who still possess some remaining motor function (D'Amico et al. 2013). This is because it would be even more difficult

for the preserved descending motor commands to activate motoneurons in the injured spinal cord (D'Amico et al. 2013). Therefore, an alternative strategy for this large group of SCI patients would be the restoration of inhibitory neuronal inputs to motoneurons via activation of G_i protein-coupled 5-HT_1 receptors on dorsal horn neurons (Murray et al. 2011b; D'Amico et al. 2013). Besides muscle spasms, an improvement in locomotion by restoring monoaminergic control in the injured spinal cord would be another potential strategy for treating SCI patients, as 5-HT and other monoamines, i.e. noradrenaline and dopamine, can control locomotor patterns in the spinal cord (Gordon and Whelan 2006).

Conclusions

Our study proposes the functional contribution of specific DDH neurons to muscle spasm mechanisms following SCI. By investigating the firing activity of DDH neurons following acute spinal transection, we show that DDH neurons exhibit distinct evoked and spontaneous firing characteristics, which can be categorized into, at least, three major types: burst, simple, and tonic neurons. The bursting behavior of the burst neurons likely contributes to muscle spasm mechanisms in response to natural sensory stimuli following SCI. We also show that administration of zolmitriptan and NMDA can elicit different responses from distinct DDH neuron types. When compared with controls, the burst neurons are the only DDH neurons that have significant changes in their firing activity during zolmitriptan and NMDA administration. Zolmitriptan suppresses the firing activity of the burst neurons, whereas NMDA moderately facilitates these neurons. These results suggest that zolmitriptan may exert an anti-spastic effect on the burst neurons via activation of 5-$HT_{1B/1D}$ receptors. In contrast, activation of NMDA receptors may facilitate the burst neurons in contributing to muscle spasm mechanisms following SCI.

Acknowledgement. We thank Mingchen Jiang for building and installing the recording chamber and Rochelle Bright for editing and proof reading. This work was supported by National Institute of Neurological Disorders and Stroke (NINDS) Grants NS047567 and NS089313 and Eunice Kennedy Shriver National Institute of Child Health and Human Development (NICHD) Grant HD084672.

III. THE FIRING CHARACTERISTICS OF BURSTING DEEP DORSAL HORN NEURONS FOLLOWING CHRONIC SPINAL TRANSECTION DURING ADMINISTRATION OF AGONISTS FOR 5-$HT_{1B/1D}$ AND NMDA RECEPTORS

Abstract. Loss of descending serotonin (5-HT) to the spinal cord contributes to muscle spasms at the chronic stage of spinal cord injury (SCI). Hyperexcitable motoneurons receive long excitatory postsynaptic potentials (EPSPs) which, in turn, activate their persistent inward currents to drive muscle spasms. Deep dorsal horn (DDH) neurons with bursting behavior could be involved in triggering the long EPSPs due to their loss of inhibition in the chronically 5-HT-deprived spinal cord. Previously, in an acutely transected preparation, we found that bursting DDH neurons were significantly affected by administration of the 5-$HT_{1B/1D}$ receptor agonist zolmitriptan, which suppressed their bursts, and by NMDA, which enhanced their bursting behavior. Non-bursting DDH neurons were not influenced by these agents. In the present study, we investigate the firing characteristics of the bursting DDH neurons following chronic spinal transection at T10 vertebral level in adult mice. Terminal experiments using our standard *in vitro* preparation of the sacral cord were carried out ~10 weeks post-transection. Compared with the acute spinal stage of our previous study, DDH neurons in the chronic stage were slightly more excitable. The suppressive effects of zolmitriptan were stronger, but the facilitative effects of NMDA were weaker. These results further support the contribution of the bursting DDH neurons to muscle spasm mechanisms following SCI.

INTRODUCTION

Reduction of raphespinal serotonin (5-HT) fibers can drive exaggerated sensory transmission and thus muscle spasms in the chronically transected spinal cord (Hadjiconstantinou et al. 1984; Murray et al. 2010; Baker and Chandler 1987; Bennett et al. 2004; Li et al. 2004a). At this chronic stage of spinal cord injury (SCI), long-lasting excitatory postsynaptic potentials (long EPSPs) activate persistent inward currents (PICs) of hyperexcitable motoneurons to trigger muscle spasms (Bennett et al. 2004; Li et al. 2004a). However, zolmitriptan, which is a selective 5-$HT_{1B/1D}$ receptor agonist, can suppress long EPSPs and muscle spasms in chronic SCI rats, without affecting PICs intrinsic to motoneurons (Murray et al. 2011b). Our previous study in the acute spinal stage suggests that these long EPSPs may be mediated by deep dorsal horn (DDH) neurons that exhibit burst firing, as zolmitriptan can suppress the bursting behavior of these DDH neurons while not affecting non-bursting neighbors (Thaweerattanasinp et al. 2016). While lacking 5-HT, the spinal cord still produces glutamate for NMDA receptor-mediated locomotion following SCI (Chau et al. 2002; Giroux et al. 2003). In contrast to zolmitriptan, NMDA can moderately facilitate the firing properties of the bursting DDH neurons in the acutely transected spinal cord (Thaweerattanasinp et al. 2016), possibly for generation of long EPSPs following SCI.

As a sequel to our previous study in acute spinal transection (Thaweerattanasinp et al. 2016), we further characterize the firing properties of the bursting DDH neurons following chronic spinal transection at T10 vertebral level. Using the *in vitro* sacral cord preparation and extracellular electrophysiology, we examine their responses to dorsal root stimulation during administration of zolmitriptan and NMDA following the 10-week period of transection recovery. Then, we compare the firing properties of the burst neurons with their counterparts from the acute transection study for all drug conditions. From acute to chronic stages of spinal transection, the

burst neurons become slightly more excitable but more sensitive to inhibition by zolmitriptan administration. In contrast, the NMDA-induced facilitation seen in the acute spinal stage is reduced in the chronic stage. Therefore, the current study in chronic spinal transection provides more evidence to support the contribution of bursting DDH neurons to generation of long EPSPs and muscle spasms following SCI.

MATERIALS AND METHODS

Animal models

Adult mice (C57BL/6; aged > 8 weeks; *N* = 55) received complete spinal transection at T10 vertebral level, which corresponds to T11-T12 spinal segments. The animals were allowed to recover from the injury for 10 weeks during which they were subject to a weekly assessment of locomotor recovery based on the Basso, Beattie, Bresnahan (BBB) Locomotor Rating Scale (Basso et al. 1995). Only the animals that exhibited little or no hindlimb movement with some isolated joint movements (BBB score ≤ 7; Basso et al. 1995) were selected (*N* = 30) for the sacral cord preparation and extracellular recordings of DDH neurons. All experimental procedures were reviewed and approved by the Institutional Animal Care and Use Committee of Northwestern University and were in accordance with the National Institute of Health Guide for the Care and Use of Laboratory Animals.

Sacral cord preparation and experimental protocol

The same procedures of sacral cord preparation and experimental protocols were used in the current study as in the acute transection study (see details in Chapter 2 or Thaweerattanasinp et al. 2016). Briefly, the whole sacral cord (S1-S3) was removed from the chronically injured

animals with a secondary complete transection at the junction of L6 and S1 spinal segments. Then, the isolated sacral cord was maintained *in vitro* in a recording chamber for extracellular recordings of DDH neurons and ventral roots. Electrode penetration was made at the dorsal surface of the sacral cord for locating the electrode tips in the vicinity of DDH neurons at 100-500 μm from the dorsal surface. At a given stimulus intensity, the corresponding sacral dorsal roots were electrically stimulated 5 times at intervals of 30 seconds for four stimulus intensities (i.e. 1X, 2X, 5X, and 10X). Bath administration of NMDA (15 and 20 μM) and zolmitriptan (1 μM) was used to study the drug effects on the firing properties of DDH neurons in response to dorsal root stimulation.

Data analysis

The same data analysis protocol was used in the current study as in the acute transection study (see details in Chapter 2 or Thaweerattanasinp et al. 2016) to measure evoked spike count, field potential, burst duration (for the burst neurons), first-spike latency, and spontaneous firing rate for the firing properties of DDH neurons. In addition, field latency was measured from the time difference between the stimulus onset and the onset of the field potential, specifically for the burst neurons in both acute and chronic transection studies. Only the non-zero values of field latency were used for statistical analyses.

Because of the unbalanced data sets, a two-way unbalanced ANOVA via multiple regression analysis ($\alpha = 0.05$) was used for all comparisons of the firing properties from DDH neuron types, drug conditions, or recovery periods from the spinal transection at four stimulus intensities. If necessary, a post-hoc pairwise comparison (*t*-test) of group means ($\alpha = 0.05$) with the Bonferroni correction was further used to specify significant differences.

Figure 7. Firing properties of the simple and burst neurons following chronic spinal transection. *A*: Distribution of the simple and burst neurons as incidence (%) across various depths measured from the dorsal surface (*N* = 61). *B-E*: group data comparing firing properties (mean ± SEM) of the burst (♦) and simple (■) neurons in response to increasing stimulus intensity in control. *B*: evoked spike count for the burst (*N* =49) and simple (*N* = 9) neurons. *C*: field potential for the burst (*N* = 49) and simple (*N* = 9) neurons. *D*: first-spike latency (only nonzero values) for the burst (*N* =49; except *N* = 46 at 1X) and simple (*N* = 9; except *N* = 7 at 1X) neurons. *E*: spontaneous firing rate for the burst (*N* = 49) and simple (*N* = 9) and neurons. Significant difference from the simple neuron (†$P < 0.001$) using a two-way unbalanced ANOVA.

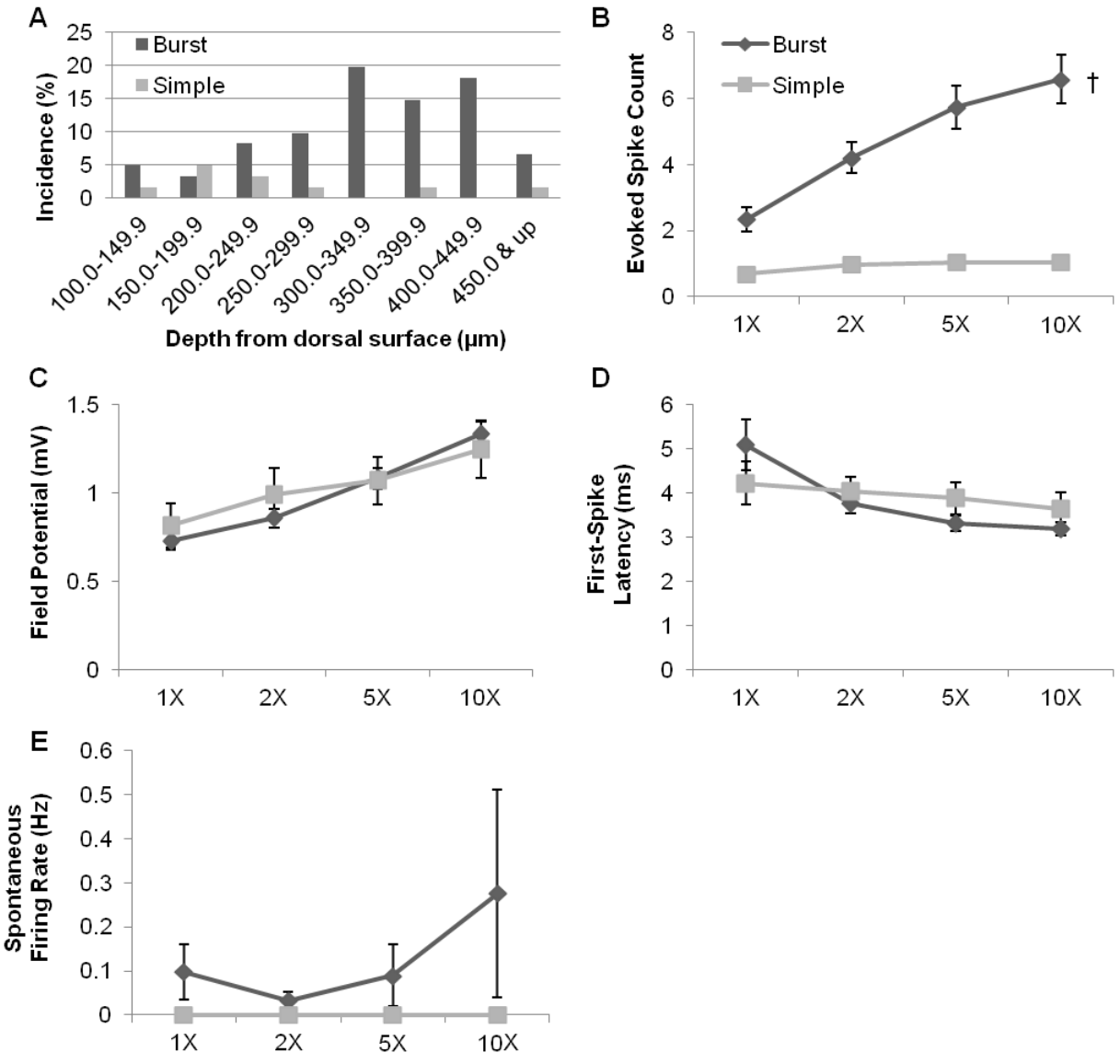
A
Incidence (%)
25
20
15
10
5
0
Burst
Simple
100.0-149.9
150.0-199.9
200.0-249.9
250.0-299.9
300.0-349.9
350.0-399.9
400.0-449.9
450.0 & up
Depth from dorsal surface (µm)
B
Evoked Spike Count
8
6
4
2
0
Burst
Simple
†
1X
2X
5X
10X
C
Field Potential (mV)
1.5
1
0.5
0
1X
2X
5X
10X
D
First-Spike Latency (ms)
6
5
4
3
2
1
0
1X
2X
5X
10X
E
Spontaneous Firing Rate (Hz)
0.6
0.5
0.4
0.3
0.2
0.1
0
1X
2X
5X
10X

RESULTS

62 DDH neurons were recorded from 30 adult mice with chronic spinal transection via extracellular recordings. Fifty of these DDH neurons from 24 adult mice were investigated during the bath administration of either NMDA (*N* = 27) or zolmitriptan (*N* = 23). We analyzed the same four firing property parameters of DDH neuron as in the acute transection study (Thaweerattanasinp et al. 2016): evoked spike count; field potential; first-spike latency; and spontaneous firing rate.

Firing response types of DDH neurons following chronic spinal transection

As in the acute transection study, the same three firing response types of DDH neurons were found upon single-pulse (0.2 ms) dorsal root stimulation: the burst (*N* = 52), simple (*N* = 9), and tonic (*N* = 1) neurons. The only tonic neuron was excluded from further analyses. Figure 7 demonstrates the statistical analyses of the firing properties of the burst and simple neurons in control, along with their depth distribution in the dorsal horn (Fig. 7A). We could not compare whether there was a change in the proportion of the burst and simple neurons from acute to chronic transection because we purposefully sought out the burst neurons following chronic transection.

Similar to those in the acute transection study, the burst neurons (4.71 ± 0.31 spikes) fired more evoked spikes than the simple (0.94 ± 0.04 spikes) neurons in response to dorsal root stimulation (Fig. 7B; two-way unbalanced ANOVA, $p = 5.38 \times 10^{-8}$). However, more intense stimulation did not evoke more spikes from DDH neurons as a group ($p = .08$). Also, there was no significant interaction between DDH neuron type and stimulus intensity ($p = .19$), indicating

the similar responses of the burst and simple neurons to activation of low- versus high-threshold afferents.

Field potentials (Fig. 7C) from the vicinity of the burst and simple neurons were not significantly different in magnitude from each other (p = .68), while more intense stimulation did evoke larger field potentials ($p = 1.47 \times 10^{-5}$). There was no significant interaction between DDH neuron type and stimulus intensity (p = 0.72). These results suggest that the burst and simple neurons are located in close proximity of each other in the dorsal horn.

First-spike latency (Fig. 7D) was not significantly different between the burst and simple neurons (p = .80). More intense stimulation could not evoke faster responses from DDH neurons (p = .16), nor was there a significant interaction between DDH neuron type and stimulus intensity (p = .61). This lack of relation between DDH neuron type and response speed contrasts with our results in the acute transection study, where the simple neurons responded most rapidly to the dorsal root stimulation (Thaweerattanasinp et al. 2016). These differing results suggest that rewiring of the sensory afferent connection to the DDH neurons may occur over time following SCI.

Lastly, spontaneous firing rate (Fig. 7E) was not significantly different between the burst and simple neurons (p = .41). Stimulus intensity did not significantly affect the spontaneous firing rate (p = .95), nor was there a significant interaction between DDH neuron type and stimulus intensity (p = .95). Thus, these results indicate that the burst and simple neurons did not contribute significantly background activity in the dorsal horn.

Taken together, these results (Fig.7B-E) demonstrated that DDH neurons with different firing characteristics continue to exist in the dorsal horn following chronic spinal transection, similar to

the acute transection study. The bursting behavior of the burst neurons makes them the potential contributor to muscle spasms mechanisms following chronic SCI.

Figure 8. Comparisons of the firing properties of the burst neurons following acute and chronic spinal transection. *A*-*F*: Group data comparing firing properties (mean ± SEM) of the burst neurons following acute (♦) and chronic (■) spinal transection in response to increasing stimulus intensity in control. *A*: evoked spike count for acute (*N* =96; except *N* = 95 at 10X) and chronic (*N* = 49 for all intensities) spinal transection. *B*: field potential for acute (*N* =96; except *N* = 95 at 10X) and chronic (*N* = 49 for all intensities) spinal transection. *C*: field latency (only nonzero values) for acute (*N* = 65, 1X; *N* = 93, 2X; *N* = 96, 5X; *N* = 94, 10X) and chronic (*N* = 49 for all intensities) spinal transection. *D*: burst duration for acute (*N* =96; except *N* = 95 at 10X) and chronic (*N* = 49 for all intensities) spinal transection. *E*: first-spike latency (only nonzero values) for acute (*N* = 64, 1X; *N* = 92, 2X; *N* = 96, 5X; *N* = 94, 10X) and chronic (*N* =49; except *N* = 46 at 1X) spinal transection. *F*: spontaneous firing rate for acute (*N* =96; except *N* = 95 at 10X) and chronic (*N* = 49 for all intensities) spinal transection. *G*-*H*: distribution comparisons between the burst neurons following acute (*N* =96) and chronic (*N* = 49) spinal transection as plots of mean field potential (*G*) and field latency (*H*) against depths measured from the dorsal surface. Significant difference (*$P < 0.05$; †$P < 0.01$; ‡$P < 0.001$) using a two-way unbalanced ANOVA.

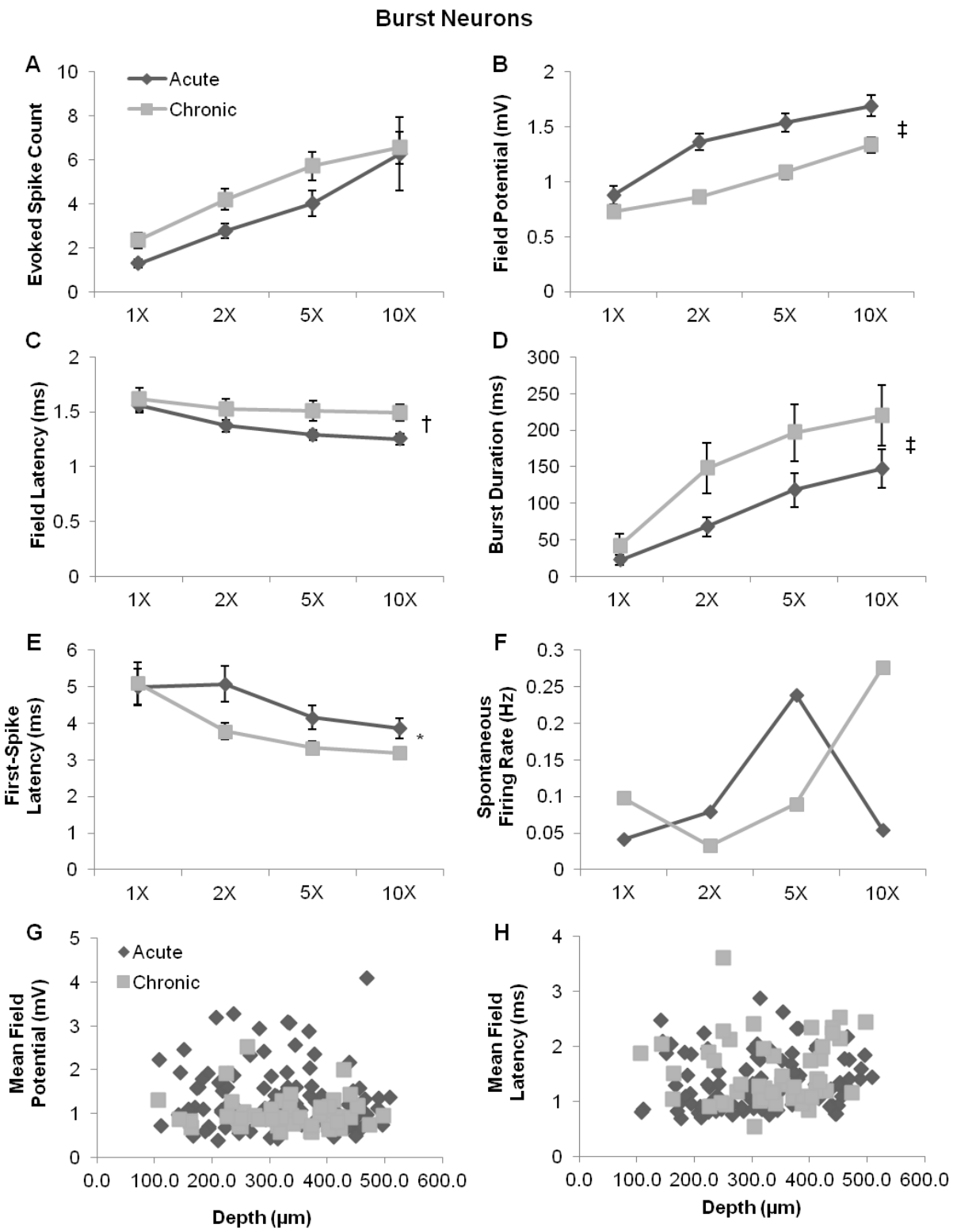
Burst Neurons
A
Evoked Spike Count
Acute
Chronic
1X
2X
5X
10X
B
Field Potential (mV)
‡
C
Field Latency (ms)
†
D
Burst Duration (ms)
‡
E
First-Spike Latency (ms)
*
F
Spontaneous Firing Rate (Hz)
G
Mean Field Potential (mV)
Depth (µm)
H
Mean Field Latency (ms)
Depth (µm)

Burst neurons become more excitable over time following SCI.

In our study of DDH neurons following acute transection, only the burst neurons had significant changes in their firing activity during administration of NMDA and zolmitriptan (Thaweerattanasinp et al. 2016). As a result, we focus on the effects of both drugs on the burst neurons following chronic spinal transection and the comparisons with their counterparts in the acute transection study. In addition to the four firing property parameters (see the previous section), we also measured burst duration and field latency specifically for the burst neurons. Compared with those in the acute transection study, the burst neurons become slightly more excitable following chronic spinal transection (Fig. 8).

In response to dorsal root stimulation, the burst neurons in chronic transection did not significantly fire more evoked spikes than those in acute transection (Fig. 8A; two-way unbalanced ANOVA, $p = .090$). There was a tendency for more evoked spikes as stimulation intensity increased ($p = 1.04 \times 10^{-5}$), but this tendency did not differ between the two stages. Nor was spontaneous firing rate (Fig. 8F) significantly different between the burst neurons in acute and chronic transection ($p = .78$). However, the burst neurons in chronic transection (151.66 ± 17.61 ms) did have significantly longer burst duration (Fig. 8D) than those in acute transection (88.95 ± 9.78 ms; $p = 5.41 \times 10^{-4}$). The response latency of the first spike in the chronic stage (3.85 ± 0.17 ms) was also shorter than the latency in acute stage (4.51 ± 0.20 ms) in response to dorsal root stimulation (Fig. 8E; $p = .023$). In both acute and chronic stages, increasing stimulus intensity increased burst duration ($p = 1.39 \times 10^{-8}$) and faster responses ($p = .001$). These results suggest the increased excitability of the burst neurons over time following SCI.

The field potentials from the vicinity of the burst neurons in chronic transection (1.00 ± 0.03 mV) were significantly smaller in magnitude (Fig. 8B) than those in acute transection (1.37 ± 0.05

mV; $p = 8.51 \times 10^{-9}$). Field potentials in chronic transection (1.53 ± 0.05 ms) was also significantly slower in latency (Fig. 8C) than that in acute transection (1.37 ± 0.03 ms; $p = .001$). In both acute and chronic stages, more intense stimulation could elicit larger ($p = 2.88 \times 10^{-14}$) and faster ($p = .018$) field potentials from the vicinity of the whole samples. These results reflect changes in the synaptic transmission and circuitry surrounding the burst neurons over time following SCI, with the center of neural activity approximately at 200-400 μm deep from the dorsal surface as suggested by the distributions of mean field potential (Fig. 8G) and field latency (Fig. 8H) of the burst neurons in acute and chronic spinal transection.

Taken together, these results (Fig.8A-F) demonstrated that the burst neurons become slightly more excitable with longer burst duration and faster responses to dorsal root stimulation, as the spinal transection transitions from acute to chronic stages. The slight increase in the excitability of the burst neurons could facilitate the generation of long EPSPs and muscle spasms following chronic SCI. However, with smaller field potential and slower field latency, some neural plasticity may occur in response to the increased excitability of the burst neurons following chronic SCI.

Figure 9. Effects of NMDA on the firing properties of the burst neurons following chronic spinal transection. *A*: Representative recording traces showing the effect of NMDA (bottom) on a burst neuron, compared with that in control (top), upon dorsal root stimulation (0.2 ms; arrow). *B-G*: group data showing the effects of NMDA (■) on the firing properties (mean ± SEM) of the burst neurons in response to increasing stimulus intensity, compared with those during control (♦) and washout (▲) conditions. *B*: evoked spike count during control (*N* = 20 for all intensities), NMDA (*N* =21; except *N* = 23 at 10X), and washout (*N* = 18 for all intensities) conditions. *C*: field potential during control (*N* = 20 for all intensities), NMDA (*N* =21; except *N* = 23 at 10X), and washout (*N* = 18 for all intensities) conditions. *D*: field latency (only nonzero values) during control (*N* = 20 for all intensities), NMDA (*N* =21; except *N* = 23 at 10X), and washout (*N* = 18 for all intensities) conditions. *E*: burst duration during control (*N* = 20 for all intensities), NMDA (*N* =21; except *N* = 23 at 10X), and washout (*N* = 18 for all intensities) conditions. *F*: first-spike latency (only nonzero values) during control (*N* =20; except *N* = 19 at 1X), NMDA (*N* = 18, 1X; *N* = 19, 2X; *N* = 21, 5X; *N* = 23, 10X), and washout (*N* = 16, 1X; *N* = 15, 2X; *N* = 18, 5X&10X) conditions. *G*: spontaneous firing rate during control (*N* = 20 for all intensities), NMDA (*N* =21; except *N* = 23 at 10X), and washout (*N* = 18 for all intensities) conditions. Significant difference from control (*$P < 0.017$) and washout (†$P < 0.017$) conditions using a post-hoc pairwise comparison (*t*-test) of group means with the Bonferroni correction.

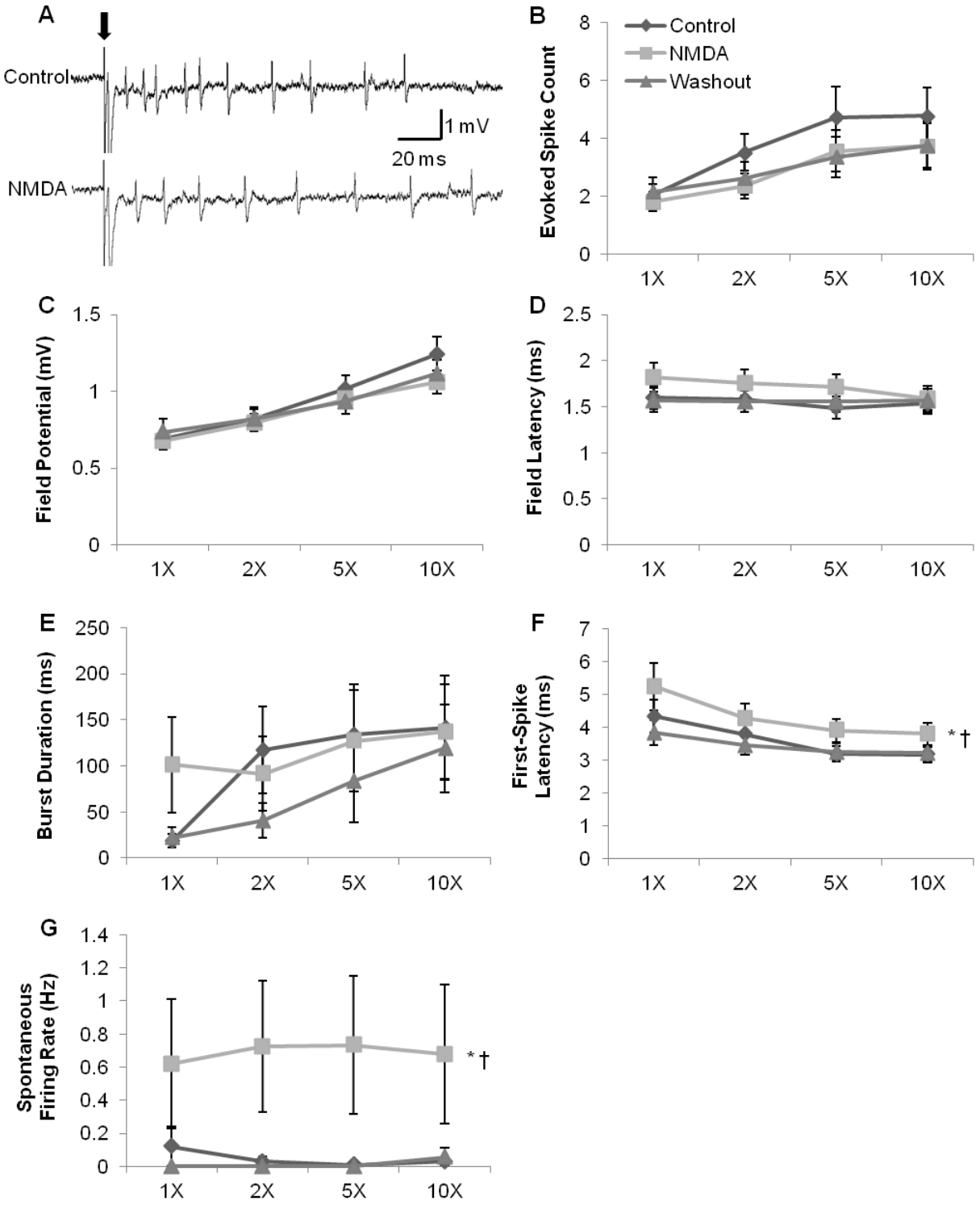
A
Control
NMDA
1 mV
20 ms
B
Control
NMDA
Washout
Evoked Spike Count
1X
2X
5X
10X
C
Field Potential (mV)
D
Field Latency (ms)
E
Burst Duration (ms)
F
First-Spike Latency (ms)
*†
G
Spontaneous Firing Rate (Hz)
*†

Figure 10. Comparisons of NMDA effects on the firing properties of the burst neurons following acute and chronic spinal transection. *A*-*F*: Group data comparing absolute changes from controls of NMDA effects (i.e. 15 μM NMDA minus control; mean ± SEM) on the firing properties of the burst neurons following acute (♦) and chronic (■) spinal transection in response to increasing stimulus intensity. *A*: evoked spike count for acute (*N* = 21 for all intensities) and chronic (*N* = 20 for all intensities) spinal transection. *B*: field potential for acute (*N* = 21 for all intensities) and chronic (*N* = 20 for all intensities) spinal transection. *C*: field latency for acute (*N* = 16, 1X; *N* = 19, 2X; *N* = 21, 5X&10X) and chronic (*N* = 20 for all intensities) spinal transection. *D*: burst duration for acute (*N* = 21 for all intensities) and chronic (*N* = 20 for all intensities) spinal transection. *E*: first-spike latency for acute (*N* = 12, 1X; *N* = 19, 2X; *N* = 20, 5X&10X) and chronic (*N* = 17, 1X; *N* = 18, 2X; *N* = 20, 5X&10X) spinal transection. *F*: spontaneous firing rate for acute (*N* = 21 for all intensities) and chronic (*N* = 20 for all intensities) spinal transection. Significant difference (*$P < 0.05$; †$P < 0.01$; ‡$P < 0.001$) using a two-way unbalanced ANOVA.

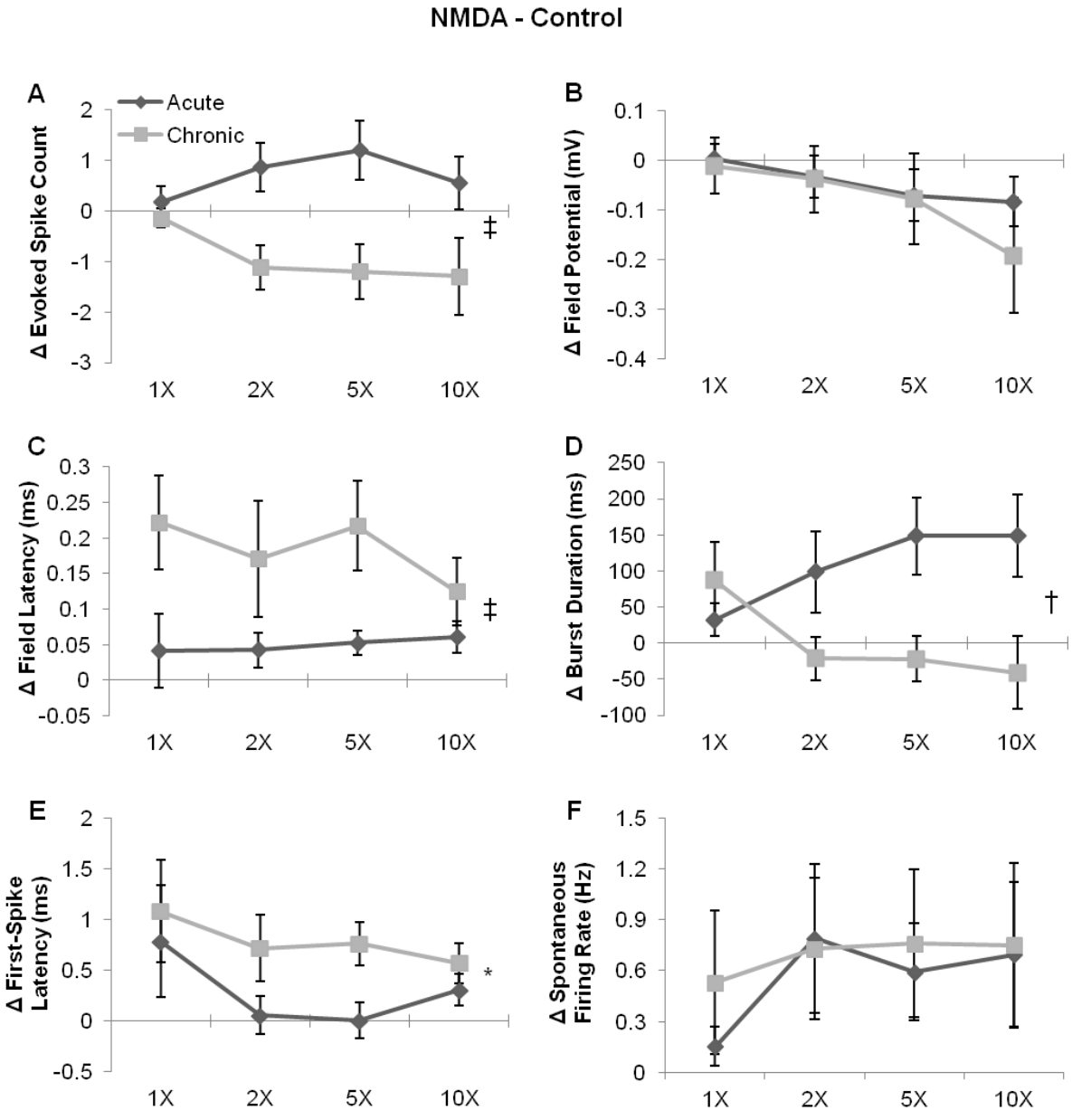
NMDA - Control
A
Acute
Chronic
Δ Evoked Spike Count
2
1
0
-1
-2
-3
‡
1X
2X
5X
10X
B
Δ Field Potential (mV)
0.1
0
-0.1
-0.2
-0.3
-0.4
1X
2X
5X
10X
C
Δ Field Latency (ms)
0.3
0.25
0.2
0.15
0.1
0.05
0
-0.05
‡
1X
2X
5X
10X
D
Δ Burst Duration (ms)
250
200
150
100
50
0
-50
-100
†
1X
2X
5X
10X
E
Δ First-Spike Latency (ms)
2
1.5
1
0.5
0
-0.5
*
1X
2X
5X
10X
F
Δ Spontaneous Firing Rate (Hz)
1.5
1.2
0.9
0.6
0.3
0
1X
2X
5X
10X

NMDA facilitates the burst neurons but with weaker effects over time following SCI.

Of a total number of 52 burst neurons, 23 neurons were studied during the bath administration of NMDA (*N* = 21 at 15 μM; *N* = 2 at 20 μM). The combined effects of both concentrations were described on the six parameters of the burst neuron firing properties following chronic spinal transection (Fig. 9). NMDA slightly facilitated the firing properties of the burst neurons (Fig. 9A) following chronic spinal transection as follows.

Similar to acute transection study, NMDA had no significant effect on the evoked spike count of the burst neurons (Fig. 9B; two-way unbalanced ANOVA; $p = .13$). The drug also had no significant effects on the field potential magnitude (Fig. 9C; $p = .38$) and latency (Fig. 9D; $p = .31$) from the vicinity of the burst neurons. However, more intense stimulation increased evoked spike count ($p = 7.45 \times 10^{-4}$) and field potential magnitude ($p = 5.16 \times 10^{-11}$) during NMDA administration, without significantly affecting field latency ($p = .81$). Unlike our acute transection study, NMDA had no significant effect on the burst duration of the burst neurons (Fig. 9E; $p = .31$), and stimulus intensity did not significantly affect burst duration ($p = .10$).

But NMDA did have a significant effect on the first-spike latency of the burst neurons (Fig. 9F; $p = .004$). Similarly to the acute transection study, NMDA delayed the first-spike latency of the burst neurons (4.30 ± 0.24 ms), compared with control (3.62 ± 0.18 ms; Bonferroni-corrected pairwise *t*-test, $p = .011$) and washout (3.44 ± 0.14 ms; $p = .002$). More intense stimulation could evoke faster responses from the burst neurons ($p = .003$), but not on the whole samples of DDH neurons (see *Firing response types of DDH neurons following chronic spinal transection*). Lastly, NMDA continued to have a significant effect on the spontaneous firing rate of the burst neurons (Fig. 9G; $p = 1.85 \times 10^{-4}$). Similar to acute transection study, NMDA significantly increased the spontaneous firing rate of the burst neurons (0.69 ± 0.20 Hz), compared with

control (0.05 ± 0.03 Hz; $p = 4.20 \times 10^{-4}$) and washout (0.01 ± 0.01 Hz; $p = 3.09 \times 10^{-4}$). Stimulus intensity did not significantly affect the spontaneous firing rate of the burst neurons ($p = 1.00$). These results support that NMDA helps raise the spontaneous firing rate of the burst neurons, similar to the acute transection study.

The facilitative effects of NMDA become weaker on the burst neurons as the spinal transection transitions from acute to chronic stages (Fig. 10). This is revealed by statistical comparisons between the firing property parameters in the current study and their counterparts in acute transection study during 15 μM NMDA administration, in each case measured as absolute changes from control conditions. Because of a large number of data with zero values in control conditions, absolute changes were used instead of relative changes for the comparisons of the drug effects with the baselines between acute and chronic transection studies. However, it is important to note that relative values are not the same as absolute values, thus possibly reaching different conclusions based on different calculation methods.

NMDA enhanced the evoked spike count of the burst neurons (Fig. 10A) in acute transection (0.70 ± 0.24 spikes) significantly more than that in chronic transection (-0.94 ± 0.26 spikes; two-way unbalanced ANOVA, $p = 9.07 \times 10^{-6}$). The drug also enhanced the burst duration of the burst neurons (Fig. 10D) in acute transection (107.01 ± 24.97 ms) significantly more than that in chronic transection (0.67 ± 21.74 ms; $p = .002$). However, NMDA delayed the field latency from the vicinity of the burst neurons (Fig. 10C) in chronic transection (0.18 ± 0.03 ms) significantly more than that in acute transection (0.05 ± 0.01 ms; $p = 3.23 \times 10^{-4}$). In addition, the drug delayed the first-spike latency of the burst neurons (Fig. 10E) in chronic transection (0.78 ± 0.16 ms) significantly more than that in acute transection (0.29 ± 0.13 ms; $p = .018$). There were no significant differences in the NMDA effects on the field potential (Fig. 10B; $p = .48$) from the

vicinity of the burst neurons, or on the spontaneous firing rate (Fig. 10F; $p = .63$) of the burst neurons in acute transection from those in chronic transection.

Taken together, these results (Fig. 9A-G) demonstrated that NMDA slightly facilitates the firing properties of the burst neurons following chronic spinal transection by enhancing only spontaneous firing rate, albeit delaying first-spike latency, when compared with controls. Although NMDA facilitates the burst neurons, its facilitative effects become weaker over time following SCI (Fig. 10A-F). The drug enhances evoked spike count and burst duration to a lesser degree and even delays field latency and first-spike latency to a greater degree as the spinal transection transitions from acute to chronic stages.

Figure 11. Effects of zolmitriptan on the firing properties of the burst neurons following chronic spinal transection. *A*: Representative recording traces showing the effect of zolmitriptan (bottom) on a burst neuron, compared with that in control (top), upon dorsal root stimulation (0.2 ms; arrow). *B*-*G*: group data showing the effects of zolmitriptan (■) on the firing properties (mean ± SEM) of the burst neurons in response to increasing stimulus intensity, compared with those during control (♦) and washout (▲) conditions. *B*: evoked spike count during control (*N* = 23 for all intensities), zolmitriptan (same as control), and washout (*N* = 21 for all intensities) conditions. *C*: field potential during control (*N* = 23 for all intensities), zolmitriptan (same as control), and washout (*N* = 21 for all intensities) conditions. *D*: field latency (only nonzero values) during control (*N* = 23 for all intensities), zolmitriptan (same as control), and washout (*N* = 21 for all intensities) conditions. *E*: burst duration during control (*N* = 23 for all intensities), zolmitriptan (same as control), and washout (*N* = 21 for all intensities) conditions. *F*: first-spike latency (only nonzero values) during control (*N* =23; except *N* = 21 at 1X), zolmitriptan (*N* = 15, 1X; *N* = 20, 2X; *N* = 21, 5X; *N* = 20, 10X), and washout (*N* = 15, 1X; *N* = 18, 2X; *N* = 19, 5X&10X) conditions. *G*: spontaneous firing rate during control (*N* = 23 for all intensities), zolmitriptan (*N* = 22 for all intensities), and washout (*N* = 21 for all intensities) conditions. Significant difference from zolmitriptan (*$P < 0.017$) and washout (†$P < 0.017$) conditions using a post-hoc pairwise comparison (*t*-test) of group means with the Bonferroni correction.

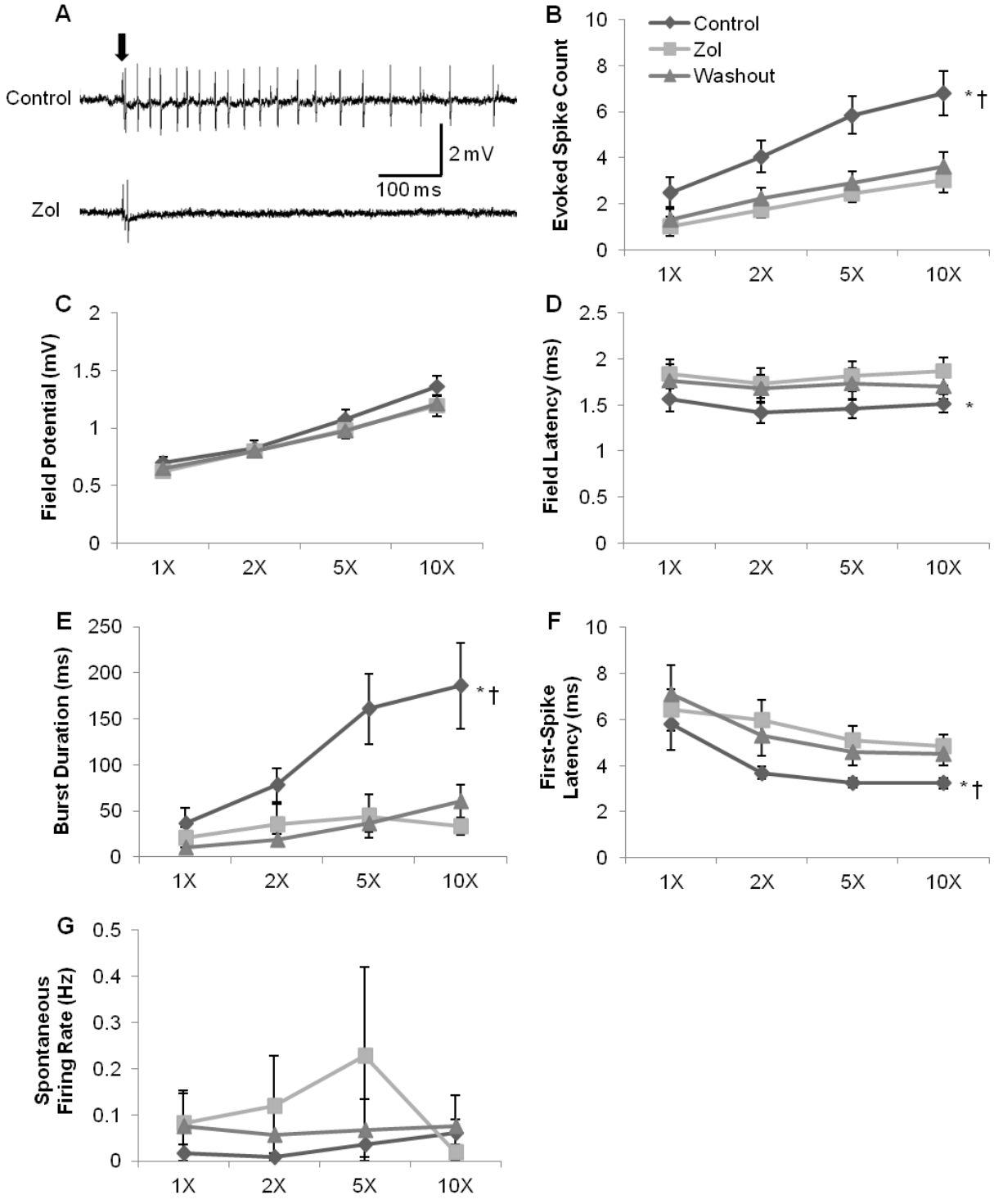
A
Control
Zol
2 mV
100 ms
B
Control
Zol
Washout
Evoked Spike Count
*†
C
Field Potential (mV)
D
Field Latency (ms)
*
E
Burst Duration (ms)
*†
F
First-Spike Latency (ms)
*†
G
Spontaneous Firing Rate (Hz)
1X
2X
5X
10X

Figure 12. Comparisons of zolmitriptan effects on the firing properties of the burst neurons following acute and chronic spinal transection. *A*-*F*: Group data comparing absolute changes from controls of zolmitriptan effects (i.e. zolmitriptan minus control; mean ± SEM) on the firing properties of the burst neurons following acute (♦) and chronic (■) spinal transection in response to increasing stimulus intensity. *A*: evoked spike count for acute (*N* =24; except *N* = 25 at 10X) and chronic (*N* = 23 for all intensities) spinal transection. *B*: field potential for acute (*N* =24; except *N* = 25 at 10X) and chronic (*N* = 23 for all intensities) spinal transection. *C*: field latency for acute (*N* = 16, 1X; *N* = 22, 2X; *N* = 23, 5X; *N* = 24, 10X) and chronic (*N* = 23 for all intensities) spinal transection. *D*: burst duration for acute (*N* =24; except *N* = 25 at 10X) and chronic (*N* = 23 for all intensities) spinal transection. *E*: first-spike latency for acute (*N* = 16, 1X; *N* = 21, 2X; *N* = 22, 5X; *N* = 21, 10X) and chronic (*N* = 14, 1X; *N* = 20, 2X; *N* = 21, 5X; *N* = 20, 10X) spinal transection. *F*: spontaneous firing rate for acute (*N* =24; except *N* = 25 at 10X) and chronic (*N* = 22 for all intensities) spinal transection. Significant difference (**P* < 0.05; †*P* < 0.01; ‡*P* < 0.001) using a two-way unbalanced ANOVA.

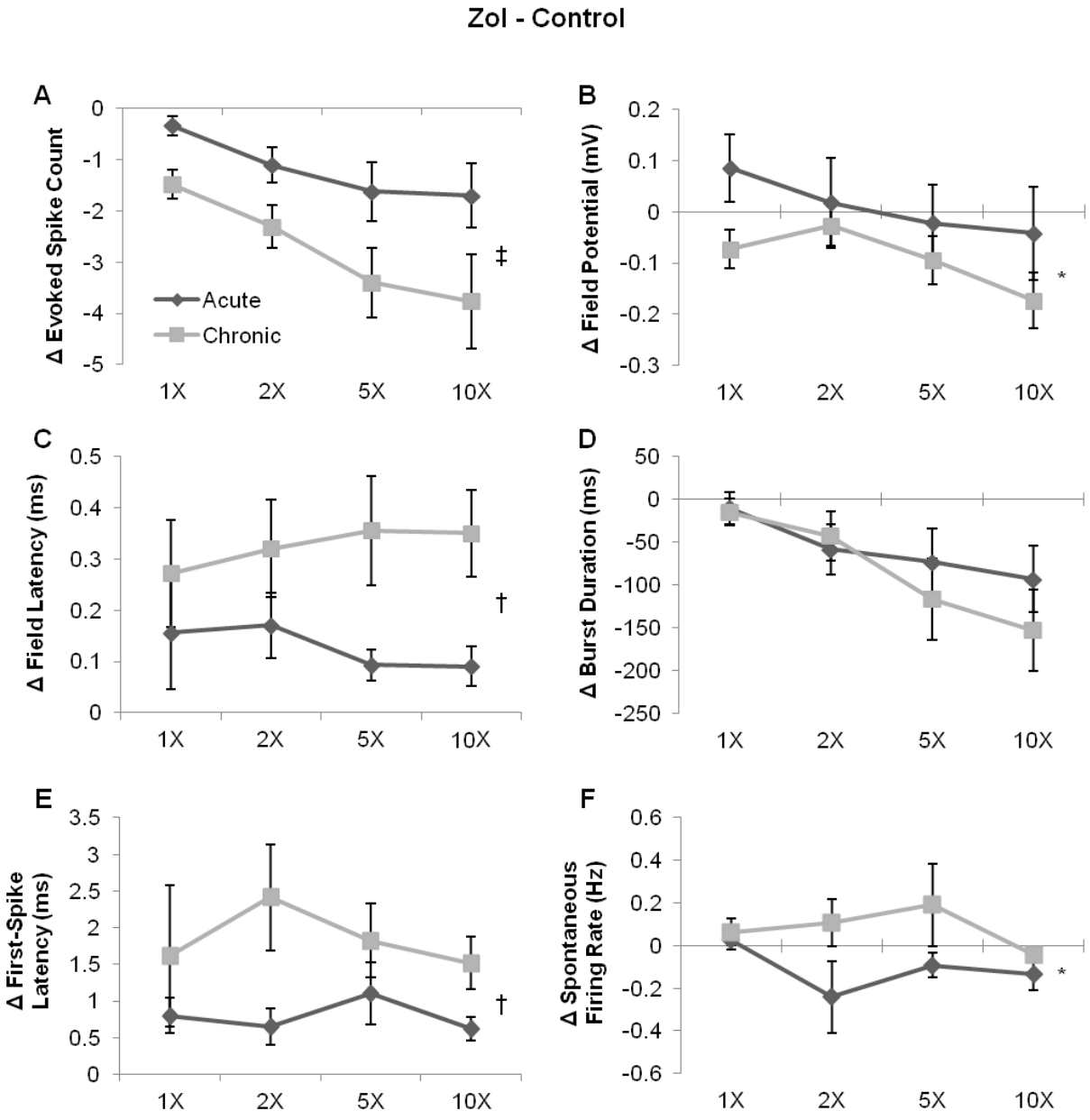
ZoI - Control
A
Δ Evoked Spike Count
0
-1
-2
-3
-4
-5
Acute
Chronic
‡
1X
2X
5X
10X
B
Δ Field Potential (mV)
0.2
0.1
0
-0.1
-0.2
-0.3
*
C
Δ Field Latency (ms)
0.5
0.4
0.3
0.2
0.1
0
†
D
Δ Burst Duration (ms)
50
0
-50
-100
-150
-200
-250
E
Δ First-Spike Latency (ms)
3.5
3
2.5
2
1.5
1
0.5
0
F
Δ Spontaneous Firing Rate (Hz)
0.6
0.4
0.2
0
-0.2
-0.4
-0.6

Zolmitriptan suppresses the burst neurons with stronger effects over time following SCI.

Of a total number of 52 burst neurons, 23 neurons were studied for their firing properties during the bath administration of zolmitriptan (1 μM; Fig. 11). Similar to our acute transection study (Thaweerattanasinp et al. 2016), there were no significant differences in all the firing properties between zolmitriptan and washout conditions because of the difficulty in washing out the drug (also reported in Murray et al. 2011b). But in the chronic transection study, we performed the recording protocol with zolmitriptan administration in only one burst neuron from each animal. Zolmitriptan suppressed the firing properties of the burst neurons (Fig. 11A) following chronic spinal transection as follows.

Similar to the acute transection study, zolmitriptan significantly decreased the evoked spike count of the burst neurons (Fig. 11B; two-way unbalanced ANOVA, $p = 3.37 \times 10^{-10}$; 2.06 ± 0.22 spikes), compared with control (4.80 ± 0.43 spikes; Bonferroni-corrected pairwise *t*-test, $p = 5.50 \times 10^{-10}$). Zolmitriptan also significantly decreased the burst duration of the burst neurons (Fig. 11E; $p = 5.65 \times 10^{-8}$; 33.43 ± 8.77 ms), compared with control (115.17 ± 17.18 ms; $p = 5.28 \times 10^{-7}$). Moreover, a significant interaction between drug condition and stimulus intensity ($p = .04$) revealed that the burst neurons exhibited prolonged burst duration over increasing stimulus intensity only in the control state ($p = 4.88 \times 10^{-4}$), with longer duration than during zolmitriptan administration at 5X (pre-drug 160.63 ± 38.40 ms vs post-drug 44.18 ± 23.26 ms; $p = 3.00 \times 10^{-4}$) and 10X (pre-drug 185.77 ± 46.22 ms vs post-drug 33.39 ± 9.52 ms; $p = 2.74 \times 10^{-6}$) intensities. These results support the effects of zolmitriptan in decreasing the evoked spike count and burst duration of the burst neurons.

Zolmitriptan significantly delayed the field latency from the vicinity of the burst neurons (Fig. 11D; $p = .005$), from a pre-drug value of 1.49 ± 0.06 ms to 1.81 ± 0.08 ms ($p = 0.002$). The drug

also significantly delayed the first-spike latency of the burst neurons (Fig. 11F; p = .002), from a pre-drug value of 3.99 ± 0.30 ms to 5.58 ± 0.36 ms (p = 0.001). However, zolmitriptan had no significant effect on the field potential magnitude from the vicinity of the burst neurons (Fig. 11C; p = .10) or on the spontaneous firing rate of the burst neurons (Fig. 11G; p = .33). These results support the effects of zolmitriptan in delaying the field latency from the vicinity of the burst neurons and the first-spike latency of the burst neurons following chronic spinal transection.

As opposed to NMDA, the suppressive effects of zolmitriptan become stronger on the burst neurons as the spinal transection transitions from acute to chronic stages (Fig. 12). This is revealed by statistical comparisons between the firing property parameters in the current study and their counterparts in the acute transection study during zolmitriptan administration measured as absolute changes from control conditions. Because of a large number of data with zero values in control conditions, absolute changes were used instead of relative changes for the comparisons of the drug effects with the baselines between acute and chronic transection studies, similarly to the comparisons of NMDA effects in the previous section. Moreover, it is possible that the relatively smaller effects of zolmitriptan in acute transection could be partly due to the inclusion of more than one DDH neuron per animal in some zolmitriptan experiments. Again, exclusion of these additional neurons in acute transection from the data analysis did not overturn any results of the statistical comparisons in which all the neurons were included. Accordingly, we described the statistical results with the inclusion of all the burst neurons below.

Zolmitriptan suppressed the evoked spike count of the burst neurons (Fig. 12A) in chronic transection (-2.74 ± 0.32 spikes) significantly more than that in acute transection (-1.19 ± 0.24 spikes; two-way unbalanced ANOVA, $p = 9.96 \times 10^{-5}$). The drug also suppressed the field potential from the vicinity of the burst neurons (Fig. 12B) in chronic transection (-0.09 ± 0.02 mV) significantly more than that in acute transection (0.01 ± 0.04 mV; p = .031). Zolmitriptan

delayed the field latency from the vicinity of the burst neurons (Fig. 12C) in chronic transection (0.32 ± 0.05 ms) significantly more than that in acute transection (0.13 ± 0.03 ms; $p = .001$). In addition, the drug delayed the first-spike latency of the burst neurons (Fig. 12E) in chronic transection (1.84 ± 0.31 ms) significantly more than that in acute transection (0.80 ± 0.15 ms; $p = .003$). Surprisingly, zolmitriptan suppressed the spontaneous firing rate of the burst neurons (Fig. 12F) in chronic transection (0.08 ± 0.06 Hz) significantly less than that in acute transection (-0.11 ± 0.05 Hz; $p = .014$). There was no significant difference in the zolmitriptan effect on the burst duration of the burst neurons in acute transection from that in chronic transection ($p = .36$).

Taken together, these results (Fig. 11A-G) demonstrated that zolmitriptan continues to suppress the firing properties of the burst neurons following chronic spinal transection by decreasing evoked spike count and burst duration and delaying field latency and first-spike latency, when compared with controls. Moreover, the suppressive effects of zolmitriptan become stronger over time following SCI (Fig. 12A-F). The drug suppresses evoked spike count and field potential and delays field latency and first-spike latency to a greater degree as the spinal transection transitions from acute to chronic stages.

DISCUSSION

Our goal was to assess the effects of 5-$HT_{1B/1D}$ and NMDA receptor activation on the firing characteristics of bursting DDH neurons following a complete-transection chronic SCI for comparisons with the results in our acute spinal transection study (Thaweerattanasinp et al. 2016). In the following discussion, we still consider the possibility that the bursting DDH neurons may contribute to generation of long EPSPs and muscle spasms as the spinal injury transitions from acute to chronic stages.

This study had two main findings. Firstly, the burst neurons still exist following chronic spinal transection, and they become slightly more excitable than their counterparts in acute spinal transection. Secondly, the burst neurons still experience significant changes in their firing activity during zolmitriptan and NMDA administration. However, zolmitriptan suppresses the burst neurons with stronger effects over time following SCI by decreasing evoked spike count and field potential and delaying field latency and first-spike latency to a greater degree than those in acute spinal transection. In contrast, NMDA slightly facilitates the burst neurons but with weaker effects over time following SCI by increasing evoked spike count and burst duration to a lesser degree and delaying field latency and first-spike latency to a greater degree than those in acute spinal transection.

Bursting DDH neurons likely contribute to muscle spasms following SCI

The slightly more excitable burst neurons could be the contributing player in generation of long EPSPs and muscle spasms following chronic SCI. Not only do they continue to fire multiple spikes (Fig. 7B&8A), the burst neurons fire with even longer burst duration (Fig. 8D) and faster responses (Fig. 8E) to a single-pulse dorsal root stimulation over time following SCI. The slight increase in the excitability of the burst neurons could result from increased excitatory synaptic drives to the burst neurons because the amplitude of spontaneous excitatory postsynaptic currents recorded from DDH neurons is increased over time following SCI (Rank et al. 2015). Changes in the intrinsic membrane properties, however, are less likely to result in the increased excitability of the burst neurons, as there are no differences in both passive and active membrane properties of DDH neurons between acute and chronic SCI (Rank et al. 2015). But we cannot rule out the possibility that an aberrant expression of specific ion channels can trigger the increased excitability of the burst neurons over time following SCI. The expression of Nav1.3

voltage-gated sodium channels has been found to be upregulated in hyperexcitable dorsal horn neurons (laminae I-VI) following chronic contusive SCI (Hains et al. 2003). Although highly expressed in neurons of rat embryos, Nav1.3 channels are virtually undetectable in adult neurons (Waxman and Hains 2006). Nav1.3 channels can generate persistent inward currents (PICs) and respond with large ramp currents to slow depolarizing stimuli below action potential threshold (Cummins et al. 2001). Moreover, the channels can rapidly recover from inactivation, thus suitable for sustaining high-frequency firing in neurons with increased excitability (Cummins et al. 2001). Reducing the expression of Nav1.3 protein via antisense oligodeoxynucleotides attenuates the hyperexcitability of dorsal horn neurons following SCI (Hains et al. 2003), but the effects are reversible after ceasing the antisense administration (Hains et al. 2003). Therefore, these studies suggest the functional relationship between Nav1.3 expression and hyperexcitability of dorsal horn neurons following SCI (Hains et al. 2003; Cummins et al. 2001).

Besides the burst neurons, the dorsal horn networks in the vicinity of the burst neurons may experience synaptic or cellular plasticity over time following SCI, as the field potential becomes smaller in magnitude (Fig. 8B) and slower in latency (Fig. 8C) from acute to chronic spinal transection. These changes in the magnitude and latency of the field potential recorded from the vicinity of the burst neurons may arise from an increased synaptic activity of inhibitory interneurons that mediate presynaptic inhibition of sensory afferents or excitatory interneurons to the burst neurons or postsynaptic inhibition of the burst neurons. A subpopulation of inhibitory GABAergic interneurons in lamina I have been found to exhibit an increase in their excitability following chronic spinal transection (Dougherty and Hochman 2008). Particularly, the neurons with tonic or initial bursting exhibit more depolarized membrane potentials, higher steady-state outward current, and larger spike heights, compared with controls (Dougherty and Hochman 2008). Moreover, the neurons with tonic firing exhibit higher firing frequencies and even

spontaneous plateau potentials likely mediated by sodium or calcium PICs (Dougherty and Hochman 2008). The increased excitability of inhibitory GABAergic interneurons may function as a compensatory homeostatic response (Dougherty and Hochman 2008) to exaggerated sensory transmission following SCI-induced loss of descending 5-HT inhibitory control (Hadjiconstantinou et al. 1984; Yoshimura and Furue 2006; Millan 2002; Murray et al. 2010; Baker and Chandler 1987; Bennett et al. 2004; Li et al. 2004a).

The burst neurons continue to show significant changes in their firing activity during zolmitriptan and NMDA administration following chronic spinal transection. Via activation of 5-$HT_{1B/1D}$ receptors, zolmitriptan can suppress long EPSPs and muscle spasms without affecting the intrinsic membrane properties of motoneurons following chronic SCI (Murray et al. 2011b). Our study demonstrates that zolmitriptan suppresses the burst neurons (Fig. 11A) by reducing their evoked spike count (Fig. 11B) and burst duration (Fig. 11E) and delaying their first-spike latency (Fig. 11G). The drug also suppresses the dorsal horn networks in the vicinity of the burst neurons by delaying their field latency (Fig. 11D). The shorter burst duration and longer first-spike latency of the burst neurons during zolmitriptan administration could also reflect changes in the EPSPs underlying the excitation of the burst neurons. Perhaps, zolmitriptan affects the sensory afferents, especially the unmyelinated C fibers (Li et al. 2016), that provide excitatory synaptic inputs to the burst neurons. When compared with the acute transection study (Thaweerattanasinp et al. 2016), zolmitriptan suppresses the burst neurons and the dorsal horn networks in their vicinity with even stronger effects over time following SCI (Fig. 12) by reducing their evoked spike count (Fig. 12A) and field potential (Fig. 12B) and delaying their field latency (Fig. 12C) and first-spike latency (Fig. 12E) to a greater degree. The increase in strength of the zolmitriptan effects could result from the supersensitivity of 5-HT_{1B} receptors via receptor upregulation following depletion of endogenous 5-HT (Sawynok and Reid, 1994), although the

underlying mechanism remains inconclusive as 5-$HT_{1B/1D}$ receptors unlikely develop supersensitivity in SCI patients (D'Amico et al. 2013). Although the mechanism underlying the anti-spastic effect of zolmitriptan in the dorsal horn is not well understood, the burst neurons could be one of its potential targets. On the other hand, activation of NMDA receptors slightly facilitates the burst neurons following chronic spinal transection (Fig. 9A). NMDA enhances only the spontaneous firing rate (Fig. 9G), despite slightly delaying the first-spike latency (Fig. 9F), of the burst neurons. When compared with the acute transection study (Thaweerattanasinp et al. 2016), NMDA facilitates the burst neurons and the dorsal horn networks in their vicinity, however, with weaker effects over time following SCI (Fig. 10) by enhancing their evoked spike count (Fig. 10A) and burst duration (Fig. 10D) to a lesser degree and delaying their field latency (Fig. 10C) and first-spike latency (Fig. 10E) to a greater degree. The decrease in strength of the NMDA effects could result from an increase in inhibitory synaptic drives to the burst neurons from hyperexcitable inhibitory interneurons, such as GABAergic interneurons in lamina I, that are involved in and regulate, albeit insufficient, NMDA receptor-mediated central sensitization and chronic pain following SCI (Woolf and Costigan 1999; Woolf and Salter 2000; Hao et al. 2004; Wang et al. 2005). Nevertheless, the small facilitative effects of NMDA on the burst neurons may intensify the generation of long EPSPs and muscle spasms following SCI.

Conclusions

Our study further supports the functional contribution of the burst neurons to generation of long EPSPs and muscle spasms following SCI. By investigating the firing activity of the burst neurons following chronic spinal transection and comparing with those following acute spinal transection, we show that the burst neurons become slightly more excitable over time following SCI. They also experience stronger suppressive effects of zolmitriptan but weaker facilitative

effects of NMDA on their firing activity over time following SCI. Nevertheless, future studies are necessary for investigating the functional connectivity of the burst neurons within the spinal networks and ultimately identifying their actual roles in the generation of long EPSPs and muscle spasms.

IV. QUANTIFICATION OF SPINAL VENTRAL ROOT ACTIVITY FOLLOWING ACUTE AND CHRONIC SPINAL TRANSECTION DURING ADMINISTRATION OF AN AGONIST FOR NMDA RECEPTOR

Abstract. An interaction between serotonin (5-HT) and NMDA receptor systems can induce and maintain the rhythmic activity in the spinal locomotor network. Depletion of raphespinal 5-HT can ultimately drive muscle spasms following chronic spinal cord injury (SCI) due to the emergence of exaggerated sensory transmission and hyperexcitable motoneurons. Despite the SCI-induced loss of 5-HT, the spinal cord continues to produce glutamates for NMDA receptor-mediated locomotion. However, what remains unknown is whether NMDA-induced rhythmic activity interacts with muscle spasm mechanisms following SCI. In this study, we quantified and compared the ventral root outputs during NMDA administration following acute and chronic spinal transection to study the relationship between NMDA-induced bursting activity and spastic ventral root reflexes. As the spinal injury transitions from acute to chronic stages, polysynaptic reflexes emerged following monosynaptic reflexes in the ventral roots. NMDA could induce bursting activity in the ventral roots but with the relatively equal effects for both acute and chronic spinal transection. These results suggest the independent functional relationship between NMDA-induced bursting activity and muscle spasm mechanisms following chronic SCI.

INTRODUCTION

Administration of NMDA can trigger rhythmic activity in the *in vitro* rodent spinal cord (Beato et al. 1997; Manuel et al. 2012). NMDA receptors have non-linear, voltage-dependent conductance (Mayer and Westbrook 1987), which results from the voltage-dependent Mg^{2+} blockade of the receptor channels (Mayer et al. 1984; Nowak et al. 1984) and thus leads to the negative slope conductance in the current-voltage relationship (i.e. I-V curve; Nowak et al, 1984; Flatman et al. 1983; MacDonald et al. 1982). Because of the voltage-dependent conductance, activation of NMDA receptors can trigger intrinsic membrane voltage oscillations in spinal motoneurons (Hochman et al. 1994b; MacLean et al. 1997; Hochman and Schmidt 1998; Manuel et al. 2012) and interneurons (Hochman et al. 1994a). Using an *in vitro* neonatal rat spinal cord preparation, MacLean and colleagues (1998) examined the effects of serotonin (5-HT) on network rhythmic activity and on tetrodotoxin (TTX)-resistant, NMDA receptor-mediated voltage oscillations. They found that application of 5-HT receptor antagonists abolished both phenomena (MacLean et al. 1998), but 5-HT itself facilitated NMDA receptor-mediated voltage oscillations (MacLean et al. 1998). However, 5-HT application alone was not sufficient for triggering voltage oscillations (MacLean et al. 1998). Therefore, the appropriate combination of neurotransmitters can elicit intrinsic membrane properties of some neurons to generate rhythmic activity for locomotor networks.

It was proposed that the generation of negative slope conductance in the I-V curve of NMDA receptors was crucial for their role in locomotor networks, rather than their collaboration with non-NMDA receptors to provide overall excitation to the networks (Schmidt and Jordan 2000). In the neonatal rat spinal cord, Schmidt and Jordan (2000) found that locomotor-like activity was poorly stable with Mg^{2+} removal, which abolishes the negative slope conductance in the I-V curve but still allows NMDA receptor activation (Schmidt and Jordan 2000). In the cord

preparations with TTX treatment, 5-HT application reintroduced the negative slope conductance in the I-V curve of healthy motoneurons failing to show the negative slope conductance in the presence of NMDA alone (Schmidt and Jordan 2000). Moreover, in other motoneurons showing the negative slope conductance in the presence of NMDA alone, 5-HT caused the negative slope conductance to shift toward the hyperpolarizing direction, which could be reversed by 5-HT antagonist mianserin (Schmidt and Jordan 2000). Reducing the bath concentration of Mg^{2+} also mimicked the hyperpolarizing shift of the negative slope conductance by 5-HT (Schmidt and Jordan 2000). Via $5\text{-}HT_2$ receptor activation, protein kinase C can enhance the hyperpolarizing shift of the negative slope conductance in the I-V curve of NMDA receptors and also reduce Mg^{2+} blockade of the receptor channels (Blank et al. 1996; Chen and Huang, 1992). Therefore, the effect of 5-HT on the negative slope conductance of NMDA receptors may result from reduction of Mg^{2+} blockade of the receptor channels.

At the chronic stage of spinal cord injury (SCI), depletion of 5-HT can trigger exaggerated sensory transmission to drive muscle spasms (Hadjiconstantinou et al. 1984; Murray et al. 2010; Baker and Chandler 1987; Bennett et al. 2004; Li et al. 2004a). While lacking 5-HT, the spinal cord still produces glutamate for NMDA receptor-mediated locomotion following SCI (Chau et al. 2002; Giroux et al. 2003). However, what remains poorly understood is how NMDA-induced rhythmic activity functions in relation with muscle spasm mechanisms following SCI. Using extracellular recordings of ventral root activity, we quantify and compare ventral root reflexes during administration of NMDA following acute and chronic spinal transection. Chronic spinal transection results in the appearance of polysynaptic reflexes, which are the triggers that start muscle spasms (Murray et al. 2011b), while only monosynaptic reflexes emerge following acute spinal transection. NMDA can induce bursting and tonic ventral root activity, but the magnitudes of this NMDA effect are not significantly different between acute and chronic spinal transection.

Therefore, the current study suggests that NMDA-induced bursting activity in the spinal cord may function independently from spastic polysynaptic ventral root reflexes following chronic SCI.

MATERIALS AND METHODS

Ventral root activity was recorded from the isolated sacral cord in response to dorsal root stimulation to reflect the activity of motoneuron populations in both acute and chronic transection studies (see details in Chapters 2 and 3). At a given stimulus intensity, the corresponding sacral dorsal roots were electrically stimulated 5 times at intervals of 30 seconds for four stimulus intensities (i.e. 1X, 2X, 5X, and 10X). Bath administration of NMDA (15, 50, and 100 μM in acute transection study; 15 and 20 μM in chronic transection study) was used to study the drug effect on the ventral root activity in response to dorsal root stimulation.

Spike2 (CED) software was used for rectifying and averaging (i.e. smoothing) the raw data of the ventral root activity. Then, the three components of the polysynaptic ventral root reflexes were quantified as the area under the curve (i.e. definite integral) in the order of their duration and latency as described in Murray et al (2011b): the short polysynaptic reflex (SPR; 10-40 ms post-stimulus); the long polysynaptic reflex (LPR; 40-500 ms post-stimulus) corresponding to the long EPSP; and the long-lasting reflex (LLR; 500-4,000 ms post-stimulus) associated with CaPIC. At a given reflex duration, mean ventral root activity was computed for all five dorsal root stimuli for each stimulus intensity. Background ventral root activity was measured over 800 ms before the first dorsal root stimulus, and it was then subtracted from the mean ventral root activity to obtain the final reflex responses. Measured as the area under the curve (mV·s in unit), the final reflex response could have a negative or zero value, corresponding to no reflex response, at a given reflex duration.

Because of the unbalanced data sets, a two-way unbalanced ANOVA via multiple regression analysis ($\alpha = 0.05$) was used for all comparisons of the ventral root activity from drug conditions or post-injury recovery periods at four stimulus intensities.

Figure 13. Comparisons of polysynaptic ventral root reflexes following acute and chronic spinal transection. *A*-*B*: Representative recording traces showing the effects of NMDA (bottom) on ventral root activities, compared with those in control (top), upon dorsal root stimulation (0.2 ms; arrow) following acute (*A*) and chronic (*B*) spinal transection. *A2*-*B2*: expanded views of the recording traces in *A1*-*B1* respectively for better views of the ventral root activities. *A3*-*B3*: the whole time course of the representative recording traces, with the shaded areas (grey) showing where the recording traces in A1-A2 and B1-B2 are taken from respectively. Vertical lines are individual dorsal root stimulation. *C*-*E*: Group data comparing the areas under the curves (mean ± SEM) in plots of the amplitudes of rectified ventral root activities against post-stimulus durations of polysynaptic ventral root reflexes following acute (♦) and chronic (■) spinal transection in response to increasing stimulus intensity in control. *C*: short polysynaptic reflex (SPR) for acute (*N* = 21 for all intensities) and chronic (*N* = 20 for all intensities) spinal transection. *D*: long polysynaptic reflex (LPR) for acute (*N* = 21 for all intensities) and chronic (*N* = 19 for all intensities) spinal transection. *E*: long-lasting reflex (LLR) for acute (*N* = 21 for all intensities) and chronic (*N* = 20 for all intensities) spinal transection. Significant difference (†$P < 0.001$) using a two-way unbalanced ANOVA.

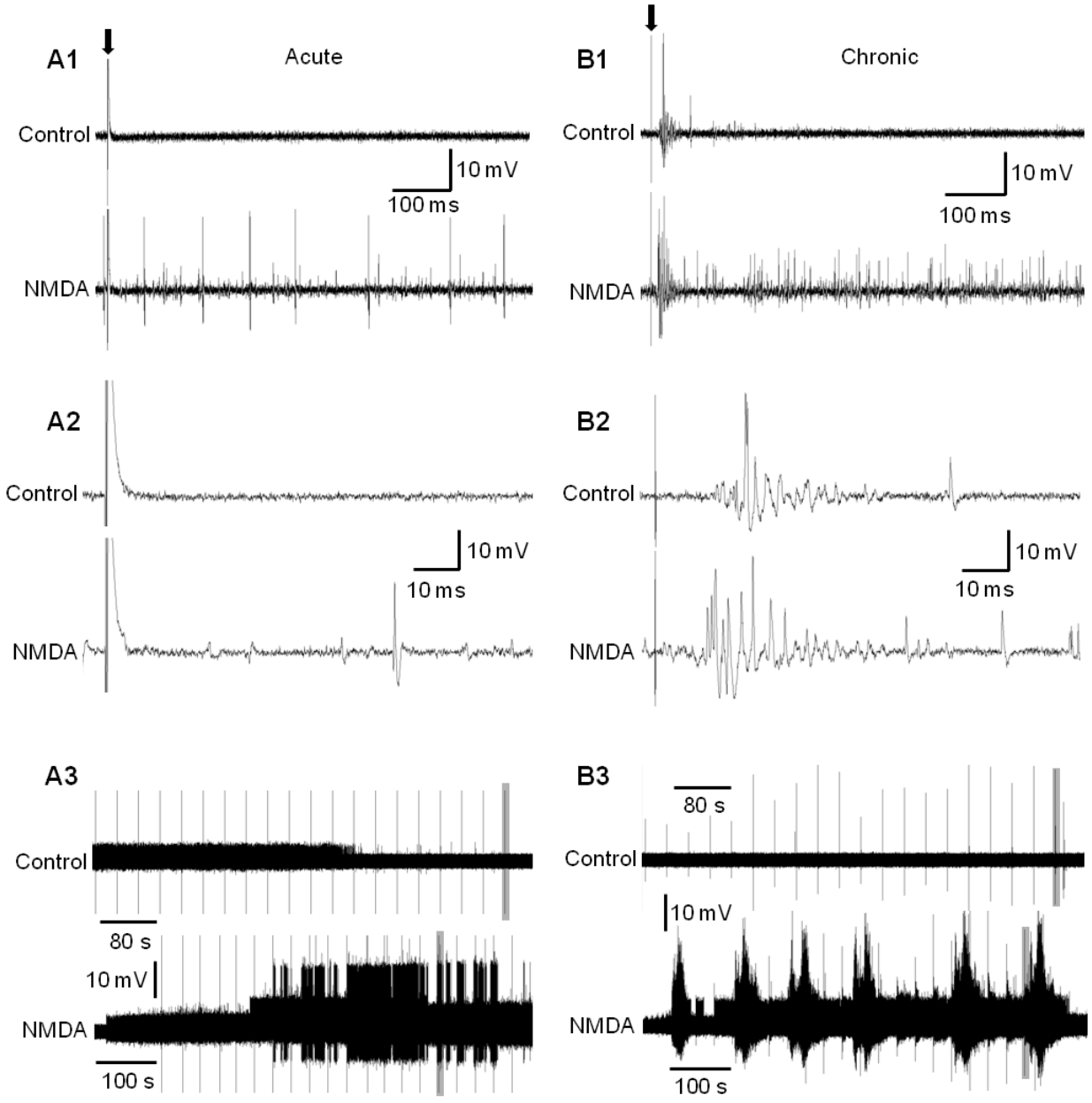

(figure continued on next page)

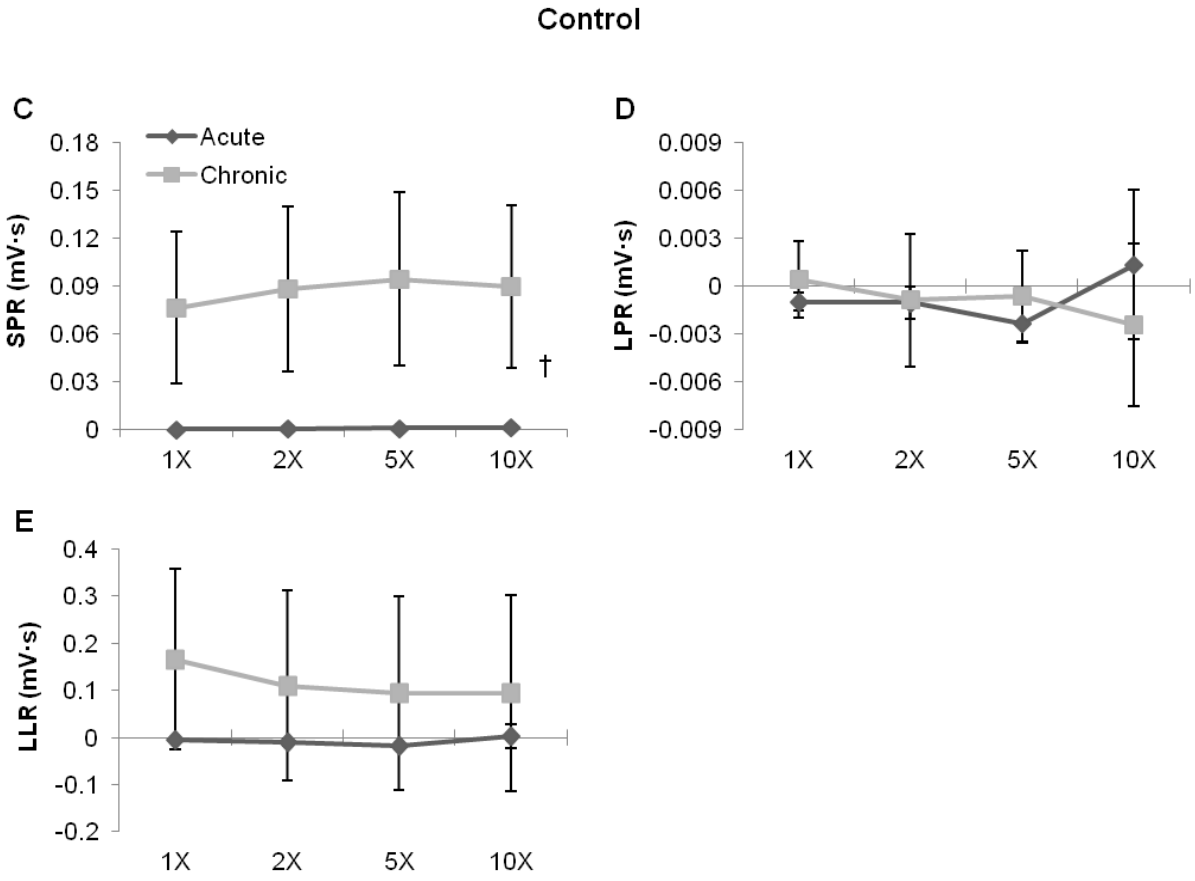
Control
C
Acute
Chronic
SPR (mV·s)
0.18
0.15
0.12
0.09
0.06
0.03
0
†
1X
2X
5X
10X
D
LPR (mV·s)
0.009
0.006
0.003
0
-0.003
-0.006
-0.009
1X
2X
5X
10X
E
LLR (mV·s)
0.4
0.3
0.2
0.1
0
-0.1
-0.2
1X
2X
5X
10X

Figure 14. Effects of NMDA on polysynaptic ventral root reflexes following acute and chronic spinal transection. *A*-*F*: Group data showing the effects of NMDA (■) on the areas under the curves (mean ± SEM) in plots of the amplitudes of rectified ventral root activities against post-stimulus durations of polysynaptic ventral root reflexes following acute (*A*-*C*) and chronic (*D*-*F*) spinal transection in response to increasing stimulus intensity, compared with those during control (♦) condition. *A*: short polysynaptic reflex (SPR) during control (*N* = 21 for all intensities) and NMDA (*N* = 13, 1X; *N* = 14, 2X; *N* = 17, 5X; *N* = 18, 10X) conditions for acute spinal transection. *B*: long polysynaptic reflex (LPR) during control (*N* = 21 for all intensities) and NMDA (*N* = 13, 1X; *N* = 14, 2X; *N* = 17, 5X; *N* = 18, 10X) conditions for acute spinal transection. *C*: long-lasting reflex (LLR) during control (*N* = 21 for all intensities) and NMDA (*N* = 13, 1X; *N* = 14, 2X; *N* = 17, 5X; *N* = 18, 10X) conditions for acute spinal transection. *D*: short polysynaptic reflex (SPR) during control (*N* = 20 for all intensities) and NMDA (*N* = 20; except *N* = 22 at 10X) conditions for chronic spinal transection. *E*: long polysynaptic reflex (LPR) during control (*N* = 20 for all intensities) and NMDA (*N* = 20; except *N* = 22 at 10X) conditions for chronic spinal transection. *F*: long-lasting reflex (LLR) during control (*N* = 20 for all intensities) and NMDA (*N* = 20; except *N* = 22 at 10X) conditions for chronic spinal transection. Significant difference (†$P < 0.001$) using a two-way unbalanced ANOVA.

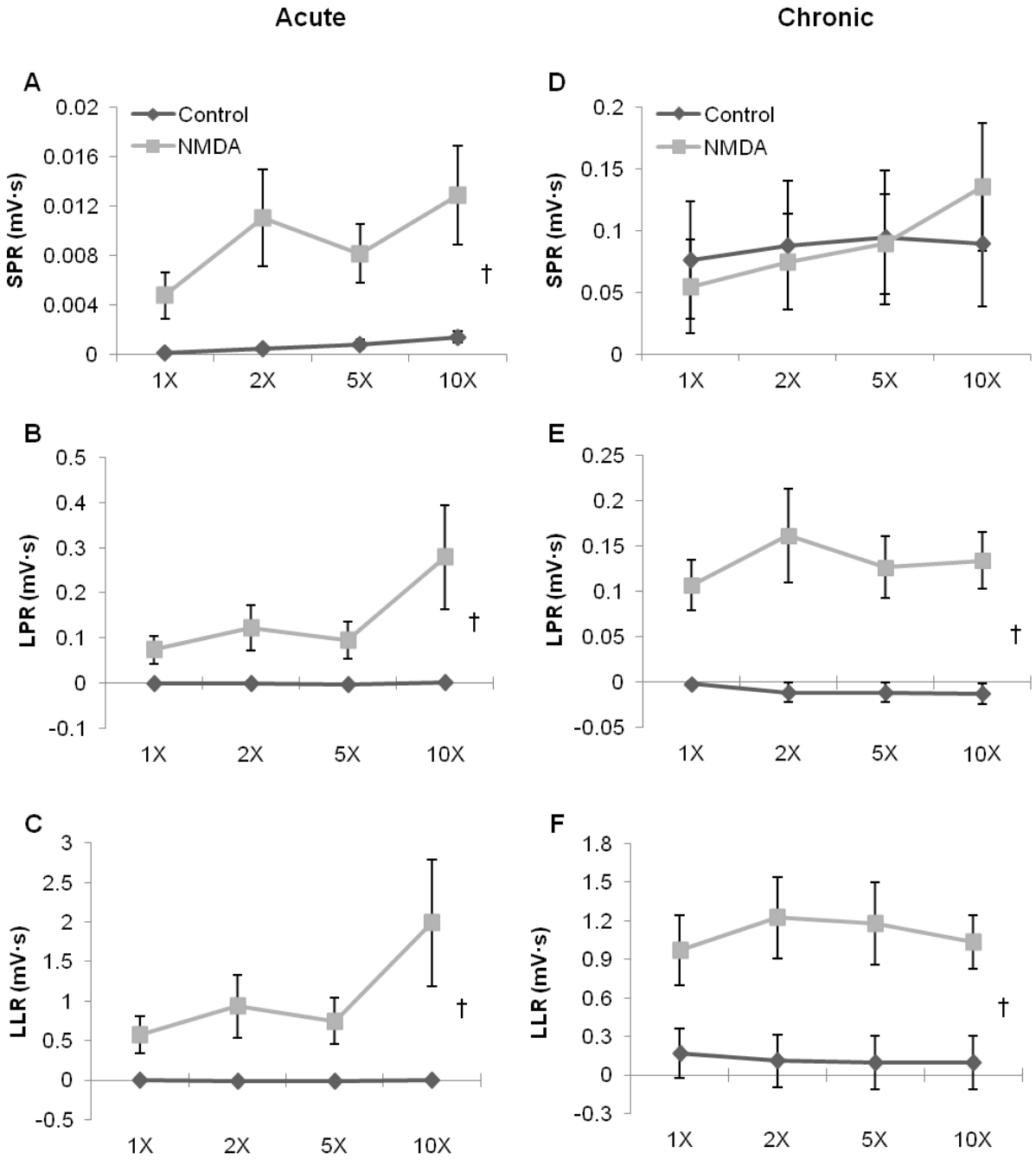
Acute
Chronic
A
D
Control
NMDA
SPR (mV·s)
0.02
0.016
0.012
0.008
0.004
0
0.2
0.15
0.1
0.05
1X
2X
5X
10X
†
B
E
LPR (mV·s)
0.5
0.4
0.3
0.2
0.1
0
-0.1
0.25
0.2
0.15
0.1
0.05
-0.05
C
F
LLR (mV·s)
3
2.5
2
1.5
1
0.5
0
-0.5
1.8
1.5
1.2
0.9
0.6
0.3
0
-0.3

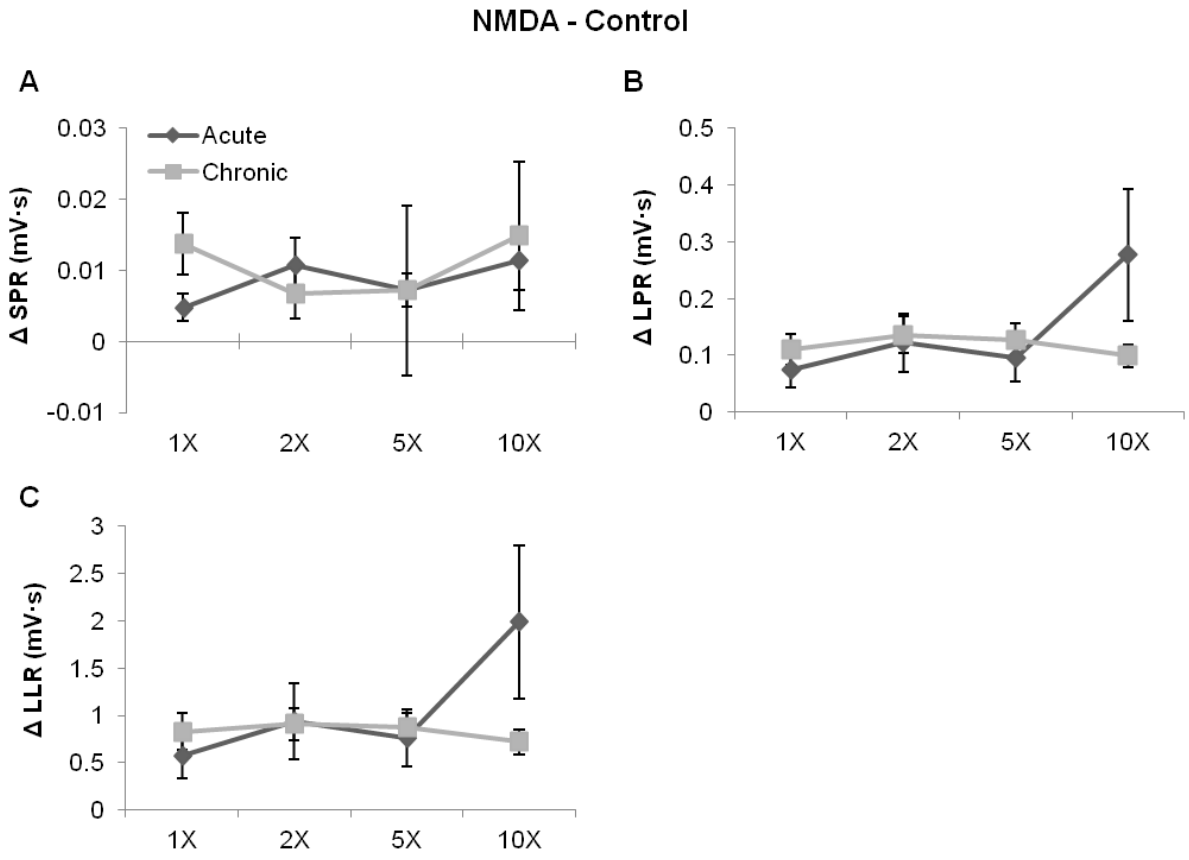

Figure 15. Comparisons of NMDA effects on polysynaptic ventral root reflexes following acute and chronic spinal transection. *A*-*C*: Group data comparing absolute changes from controls of NMDA effects (i.e. NMDA minus control; mean ± SEM) on the areas under the curves in plots of the amplitudes of rectified ventral root activities against post-stimulus durations of polysynaptic ventral root reflexes following acute (♦) and chronic (■) spinal transection in response to increasing stimulus intensity. *A*: short polysynaptic reflex (SPR) for acute (*N* = 13, 1X; *N* = 14, 2X; *N* = 17, 5X; *N* = 18, 10X) and chronic (*N* = 19 for all intensities) spinal transection. *B*: long polysynaptic reflex (LPR) for acute (*N* = 13, 1X; *N* = 14, 2X; *N* = 17, 5X; *N* = 18, 10X) and chronic (*N* = 19 for all intensities) spinal transection. *C*: long-lasting reflex (LLR) for acute (*N* = 13, 1X; *N* = 14, 2X; *N* = 17, 5X; *N* = 18, 10X) and chronic (*N* = 19 for all intensities) spinal transection.

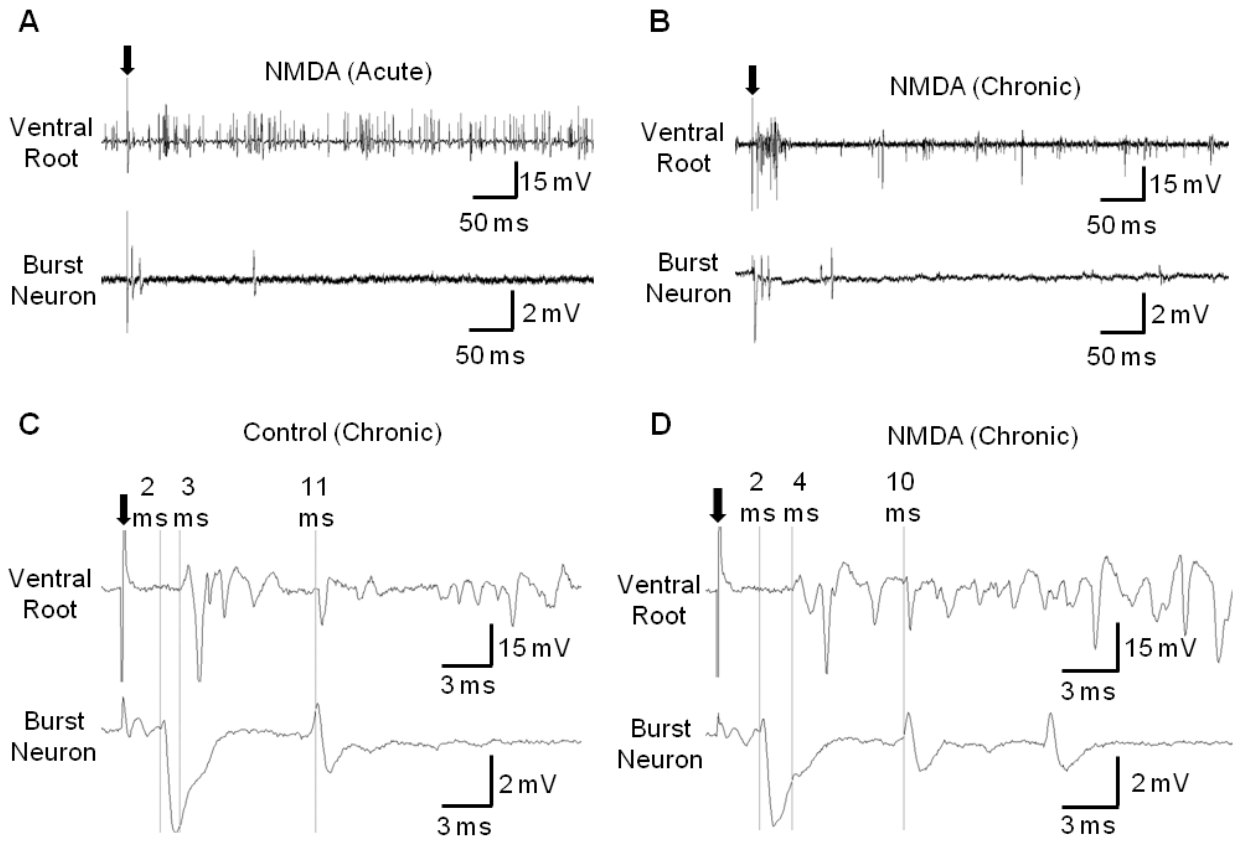

Figure 16. Correlation of the firing behavior of the burst neurons with evoked polysynaptic ventral root reflexes after chronic SCI but not with NMDA-induced bursting ventral root activity. *A-B*: representative recording traces showing the concurrent effects of NMDA on ventral root activities (top) and the burst neurons (bottom), upon dorsal root stimulation (0.2 ms; arrow) following acute (*A*) and chronic (*B*) spinal transection. *C-D*: representative recording traces showing the temporal correlations between evoked short polysynaptic reflexes (SPRs) on the ventral root and the firing activity of the burst neuron, upon dorsal root stimulation (0.2 ms; arrow) before (*C*) and during (*D*) NMDA administration following chronic spinal transection. Solid lines represent the onsets of distinct firing events: first-spike latency of the burst neuron (2 ms in *C&D*); latency of monosynaptic reflexes (3 ms in *C*; 4 ms in *D*); latency of short polysynaptic reflexes (11 ms in *C*; 10 ms in *D*).

RESULTS

NMDA-induced bursting ventral root activity may function independently from spastic ventral root reflexes.

Ventral root activity with NMDA-induced bursting was studied in extracellular sacral ventral root recordings. Ventral root recordings with a reliable effect of NMDA were selected from the experiments for Chapters 2 and 3 that recorded the burst neuron firing patterns during the bath administration of NMDA in both acute (*N* = 11 at 15 µM; *N* = 2 at 50 µM; *N* = 8 at 100 µM) and chronic (*N* = 21 at 15 µM; *N* = 2 at 20 µM) spinal transection. The results described below were derived from the combined effects of all the concentrations on the area under the curve (i.e. definite integral) in a plot of the amplitude of rectified ventral root activity against post-stimulus duration of the short polysynaptic reflex (SPR), the long polysynaptic reflex (LPR), or the long-lasting reflex (LLR; Fig. 13&14; see details in Methods). No results from washout conditions were included to allow direct comparisons between control and NMDA conditions, as washout can rapidly eliminate the NMDA-induced bursting ventral root activity (also reported in Manuel et al. 2012).

Following acute spinal transection, dorsal root stimulation evoked only short monosynaptic reflexes in the ventral roots (Fig. 13A *upper*), whereas longer-latency polysynaptic reflexes were not observed. In contrast, following chronic spinal transection, the same dorsal root stimulation evoked SPRs in addition to the monosynaptic reflexes (Fig. 13B *upper*). This is further supported by the significant difference in the area under the curve at SPR (Fig. 13C; $p = 6.80 \times 10^{-4}$) between acute (0.001 ± 0.000 mV·s) and chronic (0.087 ± 0.025 mV·s) transection in control. But LPRs and LLRs were usually not observed in response to dorsal root stimulation following chronic spinal transection (as in Fig. 13B *upper*). There were no significant differences

in the areas at LPR (Fig. 13D; p = .96) and at LLR (Fig. 13E; p = .21) between acute and chronic transection in control. These results indicate that chronic spinal transection at T10 vertebral level induces only SPRs for spastic polysynaptic reflexes in the ventral roots, not consistent with the findings by Murray et al. (2011b; see Discussion).

NMDA significantly enhanced bursting and tonic activity in the ventral roots following acute spinal transection (Fig. 13A *lower*) and thus the areas under the curves at all durations of the polysynaptic reflexes. NMDA significantly increased the area under the curve at SPR (Fig. 14A; 0.009 ± 0.002 mV·s), compared with control (0.001 ± 0.000 mV·s; two-way unbalanced ANOVA, $p = 2.40 \times 10^{-8}$). The drug also significantly increased the area at LPR (Fig. 14B; 0.142 ± 0.038 mV·s), compared with control (-0.001 ± 0.001 mV·s; $p = 2.12 \times 10^{-5}$); as well as the area at LLR (Fig. 14C; 1.061 ± 0.272 mV·s), compared with control (-0.008 ± 0.007 mV·s; $p = 8.35 \times 10^{-6}$). But stimulus intensity did not significantly affect the areas at SPR (p = .13), at LPR (p = .085), and at LLR (p = .11). NMDA continued to significantly enhance bursting and tonic activity in the ventral roots following chronic spinal transection (Fig. 13B *lower*). The drug significantly increased the area at LPR (Fig. 14E; 0.132 ± 0.018 mV·s), compared with control (-0.009 ± 0.005 mV·s; $p = 1.25 \times 10^{-11}$); as well as the area at LLR (Fig. 14F; 1.100 ± 0.138 mV·s), compared with control (0.116 ± 0.099 mV·s; $p = 6.38 \times 10^{-8}$). But NMDA had no significant effect on the area at SPR (Fig. 14D; p = .97). Stimulus intensity did not significantly affect the areas at SPR (p = .79), at LPR (p = .86), and at LLR (p = .97). These results suggest that NMDA enhances the bursting and tonic ventral root activity following both acute and chronic spinal transection, except the chronic ventral root activity at the duration of SPR.

However, NMDA-induced bursting ventral root activity likely has no functional relationship with spastic polysynaptic reflexes (Fig. 15). This is suggested by statistical comparisons of the areas under the curves at all durations of the polysynaptic reflexes between acute and chronic

transection during NMDA administration measured as absolute changes from control conditions. Because of a large number of data with zero values in control conditions, absolute changes were used instead of relative changes for the comparisons of the drug effects with the baselines between acute and chronic transection studies, similarly to the comparisons of NMDA and zolmitriptan effects on the burst neurons in Chapter 3.

There were no significant differences in the NMDA effect on the areas at SPR (Fig. 15A; p = .67), at LPR (Fig. 15B; p = .52), and at LLR (Fig. 15C; p = .37) in acute transection from those in chronic transection. Moreover, there were no temporal correlations between the NMDA-induced bursting ventral root activities and the firing behavior of none of the burst neurons (N = 0) following both acute (Fig. 16A) and chronic (Fig. 16B) spinal transection. However, the firing behavior of all the burst neurons, the potential contributor to muscle spasms (Thaweerattanasinp et al. 2016), correlated in time with the evoked ventral root activity at the duration of SPR following chronic spinal transection (Fig. 16C-D). The burst neurons had the response latency of their first spikes (3.85 ± 0.17 ms; Chapter 3) well before the SPR latency (Fig. 16C-D; 10 ms; Murray et al. 2011b). In addition, their burst duration (151.66 ± 17.61 ms; Chapter 3) could last until the latency and duration of LPR (40-500 ms; Murray et al. 2011b), which arises from long EPSPs in motoneurons (Murray et al. 2011b).These results suggest that the effects of NMDA on the ventral root activities do not correlate with the evoked polysynaptic reflexes and burst neurons related to muscle spasms following chronic SCI.

Taken together, besides the facilitation of the burst neurons, NMDA could induce bursting activity in the ventral roots following both acute and chronic spinal transection (Fig. 13&14). However, the NMDA-induced bursting ventral root activity may function independently from spastic ventral root reflexes (i.e. SPR, LPR, and LLR; Fig. 15) following chronic SCI.

DISCUSSION

Our goal was to assess the effects of NMDA receptor activation on the ventral root reflexes following both acute and chronic spinal transection. In the following discussion, we still consider the possibility that NMDA-induced bursting ventral root activity may function independently from muscle spasm mechanisms following SCI. The main finding of this study is that NMDA triggers bursting activity in the ventral roots following both acute and chronic spinal transection. But the magnitude of this NMDA effect on the weak ventral root activity in acute spinal transection is comparable with that on the relatively stronger ventral root activity in chronic spinal transection, where only short polysynaptic reflexes emerge.

Spinal locomotor network may function independently from muscle spasm-generating network

Dorsal root stimulation evokes only short monosynaptic reflexes following acute spinal transection (Fig. 13A *upper*), as the excitability of motoneurons plummets due to loss of descending monoaminergic control (Li et al. 2004a; Heckman et al. 2005; Miller et al. 1996). Consequently, no muscle spasms or long-lasting ventral root reflexes arise, despite the presence of the burst neurons (Thaweerattanasinp et al. 2016) and the consequent long EPSPs in motoneurons (Murray et al. 2011b; Baker and Chandler 1987; Bennett et al. 2004; Li et al. 2004a). In other words, the input that could trigger spasms in motoneurons is present but their low excitability prevents spasms from being generated. In addition to the monosynaptic reflexes, dorsal root stimulation evokes only short polysynaptic reflexes (SPRs) following chronic spinal transection (Fig. 13B *upper* & 13C), without any significant development of long polysynaptic reflexes (LPRs; Fig. 13D) and long-lasting reflexes (LLRs; Fig. 13E). The results are inconsistent with the findings by Murray et al. (2011b), in which dorsal root stimulation in chronic spinal rats can evoke all the three polysynaptic reflexes. The inconsistency likely results

from the fact that we made a secondary acute transection at between L6-S1 spinal segments during the sacral cord preparation in addition to the primary chronic transection at T10 vertebral level. This secondary injury could unexpectedly induce the increased synaptic activity of inhibitory spinal interneurons which, in turn, suppress and prevent hyperexcitable motoneurons from generating spastic long-lasting reflexes (Bennett et al. 2004; Li et al. 2004a). According to Murray et al. (2011b), SPR is a large, transient reflex with short latency that arises from short-duration polysynaptic EPSP. Next, longer-lasting LPR follows and arises from long-duration polysynaptic EPSP which also activates PICs intrinsic to motoneurons to further amplify and prolong LPR (Murray et al. 2011b). Lastly, long-lasting tonic LLR arises from the activated sodium and calcium PICs to ultimately drive muscle spasms (Murray et al. 2011b).

NMDA administration can induce bursting and tonic activity in the ventral roots following both acute and chronic spinal transection (Fig. 13A *lower*, 13B *lower* &14). The results are consistent with the previous discovery of NMDA-induced rhythmic bursting in the ventral roots of the isolated spinal cords (Cazalets et al. 1992; Sqalli-Houssaini et al. 1993; Manuel et al. 2012). At the low NMDA concentrations (15&20 μM), the bursting ventral root activity of our preparations (data not shown) likely results from the NMDA receptor activation of spinal interneurons participating in the central pattern generator (CPG) for locomotion (Hochman et al. 1994a; Cazalets et al. 1992; Sqalli-Houssaini et al. 1993). The voltage dependence of NMDA receptor activation can contribute to the rhythmic bursting in the CPG interneurons (Hochman et al. 1994a), but the cellular mechanisms of the mammalian CPG remain poorly understood nonetheless. At the higher NMDA concentrations (≥ 30 μM), NMDA receptor activation starts to induce the rhythmic bursting in motoneurons (Manuel et al. 2012), also contributing to the bursting ventral root activity in our preparations. This rhythmic bursting results from the alternating activation of persistent inward current (NMDA PIC) and persistent outward current

(NMDA POC) in motoneurons (Manuel et al. 2012). NMDA PIC depolarizes motoneurons and sustains the depolarizing phase of NMDA plateau, which is the slow-wave depolarization, while NMDA POC, which is likely produced by a calcium-dependent potassium current (SK), hyperpolarizes the motoneurons and terminates the NMDA plateau (Manuel et al. 2012). After NMDA POC subsides, NMDA PIC resumes, thus resulting in oscillations in membrane potentials of the motoneurons (Manuel et al. 2012). These NMDA-mediated oscillations in the motoneurons may contribute to rhythmic locomotor activity by amplifying and regulating oscillatory drives from interneuronal locomotor networks to the motoneuron pools (Manuel et al. 2012), which is consistent with the role of NMDA receptors in locomotor rhythm production (Schmidt and Jordan 2000; Chau et al. 2002; Giroux et al. 2003).

Although NMDA induces bursting ventral root activity, the magnitudes of its effect are not significantly different between acute and chronic spinal transection (Fig. 15 A-C). Moreover, the burst firing of the burst neurons does not clearly show any temporal correlation with the NMDA-induced bursting ventral root activities (Fig. 16A-B). Instead, it correlates in time with the evoked ventral root activity at the duration of SPR following chronic spinal transection (Fig. 16C-D). These results may suggest the independent functional relationship between spinal locomotor network and muscle spasm-generating network following chronic SCI. However, we cannot rule out the possible antagonistic relationship between the two spinal networks, as the emergence of SPR may prevent NMDA from inducing bursting ventral root activity resulting in no significant effect of NMDA at the duration of SPR (Fig. 14D). At the same time, the NMDA-induced bursting ventral root activity may reciprocally suppress the generation of SPR (Fig. 14D). Muscle spasms can impede locomotion following SCI (Lewek et al., 2007; de Leon et al. 1999). Reversely, locomotor training can reduce muscle spasms in SCI patients (D'Amico et al. 2014), which is consistent with the reduction of reflex transmission during locomotor activity in cats (Bennett et

al. 1996). Nevertheless, whether the mutual inhibition of spinal networks for locomotion and muscle spasms exists following chronic SCI remains unknown.

Conclusions

Our study proposes the independent functional relationship between NMDA-induced bursting ventral root activity and spastic ventral root reflexes following SCI. By quantifying and comparing the ventral root reflexes during NMDA administration following acute and chronic spinal transection, we show that NMDA can induce bursting activity in the ventral roots following both acute and chronic spinal transection but with the comparable magnitudes of its effect on both transection conditions. These ventral root reflex results suggest that spinal locomotor network may function independently from muscle spasm-generating network following chronic SCI. Nevertheless, future studies are necessary for investigating the functional connectivity between interneuronal networks for reflex control and rhythmic locomotion.

V. CONCLUDING REMARKS

SUMMARY OF RESEARCH

In Chapter 2, we characterized and assessed the firing properties of DDH neurons upon activation of 5-$HT_{1B/1D}$ and NMDA receptors following acute spinal transection. DDH neurons could respond to short-duration dorsal root stimulation with bursting, single-spiking, or tonic-firing behaviors. Zolmitriptan and NMDA administration could influence only the firing activity of the bursting DDH neurons. Zolmitriptan suppressed the bursting DDH neurons by decreasing their evoked spike count, burst duration, and spontaneous firing rate. On the other hand, NMDA moderately facilitated them by increasing their burst duration and spontaneous firing rate. These results validate my hypothesis that the bursting DDH neurons emerge and respond significantly to the effects of zolmitriptan and NMDA following SCI. Moreover, the results suggest the possible functional contribution of the bursting DDH neurons to generation of long EPSPs in motoneurons and thus muscle spasms that develop over time following SCI. The results also suggest that activation of 5-$HT_{1B/1D}$ receptors on the bursting DDH neurons may mediate the anti-spastic effect of zolmitriptan, whereas activation of NMDA receptors may facilitate the bursting DDH neurons in contributing to muscle spasm mechanisms following SCI.

In Chapter 3, we further assessed the firing properties of the bursting DDH neurons upon activation of 5-$HT_{1B/1D}$ and NMDA receptors following chronic spinal transection. There were still DDH neurons with bursting responses to short-duration dorsal root stimulation following chronic spinal transection. The bursting DDH neurons also became slightly more excitable and continued to experience the effects of zolmitriptan and NMDA over time following SCI. Zolmitriptan suppressed the bursting DDH neurons with stronger effects by decreasing the evoked spike count and field potential and delaying the field latency and first-spike latency to a

greater degree over time following SCI. On the other hand, NMDA slightly facilitated the bursting DDH neurons with weaker effects by increasing the evoked spike count and burst duration to a lesser degree and delaying the field latency to a greater degree over time following SCI. These results reinforce my hypothesis that the bursting DDH neurons continue to exhibit their burst firing behavior which can be influenced by the effects of zolmitriptan and NMDA over time following SCI, thus supporting the functional contribution of the bursting DDH neurons to muscle spasm mechanisms as acute spinal injury transitions to chronic injury.

In chapter 4, we assessed the ventral root reflexes upon NMDA receptor activation following acute and chronic spinal transection. NMDA induced bursting activity in the ventral roots following both stages of complete spinal transection. Although short polysynaptic reflexes emerged in the ventral roots following chronic spinal transection, the magnitude of the NMDA-induce bursting activity did not differ significantly from that in acute spinal transection. These results suggest the independent functional relationship between different mechanisms underlying NMDA-induced bursting ventral root activity and spastic ventral root reflexes following SCI.

FUTURE STUDIES

This research project has provided evidence that the bursting DDH neurons may contribute to generation of long EPSPs and muscle spasms following SCI. These DDH neurons fire bursting responses upon dorsal root stimulation, which can be suppressed by the anti-spastic effect of zolmitriptan via 5-$HT_{1B/1D}$ receptor activation. In contrast, the burst firing of these DDH neurons can be facilitated by NMDA receptor activation which is known to produce longer-lasting EPSPs than AMPA receptor activation. Future studies may employ molecular and cellular techniques, such as genetic labeling, to further identify and characterize the bursting DDH neurons and their

functional connectivity with other neurons in the spinal networks, including interneuronal networks for reflex control and rhythmic locomotion. Moreover, simultaneous recordings of the bursting DDH neurons and motoneurons would give us new insights into the functional role of these interneurons in the generation of long EPSPs and muscle spasms following SCI. In the end, a thorough understanding of the bursting DDH neurons would provide an alternative strategy for treating SCI and its related complications with drugs that restore inhibitory control of sensory transmission in the injured spinal cord.

REFERENCES

Abbinanti MD, Zhong G, Harris-Warrick RM. Postnatal emergence of serotonin-induced plateau potentials in commissural interneurons of the mouse spinal cord. *J Neurophysiol* 108: 2191-2202, 2012.

Abraira VE, Ginty DD. The sensory neurons of touch. *Neuron* 79: 618-639, 2013.

Andersen P, Eccles JC, Sears TA. Cortically evoked depolarization of primary afferent fibres in the spinal cord. *J Neurophysiol* 27: 63-77, 1964.

Baker LL, Chandler SH. Characterization of postsynaptic potentials evoked by sural nerve stimulation in hindlimb motoneurons from acute and chronic spinal cats. *Brain Res* 420: 340-350, 1987.

Basso D, Beattie M, Bresnahan J. A sensitive and reliable locomotor rating scale for open field testing in rats. J Neurotrauma 12: 1-21, 1995.

Beato M, Bracci E, Nistri, A. Contribution of NMDA and non-NMDA glutamate receptors to locomotor pattern generation in the neonatal rat spinal cord. *Proc R Soc Lond B* 264: 877-884, 1997.

Bennett DJ, De Serres SJ, Stein RB. Gain of the triceps surae stretch reflex in decerebrate and spinal cats during postural and locomotor activities. *J Physiol* 496: 837-850, 1996.

Bennett DJ, Sanelli L, Cooke C, Harvey PJ, Gorassini MA. Spastic long-lasting reflexes in the awake rat after sacral spinal cord injury. *J Neurophysiol* 91: 2247–2258, 2004.

Bennett GJ, Abdelmoumene M, Hayash H, Dubner R. Physiology and morphology of substantia gellatinosa neurones intracellularly stained with horseradish peroxidase. *J Comp Neurol* 194: 809-827, 1980.

Bennett GJ, Nishikawa N, Lu GW, Hoffert MJ, Dubner R. The morphology of dorsal column postsynaptic spinomedullary neurons in the cat. *J Comp Neurol* 224: 568-578, 1984.

Blank T, Zwart R, Nijholt I, Spiess J. Serotonin 5-HT2 receptor activation potentiates NMDA receptor-mediated ion currents by protein kinase C-dependent mechanism. *J Neurosci Res* 45: 153-160, 1996.

Blanke ML, VanDongen AM. Activation mechanisms of the NMDA receptor. In: *Biology of the NMDA Receptor,* edited by VanDongen AM. Boca Raton, FL: CRC Press/Taylor & Francis, 2009.

Brown AG. REVIEW ARTICLE THE DORSAL HORN OF THE SPINAL CORD. *Exp Physiol* 67: 193-212, 1982.

Brown AG, Fyffe RE. Synaptic contacts made by identified Ia afferent fibres upon motoneurones. *J Physiol* 284: 43P-44P, 1978.

Bui TV, Akay T, Loubani O, Hnasko TS, Jessell TM, Brownstone RM. Circuits for grasping: spinal dI3 interneurons mediate cutaneous control of motor behavior. *Neuron* 78: 191-204, 2013.

Carstens E, Trevino DL. Laminar origins of spinothalamic projections in the cat as determined by the retrograde transport of horseradish peroxidase. *J Comp Neurol* 182: 161-165, 1978.

Cazalets JR, Sqalli-Housaaini Y, Clarac F. Activation of the central pattern generator for locomotion by serotonin and excitatory amino acids in neonatal rat. *J Physiol* 455:187-204, 1992.

Cervero F, Handwerker HO, Laird JM. Prolonged noxious mechanical stimulation of the rat's tail: responses and encoding properties of dorsal horn neurones. *J Physiol* 404: 419-436, 1988.

Chau C, Giroux N, Barbeau H, Jordan L, Rossignol S. Effects of intrathecal glutamatergic drugs on locomotion I. NMDA in short-term spinal cats. *J Neurophysiol* 88: 3032-3045, 2002.

Chen L, Huang LM. Protein kinase C reduces Mg^{2+} block of NMDA-receptor channels as a mechanism of modulation. *Nature* 356: 521-523, 1992.

Christensen BN, Perl ER. Spinal neurons specifically excited by noxious or thermal stimuli: marginal zone of the dorsal horn. *J Neurophysiol* 33: 293-307, 1970.

Cummins TR, Aglieco F, Renganathan M, Herzog RI, Dib-Hajj SD, Waxman SG. Nav1.3 sodium channels: rapid repriming and slow closed-state inactivation display quantitative differences after expression in a mammalian cell line and in spinal sensory neurons. *J Neurosci* 21: 5952–5961, 2001.

D'Amico JM, Li Y, Bennett DJ, Gorassini MA. Reduction of spinal sensory transmission by facilitation of $5\text{-}HT_{1B/D}$ receptors in noninjured and spinal cord-injured humans. *J Neurophysiol* 109: 1485-1493, 2013.

D'Amico JM, Condliffe EG, Martins KJ, Bennett DJ, Gorassini MA. Recovery of neuronal and network excitability after spinal cord injury and implications for spasticity. *Front Integr Neurosci* 8: 36, 2014.

De Koninck Y, Ribeiro-da-Silva A, Henry JL, Cuello AC. Spinal neurons exhibiting a specific nociceptive response receive abundant substance P-containing synaptic contacts*. Proc Natl Acad Sci USA* 89: 5073-5077, 1992.

de Leon RD, Tamaki H, Hodgson JA, Roy RR, Edgerton VR. Hindlimb locomotor and postural training modulates glycinergic inhibition in the spinal cord of the adult spinal cat. *J Neurophysiol* 82: 359-369, 1999.

Derjean D, Bertrand S, Le Masson G, Landry M, Morisset V, Nagy F. Dynamic balance of metabotropic inputs causes dorsal horn neurons to switch functional states. *Nat Neurosci* 6: 274-281, 2003.

Ditunno JF, Little JW, Tessler A, Burns AS. Spinal shock revisited: a four-phase model. *Spinal Cord*, 42: 383-395, 2004.

Dougherty KJ, Bannatyne BA, Jankowska E, Krutki P, Maxwell DJ. Membrane receptors involved in modulation of responses of spinal dorsal horn interneurons evoked by feline group II muscle afferents. *J Neurosci* 25: 584–593, 2005.

Dougherty KJ, Hochman S. Spinal cord injury causes plasticity in a subpopulation of lamina I GABAergic interneurons. *J Neurophysiol* 100: 212-223, 2008.

Duysens J, and Pearson KG. The role of cutaneous afferents from the distal hindlimb in the regulation of the step cycle of thalamic cats. *Exp Brain Res* 24: 245-255, 1976.

Ferrington DG, Sorkin LS, Willis WD Jr. Responses of spinothalamic tract cells in the superficial dorsal horn of the primate lumbar spinal cord. *J Physiol* 388: 681-703, 1987.

Fetz, EE. Pyramidal tract effects on interneurons in the cat lumbar dorsal horn. *J Neurophysiol* 31: 69-80, 1968.

Fields HL, Basbaum AI, Clanton CH, Anderson SD. Nucleus raphe magnus inhibition of spinal cord dorsal horn neurons. *Brain Res* 126: 441-453, 1977.

Flatman JA, Schwindt PC, Crill WE, Stefstrom CE. Multiple actions of N-methyl-D-aspartate on cat neocortical neurons in vitro. *Brain Res* 266: 169-173, 1983.

Giroux N, Chau C, Barbeau H, Reader TA, Rossignol S. Effects of intrathecal glutamatergic drugs on locomotion. II. NMDA and AP-5 in intact and late spinal cats. *J Neurophysiol* 90: 1027-1045, 2003.

Gordon IT, Whelan PJ. Monoaminergic control of cauda-equina-evoked locomotion in the neonatal mouse spinal cord. *J Neurophysiol* 96: 3122–3129, 2006.

Grudt TJ, Perl ER. Correlations between neuronal morphology and electrophysiological features in the rodent superficial dorsal horn. *J Physiol* 540: 189–207, 2002.

Hadjiconstantinou M, Panula P, Lackovic Z, Neff NH. Spinal cord serotonin: a biochemical and immunohistochemical study following transection. *Brain Res* 322: 245–254, 1984.

Hains BC, Klein JP, Saab CY, Craner MJ, Black JA, Waxman SG. Upregulation of sodium channel Nav1.3 and functional involvement in neuronal hyperexcitability associated with central neuropathic pain after spinal cord injury. *J Neurosci* 23: 8881–8892, 2003.

Han ZS, Zhang ET, Craig AD. Nociceptive and thermoreceptive lamina I neurons are anatomically distinct. *Nat Neurosci* 1: 218-225, 1998.

Hantman AW, van den Pol AN, Perl ER. Morphological and physiological features of a set of spinal substantia gelatinosa neurons defined by green fluorescent protein expression. *J Neurosci* 24: 836–842, 2004.

Hao JX, Kupers RC, Xu XJ. Response characteristics of spinal cord dorsal horn neurons in chronic allodynic rats after spinal cord injury. *J Neurophysiol* 92: 1391-1399, 2004.

Harvey PJ, Li X, Li Y, Bennett DJ. 5-HT2 receptor activation facilitates a persistent sodium current and repetitive firing in spinal motoneurons of rats with and without chronic spinal cord injury. *J Neurophysiol* 96: 1158-1170, 2006a.

Harvey PJ, Li X, Li Y, Bennett DJ. Endogenous monoamine receptor activation is essential for enabling persistent sodium currents and repetitive firing in rat spinal motoneurons. *J Neurophysiol* 96: 1171–1186, 2006b.

Heckman CJ, Gorassini MA, Bennett DJ. Persistent inward currents in motoneuron dendrites: implications for motor output. *Muscle Nerve* 31: 135–156, 2005.

Heise C, Kayalioglu G. Cytoarchitecture of the spinal cord. In: *The Spinal Cord: A Christopher and Dana Reeve Foundation Text and Atlas*, edited by Watson C, Paxinos G, Kayalioglu G. Burlington, MA: Academic press, 2009.

Hochman S, Garraway SM, Pockett S. Membrane properties of deep dorsal horn neurons from neonatal rat spinal cord in vitro. *Brain Res* 767: 214-219, 1997.

Hochman S, Garraway SM, Machacek DW, Shay BL. 5-HT receptors and the neuromodulatory control of spinal cord function. In: *Motor Neurobiology of the Spinal Cord*, edited by Cope TC. Boca Raton, FL: CRC Press, 2001.

Hochman S, Jordan LM, MacDonald JF. N-methyl-D-aspartate receptor-mediated voltage oscillations in neurons surrounding the central canal in slices of rat spinal cord. *J Neurophysiol* 72: 565–577,1994a.

Hochman S, Jordan LM, Schmidt BJ. TTX-resistant NMDA receptor-mediated voltage oscillations in mammalian lumbar motoneurons. *J Neurophysiol* 72: 2559–2562, 1994b.

Hochman, S, Schmidt BJ. Whole cell recordings of lumbar motoneurons during locomotor-like activity in the in vitro neonatal rat spinal cord. *J Neurophysiol* 79: 743–752, 1998.

Jankowska E, Slawinska U, Hammar I. On organization of a neuronal network in pathways from group II muscle afferents in feline lumbar spinal segments. *J Physiol* 542: 301-314, 2002.

Jiang MC, Heckman CJ. In vitro sacral cord preparation and motoneuron recording from adult mice. *J Neurosci Methods* 156: 31-36, 2006.

Jiang MC, Schuster JE, Fu R, Siddique T, Heckman CJ. Progressive changes in synaptic inputs to motoneurons in adult sacral spinal cord of a mouse model of amyotrophic lateral sclerosis. *J Neurosci* 29: 15031-15038, 2009.

Levine AJ, Hinckley CA, Hilde KL, Driscoll SP, Poon TH, Montgomery JM, Pfaff SL. Identification of a cellular node for motor control pathways. *Nat Neurosci* 17: 586-593, 2014.

Lewek MD, Hornby TG, Dhaher YY, Schmit BD. Prolonged quadriceps activity following imposed hip extension: a neurophysiological mechanism for stiff-knee gait? *J Neurophysiol* 98: 3153-3162, 2007.

Li L, Rutlin M, Abraira VE, Cassidy C, Kus L, Gong S, Jankowski MP, Luo W, Heintz N, Koerber HR, Woodbury CJ, Ginty DD. The functional organization of cutaneous low-threshold mechanosensory neurons. *Cell* 147: 1615-1627, 2011.

Li X, Murray K, Harvey PJ, Ballou EW, Bennett DJ. Serotonin facilitates a persistent calcium current in motoneurons of rats with and without chronic spinal cord injury. *J Neurophysiol* 97: 1236-1246, 2007.

Li Y, Bennett DJ. Persistent sodium and calcium currents cause plateau potentials in motoneurons of chronic spinal rats. *J Neurophysiol* 90: 857-869, 2003.

Li Y, Gorassini MA, Bennett DJ. Role of persistent sodium and calcium currents in motoneuron firing and spasticity in chronic spinal rats. *J Neurophysiol* 91: 767-783, 2004a.

Li Y, Harvey PJ, Li X, Bennett DJ. Spastic long-lasting reflexes of the chronic spinal rat studied in vitro. *J Neurophysiol* 91: 2236-2246, 2004b.

Li Y, Lucas-Osma AM, Black S, Stephens MJ, Fenrich KK, Fouad K, Bennett DJ. Sensory transmission to motoneurons is facilitated by cold-sensing C fibres expressing TRPM8 and 5-HT_{1D} receptors: links between management of spasticity and migraines. In: Proceedings from the 46th Annual Meeting of the Society for Neuroscience; November 12-16, 2016; San Diego, CA. Abstract 612.29.

Light AR, Kavookjian AM. Morphology and ultrastructure of physiologically identified substantia gelatinosa (lamina II) neurons with axons that terminate in deeper dorsal horn laminae (III-V). *J Comp Neurol* 267: 172-189, 1988.

Light AR, Perl ER. Spinal termination of functionally identified primary afferent neurons with slowly conducting myelinated fibers. *J Comp Neurol* 186: 133-150, 1979.

Light AR, Trevino DL, Perl ER. Morphological features of functionally defined neurons in the marginal zone and substantia gelatinosa of the spinal dorsal horn. *J Comp Neurol* 186: 151-171, 1979.

Light AR, Willcockson HH. Spinal laminae I-II neurons in rat recorded in vivo in whole cell, tight seal configuration: properties and opioid responses. *J Neurophysiol* 82: 3316-3326, 1999.

MacDonald JK, Porietis AV, Wojtowicz JM. L-aspartic acid induces a region of negative slope conductance in the current-voltage relationship of cultured spinal neurons. *Brain Res* 237: 248-253, 1982.

MacLean JN, Cowley KC, Schmidt BJ. NMDA receptor mediated oscillatory activity in the neonatal rat spinal cord is serotonin dependent. *J Neurophysiol* 79: 2804 –2808, 1998.

MacLean JN, Schmidt BJ, Hochman S. NMDA receptor activation triggers voltage oscillations, plateau potentials and bursting in neonatal rat motoneurons in vitro. *Eur J Neurosci* 9: 2702–2711, 1997.

Manuel M, Li Y, Elbasiouny SM, Murray K, Griener A, Heckman CJ, Bennett DJ. NMDA induces persistent inward and outward currents that cause rhythmic bursting in adult rodent motoneurons. *J Neurophysiol* 108: 2991-2998, 2012.

Maxwell DJ. Combined light and electron microscopy of Golgi-labelled neurons in lamina III of the feline spinal cord. *J Anat* 141: 155-169, 1985.

Maxwell DJ, Fyffe RE, Rethelyi M. Morphological properties of physiologically characterized lamina III neurons in the cat spinal cord. *Neuroscience* 10: 1-22, 1983.

Mayer ML, Westbrook GL. The physiology of excitatory amino acids in the vertebrate central nervous system. *Prog Neurobiol* 28: 197-276, 1987.

Millan MJ. The induction of pain: an integrative review. *Prog Neurobiol* 57: 1-164, 1999.

Millan MJ. Descending control of pain. *Prog Neurobiol* 66: 355–474, 2002.

Miller JF, Paul KD, Lee RH, Rymer WZ, Heckman CJ. Restoration of extensor excitability in the acute spinal cat by the 5-HT2 agonist DOI. *J Neurophysiol* 75: 620-628, 1996.

Morisset V, Nagy F. Modulation of regenerative membrane properties by stimulation of metabotropic glutamate receptors in rat deep dorsal horn neurons. *J Neurophysiol* 76: 2794–2798, 1996.

Morisset V, Nagy F. Nociceptive integration in the rat spinal cord: role of nonlinear membrane properties of deep dorsal horn neurons. *Eur J Neurosci* 10: 3642–3652, 1998.

Morisset V, Nagy F. Ionic basis for plateau potentials in deep dorsal horn neurons of the rat spinal cord. *J Neurosci* 19: 7309-7316, 1999.

Murray K, Nakae A, Stephens MJ, Rank M, D'Amico J, Harvey P, Li X, Harris L, Ballou EW, Anelli R, Heckman CJ, Mashimo T, Vavrek R, Sanelli L, Gorassini MA, Bennett DJ, Fouad K. Recovery of motoneuron and locomotor function after spinal cord injury depends on constitutive activity in 5-HT_{2C} receptors. *Nat Med* 16: 694–700, 2010.

Murray K, Stephens MJ, Ballou EW, Anelli R, Heckman CJ, Bennett DJ. Motoneuron excitability and muscle spasms are regulated by 5-HT_{2B} and 5-HT_{2C} receptor activity. *J Neurophysiol* 105: 731–278, 2011a.

Murray K, Stephens MJ, Rank M, D'Amico J, Gorassini MA, Bennett DJ. Polysynaptic excitatory postsynaptic potentials that trigger spasms after spinal cord injury in rats are inhibited by 5-HT_{1B} and 5-HT_{1F} receptors. *J Neurophysiol* 106: 925-943, 2011b.

Nowak L, Bregetovski P, Ascher P, Herbet A, Prochiantz A. Magnesium gates glutamate activated channels in mouse central neurones. *Nature* 307: 462-465, 1984.

Perl ER. Afferent basis of nociception and pain: evidence from the characteristics of sensory receptors and their projections to the spinal dorsal horn. *Res Publ Assoc Res Nerv Ment Dis* 58: 19-45, 1980.

Prescott SA, De Koninck Y. Four cell types with distinctive membrane properties and morphologies in lamina I of the spinal dorsal horn of the adult rat. *J Physiol* 539: 817-836, 2002.

Quevedo J, Stecina K, Gosgnach S, and McCrea DA. Stumbling corrective reaction during fictive locomotion in the cat. *J Neurophysiol* 94: 2045-2052, 2005.

Rank MM, Flynn JR, Battistuzzo CR, Galea MP, Callister R, Callister RJ. Functional changes in deep dorsal horn interneurons following spinal cord injury are enhanced with different duration of exercise training. *J Physiol* 593: 331-345, 2015.

Ritz LA, Greenspan JD. Morphological features of lamina V neurons receiving nociceptive input in cat sacrocaudal spinal cord. *J Comp Neurol* 238: 440-452, 1985.

Ruscheweyh R, Sandkühler J. Lamina-specific membrane and discharge properties of rat spinal dorsal horn neurones in vitro. *J Physiol* 541: 231-244, 2002.

Sawynok J, Reid A. Spinal supersensitivity to 5-HT_1, 5-HT_2 and 5-HT_3 receptor agonists following 5,7-dihydroxytryptamine. *Eur J Pharmacol* 264: 249-257, 1994.

Schmidt BJ, Jordan LM. The role of serotonin in reflex modulation and locomotor rhythm production in the mammalian spinal cord. *Brain Res Bull* 53: 689-710, 2000.

Schoenen J. The dendritic organization of the human spinal cord: the dorsal horn. *Neuroscience* 7: 2057-2087, 1982.

Schouenborg J, Sjolund BH. Activity evoked by A-and C-afferent fibers in rat dorsal horn neurons and its relation to a flexion reflex. *J Neurophysiol* 50: 1108-1121, 1983.

Sqalli-Houssaini Y, Cazalets JR, Clarac F. Oscillatory properties of the central pattern generator for locomotion in neonatal rats. *J Neurophysiol* 70: 803-813, 1993.

Thaweerattanasinp T, Heckman CJ, Tysseling VM. Firing characteristics of deep dorsal horn neurons after acute spinal transection during administration of agonists for 5-$HT_{1B/1D}$ and NMDA receptors. *J Neurophysiol* 116: 1644-1653, 2016.

Todd AJ. Cells in lamina III and IV of rat spinal dorsal horn receive monosynaptic primary afferent input in lamina II. *J Comp Neurol* 289: 676-686, 1989.

Todd AJ. Neuronal circuitry for pain processing in the dorsal horn. *Nat Rev Neurosci* 11: 823-836, 2010.

Voisin DL, Nagy F. Sustained L-type calcium currents in dissociated deep dorsal horn neurons of the rat: characteristics and modulation. *Neurosci* 102: 461-472, 2001.

Wang J, Kawamata M, Namiki A. Changes in properties of spinal dorsal horn neurons and their sensitivity to morphine after spinal cord injury in the rat. *Anesthesiology* 102: 152-164, 2005.

Watson C, Kayalioglu G. The organization of the spinal cord. In: *The Spinal Cord: A Christopher and Dana Reeve Foundation Text and Atlas*, edited by Watson C, Paxinos G, Kayalioglu G. Burlington, MA: Academic press, 2009.

Watson C, Harvey AR. Projections from the brain to the spinal cord. In: *The Spinal Cord: A Christopher and Dana Reeve Foundation Text and Atlas*, edited by Watson C, Paxinos G, Kayalioglu G. Burlington, MA: Academic press, 2009.

Watson C, Paxinos G, Kayalioglu G, Heise C. Atlas of the mouse spinal cord. In: *The Spinal Cord: A Christopher and Dana Reeve Foundation Text and Atlas*, edited by Watson C, Paxinos G, Kayalioglu G. Burlington, MA: Academic press, 2009.

Waxman SG, Hains BC. Fire and phantoms after spinal cord injury: Na^+ channels and central pain. *Trends Neurosci* 29: 207-215, 2006.

Willis WD, Kenshalo DR Jr, Leonard RB. The cells of origin of the primate spinothalamic tract. *J Comp Neurol* 188: 543-573, 1979.

Woolf CJ. Central terminations of cutaneous mechanoreceptive afferents in the rat lumbar spinal cord. *J Comp Neurol* 261: 105-119, 1987.

Woolf CJ, Costigan M. Transcriptional and posttranslational plasticity and the generation of inflammatory pain. *Proc Natl Acad Sci USA* 96: 7723–7730, 1999.

Woolf CJ, Salter MW. Neuronal plasticity: increasing the gain in pain. *Science* 288: 1765–1769, 2000.

Yoshimura M, Furue H. Mechanisms for the anti-nociceptive actions of the descending noradrenergic and serotonergic systems in the spinal cord. *J Pharmacol Sci* 101: 107–117, 2006.

Young RR. Spasticity: a review. *Neurology* 44: S12-S20, 1994.